The Effect of Deglacial Meltwater Processes on Kimberlite Indicator Mineral Concentrations in Glacial Sediments

by

Patrick DesRosiers

BSc (Hons), Queens University, 2018

Thesis Submitted in Partial Fulfillment of the
Requirements for the Degree of
Master of Science

in the
Department of Earth Sciences
Faculty of Science

SIMON FRASER UNIVERSITY
Spring 2021

Declaration of Committee

Name:	**Patrick DesRosiers**
Degree:	**Master of Science**
Thesis title:	**The Effect of Deglacial Meltwater Processes on Kimberlite Indicator Mineral Concentrations in Glacial Sediments**
Committee:	**Chair:** Dan Gibson Professor, Earth Sciences
	Brent Ward Supervisor Professor, Earth Sciences
	David Sacco Committee Member Senior Surficial Exploration Specialist, Palmer
	Daniel Layton-Matthews Committee Member Associate Professor, Geological Sciences and Geological Engineering Queen's University
	Isabelle McMartin Examiner Research Scientist Geological Survey of Canada

Abstract

Successful diamond exploration projects in glaciated terrain depend on effective drift prospecting methods. This thesis assesses the effects of deglacial meltwater on kimberlite indicator mineral contents in subglacial meltwater corridor sediments. Located 100 km west of Lac de Gras, NWT, the study area has diamond potential and contains subglacial meltwater corridors and unmodified till. A 1:15 000 surficial geology map was produced. Meltwater corridors bisect areas of till veneer and blanket and contain glaciofluvial deposits including eskers and glaciofluvial hummocks. These hummocks form by subglacial meltwater erosion of till and rapid deposition. Till has more silt and clay than meltwater-affected sediments; this affects normalization of analytical results with glaciofluvial hummocks containing higher counts of pyropes. Identification of subglacial meltwater corridor sediments including glaciofluvial hummocks is crucial as they have different compositions and transport histories than till. These differences must be considered when interpreting surficial exploration datasets and planning sampling programs.

Keywords: Quaternary Geology, Surficial mapping, Drift prospecting, Glacial landform genesis, Subglacial meltwater corridor

Acknowledgements

Thank you to Barrett Elliott and the Northwest Territories Geological Survey for logistical and financial support with fieldwork and laboratory analysis; without your support this project would not have been possible. Thank you to Dave Kelsch and GGL Resources Inc. for allowing us to use your exploration property and facilitating the setup, use, and management of your field camp. Your support made the field component of this project one of the best field experiences I have ever had. Crey Ackerson is thanked for both his exceptional assistance in the field and the photogrammetry work he completed for this project. Your positive can-do attitude helped get me through those tougher field days and your commitment to learning new skills led to the creation of great DEMs of the project area.

Beth McClenaghan is thanked for her time, mentorship and guidance with drift prospecting standards, the selection of analytical methods and for providing till sample standards. It was very kind of you to take the time to support me as I navigated my way through this project.

I would like to acknowledge the Natural Science and Engineering Research Council of Canada for the Canadian graduate student scholarship and to Simon Fraser University for the graduate fellowship. These financial supports allowed me to focus on my research during my graduate degree and for that I am very grateful.

Finally, I would like to thank all the members of my supervisory committee. Your combined expertise facilitated my learning in all aspects of this multidisciplinary project, and I could not have asked for a better group of mentors. Thank you to Dave Sacco for sharing your expertise in surficial geology mapping and surficial exploration in the Slave Geological Province. You also taught me how to use Summit Evolution, one of the coolest programs I have ever had the opportunity to use and for that I am very thankful.

Daniel Layton Matthews is thanked for his time and mentorship in applied geochemistry. When we ran into pandemic related issues with data analysis, Dan and his team at Queen's Facility for Isotope Research were able to complete sample preparation and mineral chemistry analysis quickly and on short notice, and for that I am very grateful.

Thank you to my senior supervisor Brent Ward for your mentorship and support throughout all aspects of my graduate studies. Whenever I had questions or needed help you always had time for me, and I am very grateful for that. You facilitated all my learning in the study of Quaternary Geology, and I hope to make you proud as I take everything you have taught me into my future endeavors.

Table of Contents

List of Tables

List of Figures

List of Acronyms

3D	Three dimensional
GSC	Geological Survey of Canada
KIM	Kimberlite indicator mineral
LGM	Last glacial maximum
LIS	Laurentide Ice Sheet
MLA	Mineral Liberation Analysis
REE	Rare earth elements
SGP	Slave Geological Province

Chapter 1. Introduction

At the last glacial maximum (LGM), the Laurentide Ice Sheet (LIS) covered the Canadian Shield and most of Canada. The last glaciation resulted in erosion and widespread deposition of glacial sediments, covering both bedrock and associated mineral deposits. The glaciated terrain in Canada includes a wide range of sediments that are variable in both material genesis and transport history, complicating surficial mineral exploration in these regions. In glaciated terrains, conventional surficial mineral exploration methods, where geochemical anomalies in surface sediments are interpreted to target buried mineral deposits (Cameron et al., 2004), can be ineffective without taking into consideration the transport history of the sample media.

The Slave Geological Province (SGP) of the Northwest Territories is previously glaciated terrain and prospective for diamond and other mineral deposits. The success of diamond exploration projects in the SGP depends on the implementation of appropriate drift prospecting methods due to the differences in material genesis of glacial sediments. Conventional methods of drift prospecting combine geochemical and mineralogical surficial sediment sampling techniques with knowledge of sediment genesis so that anomalous samples can be properly interpreted and traced back to their source (McClenaghan et al., 2020). Subglacial till is an optimal sediment for drift prospecting programs as it is common and widely distributed in glaciated terrains, is derived directly from a bedrock source and transport histories can be interpreted (McClenaghan, 2005; McClenaghan et al., 2020). Geochemical and indicator mineral anomalies in subglacial till are significantly larger than their bedrock source, creating large exploration targets (Levson, 2001). However, deglacial meltwater processes that may rework and erode till are commonly overlooked or misidentified in sample collection and data interpretation. This thesis evaluates the sedimentology, mineralogy, matrix geochemistry, and mineral chemistry of sediments in subglacial meltwater corridors. These processes may alter kimberlite indicator mineral (KIM) concentrations in modified sediments, potentially masking primary dispersal of the indicator minerals in till. It is possible that kimberlite anomalies are being misinterpreted or completely missed in areas where deglacial meltwater processes have modified the sediments.

The effect of deglacial meltwater processes on KIM concentrations in meltwater-modified glacial sediments is poorly understood and there is limited published literature. The aim of this project is to quantify if and how these processes affect KIM concentrations in meltwater-modified sediments. The results of this project have significant implications for the planning and interpretation of surficial diamond exploration programs in the Northwest Territories and similar glaciated areas worldwide with subglacial meltwater corridors.

1.1. Setting

The study area is located north of Beauparlant Lake, Northwest Territories. It is in the central SGP, ~260 km northeast of Yellowknife and ~100 km west of Diavik Diamond mine on Lac de Gras (Figure 1.1). It is part of the Beauparlant Lake map sheet (NTS 86A09), located on the western edge of the 1:250 000 Winter Lake map sheet (NTS 86A). It was chosen because it contains multiple subglacial meltwater corridors, meltwater related landforms, unmodified glacial sediments, and has diamond potential. The study area is 144 km^2, centered around an existing exploration camp. The area has low rolling relief, generally not exceeding tens of metres overall. It has many lakes, small ponds, and small areas of shallow organic wetlands. Small outcrops of bedrock are common, though the dominant surficial materials in the area are glacial sediments, the most common of which is till (Kerr et al.,1996).

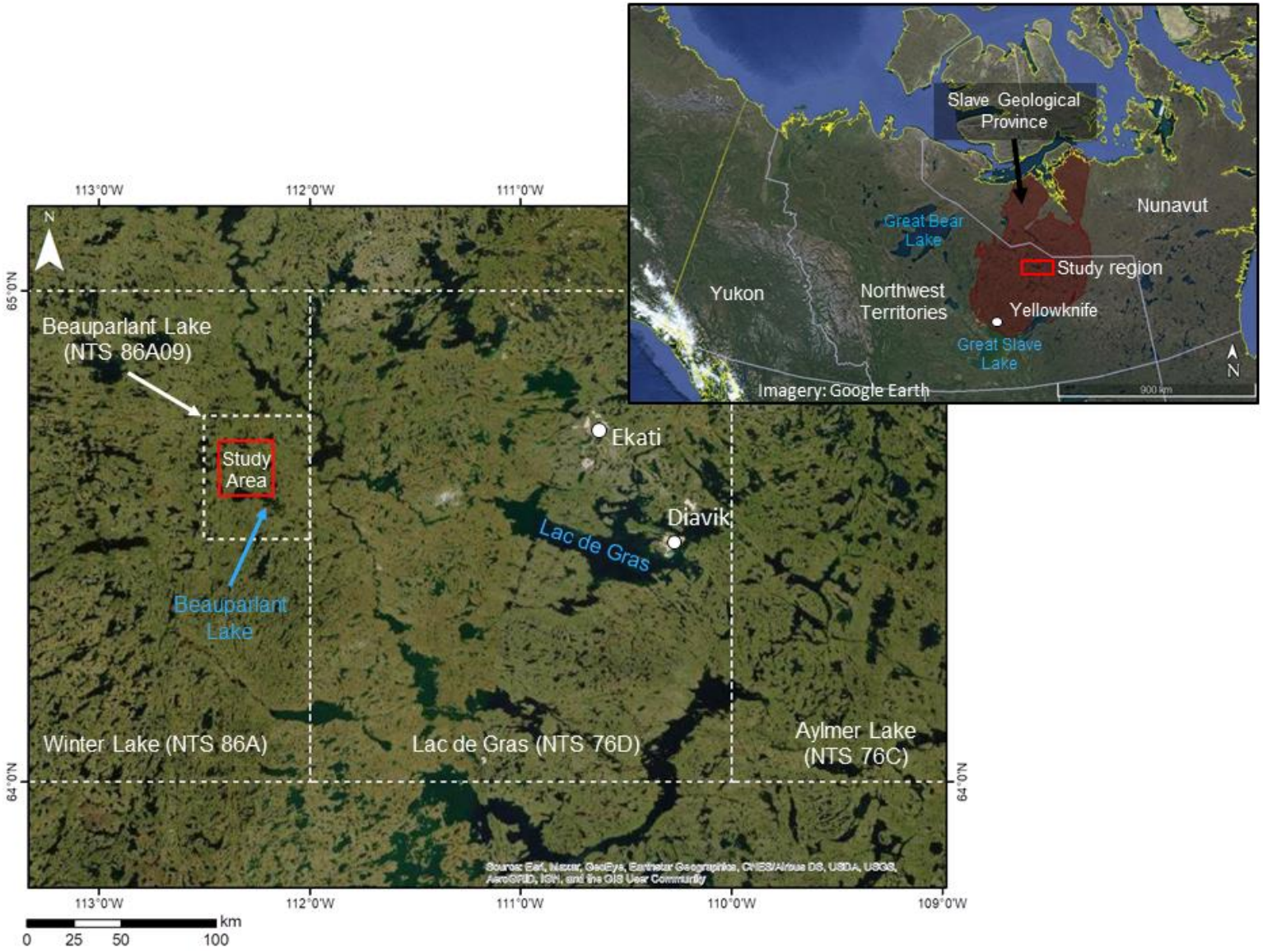

Figure 1.1: Location of the study area with insert map displaying the region in the Northwest Territories. The study area is highlighted in red and relevant locations and NTS map sheets are included.

1.2. Regional Glacial History

The Geological Survey of Canada (GSC) completed an investigation of the surficial geology and glacial history of the central SGP (Dredge et al., 1994) following the discovery of diamond bearing kimberlites in the early 1990's. As part of this investigation three 1:125 000 scale surficial geology maps were produced that cover the Winter Lake, Lac de Gras, and Aylmer Lake map sheets (Figure 1.1; Dredge et al., 1995; Kerr et al., 1996; Ward et al., 1997). In this thesis the Winter Lake region refers to the Winter Lake map area. Recently larger scale mapping (Haiblen et al., 2018; Sacco et al., 2018) provides detailed surficial geology and glacial history of smaller areas surrounding Lac de Gras, to the east of the study area. These maps and accompanying reports provide a framework for the interpretation of the regional surficial geology and glacial history.

During the LGM, the LIS covered a significant portion of Canada and parts of the northern United States. The LIS grew in three major sectors: Labrador, Keewatin, and Baffin (Dyke, 2004). The Keewatin Sector covered the Winter Lake region, and the Keewatin ice divide controlled the direction of ice flow (Dalton et al., 2020; Dyke, 2004). During deglaciation, the position of the Keewatin Ice Divide evolved (Dyke and Prest, 1987), and this led to changes in the direction of ice flow in the Winter Lake region. Radiocarbon and terrestrial cosmogenic nuclide ages indicate that the study area deglaciated between 9.5 and 9 ^{14}C ka BP (Dalton et al., 2020; Dyke, 2004).

Alysworth and Shilts (1989) defined four broad landform assemblage zones within the Keewatin Sector of the LIS. The Winter Lake region is within landform assemblage zones three and four, suggesting that the landform assemblage in the area varies between thick drumlinized drift cover with infrequent eskers to areas of thin to minimal drift cover with significant areas of exposed bedrock.

Regional Quaternary geology research identified three main phases of ice flow history in the central SGP (Figure 1.2) based on striation sequencing and orientation of streamlined macroforms (Dredge et al., 1994). The first phase is oriented towards the southwest, which is followed by flow to the west and then flow to the west-northwest (Dredge et al., 1994). There is evidence of small local deviations in ice flow after this third phase, with flow to the southwest in the north-eastern portion of the Aylmer Lake map area and flow to the west in the northern portion of the Winter Lake map area (Dredge et al., 1994). The third

phase of ice flow is thought to be the dominant ice flow direction in the region in terms of its ability to transport sediments and shape the landscape (Dredge et al., 1994; Ward et al., 1997).

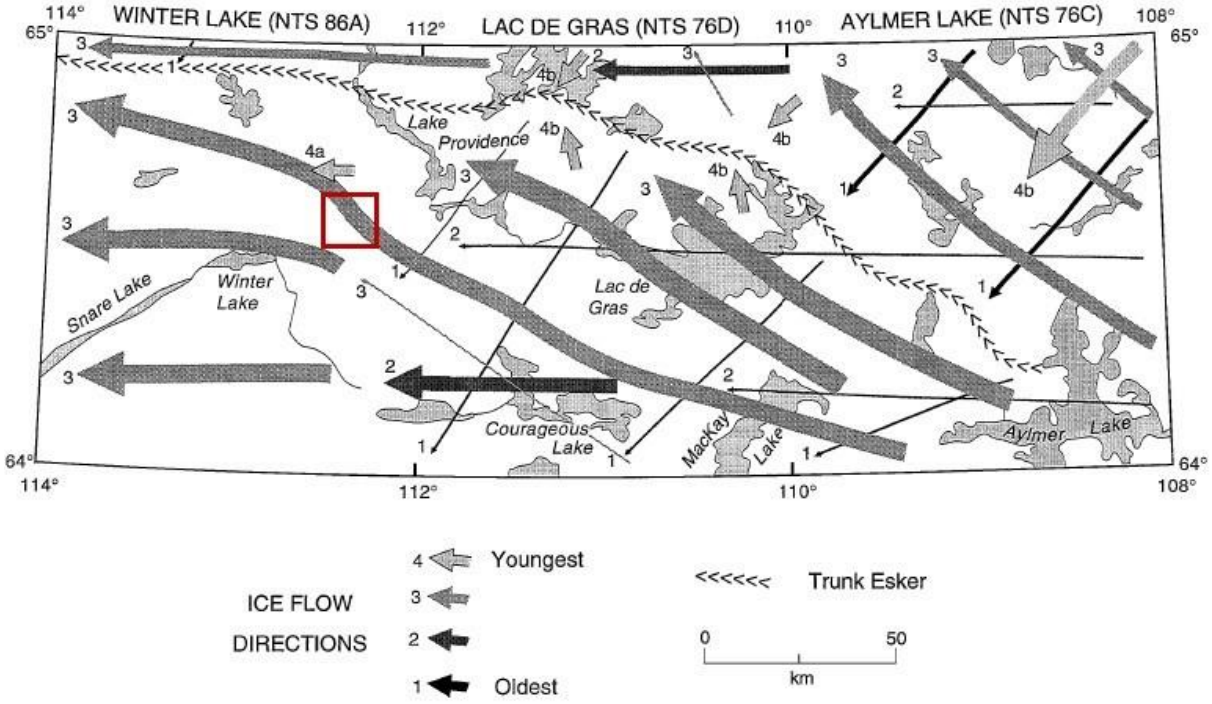

Figure 1.2: Generalized ice flow diagram for the cental SGP (Dredge et al., 1994), the red box highlights the study area. Flow directions are numbered and the thickness of each arrow denotes the relative effect of the flow on sediment transport and landscape modification.

1.3. Subglacial Meltwater Corridors

Subglacial meltwater corridors are elongated, sublinear geomorphic features that contain sediment and landform assemblages resulting from meltwater erosion and deposition by subglacial meltwater. Erosion and reworking by meltwater have been observed worldwide in a wide range of glaciated environments (e.g, Peterson and Johnson, 2018; Peterson et al., 2018; Rampton, 2000; St Onge, 1984) and subglacial meltwater corridors are common in the SGP (Dredge et al., 1985; Dredge et al., 1995; Haiblen, 2016; Kerr et al., 1996; Kerr et al., 2014a; Kerr et al., 2014b; Knight, 2018; Sacco et al., 2018; St Onge and Kerr, 2014; Ward et al., 1997). These features have also been observed in southern Sweden, where subglacial meltwater corridors are referred to as tunnel valleys or hummock corridors (Ojala et al., 2019; Peterson and Johnson, 2018; Peterson et al., 2018).

Subglacial meltwater corridors include areas of glaciofluvial material occurring as veneers of sand and gravel, boulder concentrations, reworked till and scoured bedrock. Landforms including eskers, deltas, and hummocks are common. Hummocks and mounds have been found within subglacial meltwater corridors in many of the locations where these corridors are described (Campbell et al., 2013; Dahlgren, 2013; Dredge et al., 1995; Haiblen, 2016; McMartin et al., 2020; Rampton, 2000; Rampton and Sharpe, 2014; Sacco et al., 2018; Utting et al., 2009; Ward et al., 1997). In older literature these hummocks are mapped as kames and ribbed moraines (Aylsworth and Shilts, 1989; Dredge et al., 1995; Kerr et al., 1996; Ward et al., 1997). These hummock landforms were targeted for investigation to better understand their genesis.

There are multiple hypotheses regarding the formation of subglacial meltwater corridors. One hypothesis is that subglacial meltwater corridors formed from outburst floods associated with the drainage of large subglacial lakes (Rampton, 2000). Corridors formed when multiple sustained pulses of high energy, subglacial meltwater travelled long distances across the SGP at the ice-bed interface (Rampton, 2000). Another hypothesis is that subglacial meltwater corridor formation is a time transgressive process, with relatively short segments of the corridor forming through time as the margin of the LIS retreated (Campbell et al., 2013; Utting et al., 2009). In this hypothesis the source of meltwater is supraglacial with meltwater reaching the ice-bed interface as it approaches the margin (Campbell et al., 2013; St Onge, 1984; Utting et al., 2009). A third hypothesis that combines aspects of both previously mentioned genesis models suggests that subglacial meltwater corridors formed in a time transgressive manner from high energy sheet-type meltwater flows originating supraglacially which evolved into channelized drainage systems (Haiblen, 2016). Regardless of how subglacial meltwater corridors form it is evident that they lead to erosion, reworking and deposition of remobilized surficial sediments (Haiblen, 2016; Rampton, 2000; Utting et al., 2009).

1.4. Drift Prospecting in the Slave Geological Province

Diamond bearing kimberlites were discovered in the Lac de Gras region of the Northwest Territories in 1991 when exploration across the region led to the discovery of the point lake kimberlite (Fipke et al., 1995). Since then, significant effort has been placed on developing methods for diamond exploration in glaciated terrains. Drift prospecting

guidelines and best practices have been released and are continuously revised by the GSC (McClenaghan et al., 2013; McClenaghan et al., 2020; Spirito et al., 2011)

There are two main types of surficial materials commonly sampled for KIMs, till and glaciofluvial sediments (Cummings et al., 2011; McClenaghan, 2005,). Till is the most common sampling media in property-scale investigations as it is widespread in glaciated terrains and geochemical and mineral anomalies in till can create large exploration targets, significantly larger than their bedrock source (Levson, 2001). Till is a first derivative of bedrock and when combined with knowledge of the sediment transport history, allows for vectoring back to the bedrock source (McClenaghan, 2005; Spirito et al., 2011).

Kimberlites have a distinct mineral and geochemical signature (Sparks et al., 2006) and are usually relatively soft compared to the surrounding bedrock. When glaciers flow over kimberlites or other mineral deposits they can easily erode and deposit them in the till down ice (McClenaghan et al., 2002; McClenaghan 2005; Miller, 1984); this creates patterns of anomalous indicator mineral concentrations, referred to as dispersal trains. Once a dispersal train has been discovered, vectoring in the up-ice (inverse to ice flow) direction can lead to the kimberlite source. These dispersal train anomalies can be an extremely useful exploration tool for vectoring towards kimberlites in the SGP (Dredge et al., 1994; McClenaghan et al., 2002).

The process of vectoring can be complicated by non-linear dispersal due to multiple ice flow directions as is the case in the SGP; the complex ice flow history can produce non-linear, palimpsest dispersal trains (McClenaghan et al., 2000). The formerly linear, almost cigar shaped anomaly can be smeared out into a fan shape or even more complex forms depending on the different directions of ice flow (McClenaghan et al., 2000). Therefore, it is important to understand the glacial history when interpreting surficial exploration datasets.

Esker sediments can also be used for KIM sampling. Usually, glaciofluvial sediments are sampled during regional scale reconnaissance exploration (e.g, Cummings et al., 2011; Henderson, 2000; Parent et al., 2004; Tremblay et al., 2009). Esker sediments are generally further travelled from their source and represent a second derivative of bedrock because they are commonly derived from till (Cummings et al., 2011). Esker sediments may also be derived directly from bedrock. The most likely transport history of KIMs in

glaciofluvial material is that subglacial meltwater intersects and erodes a KIM dispersal train in till and deposits it further downstream (Cummings et al., 2011). The derivative nature of glaciofluvial sediment transport history must be considered when sampling any subglacial meltwater corridor sediments and the secondary meltwater transport considered when vectoring towards mineralization.

1.5. Thesis Objectives

The main research question addressed in this thesis is:

How do deglacial meltwater processes affect kimberlite indicator mineral concentrations and distributions in glacial sediments?

To effectively complete this thesis, the research question was divided into several components, and smaller research objectives were generated to address each element. Results were then synthesized to form a general conclusion. The specific research questions of this project are:

1. What is the nature, genesis, and distribution of glacial sediments in the area?

2. What is the glacial history of the study area?

3. What are the sedimentological differences between glacial sediments?

4. What are the concentrations of KIMs in samples collected from different surficial materials?

5. What are the relationships between indicator mineral chemistry and matrix geochemistry of material types with different geneses?

The hypothesis is that meltwater-modified sediments will have higher concentrations of KIMs, similar to esker or stream sediments.

1.6. Methods

This project includes surficial geology mapping, field work, granulometry, clast lithology, KIM analysis and matrix geochemical analysis. The methods utilized in completing these project elements are described in detail in the relevant chapters. Mapping methods are described in Chapter 2. Granulometry and clast lithology methods are described in Chapter 3. Methods of KIM analysis, and methods of geochemical analysis are described in Chapter 4.

1.7. Thesis Organization

This is a modified paper-format thesis, so several of the chapters have been presented as stand-alone articles. As a result, there is some repetition of information amongst chapters. The thesis consists of five chapters. Chapter 1 introduces the project, study area, and background information. Chapter 2 contains a summary of previous regional and local surficial geology and presents new, high-resolution surficial geology mapping for a portion of the Beauparlant Lake map sheet (NTS 86A09) (Appendix A). In Chapter 2 surficial geology is described, distribution of sediments is discussed, and the glacial history presented. Chapter 3 includes a summary of previous research in the genesis of subglacial meltwater corridors and glaciofluvial hummocks and presents the granulometry dataset from three transects that cross the margins of subglacial meltwater corridors. The results of this work and local surficial mapping completed in Chapter 2 are used to interpret the genesis of glaciofluvial hummocks. Chapter 4 examines and compares KIM counts, mineral chemistry and matrix geochemistry datasets from till and subglacial meltwater corridor sediments. The effects of deglacial meltwater processes on KIM concentrations and distributions, and implications for drift prospecting are discussed. Chapter 5 summarizes the significant contributions of this thesis. Future work is proposed for furthering our understanding of the genesis of subglacial meltwater landforms and applications to drift prospecting.

Chapter 2. Surficial Geology and Glacial History of the Beauparlant Lake Area

2.1. Introduction

This chapter includes the surficial geology, ice flow history and glacial history of the study area interpreted from descriptions of surficial materials, surface expressions, landforms, and ice flow indicators. The results of high-resolution mapping completed north of Beauparlant Lake are described and local glacial history is discussed. A 1:15 000-scale surficial geology map of a portion of the Beauparlant Lake map sheet (NTS 86A09) (Appendix A) accompanies this chapter. The purpose of this chapter is to complete two of the main research objectives of this project: determine the distribution and nature of surficial sediments at a high resolution and refine the glacial history of the Beauparlant Lake area.

2.2. Setting

The study area is located north of Beauparlant Lake, Northwest Territories. It is in the central SGP, ~260 km northeast of Yellowknife and ~100 km west of Diavik Diamond mine on Lac de Gras (Figure 2.1). It is part of the Beauparlant Lake map sheet (NTS 86A09), located on the western edge of the 1:250 000 Winter Lake map sheet (NTS 86A). It was chosen because it contains multiple subglacial meltwater corridors, meltwater related landforms, unmodified glacial sediments, and has diamond potential. The study area is 144 km^2, centered around an existing exploration camp. The area has low rolling relief, generally not exceeding tens of metres overall. It has many lakes, small ponds, and small areas of shallow organic wetlands. Small outcrops of bedrock are common, though the dominant surficial materials in the area are glacial sediments, the most common of which is till (Kerr et al.,1996).

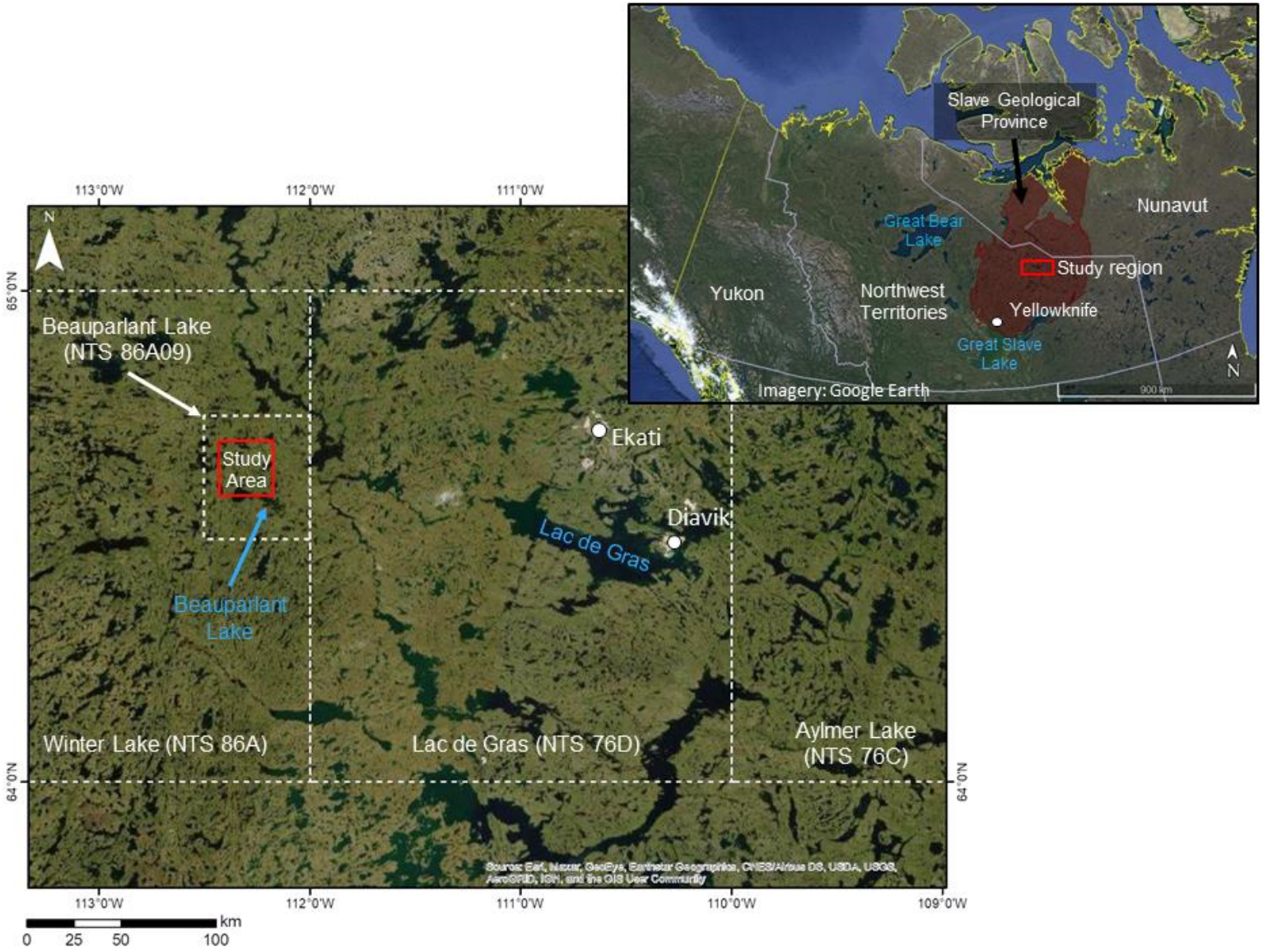

Figure 2.1: Location of mapping area with insert map displaying the region in the Northwest Territories. The study area is highlighted in red and relevant locations and NTS map sheets are included.

2.3. Previous Work

2.3.1. Regional Glacial History

The GSC completed an investigation of the surficial geology and glacial history of the central SGP (Dredge et al., 1994) following the discovery of diamond bearing kimberlites in the early 1990's. As part of this investigation three, 1:125 000 scale surficial geology maps were produced that cover the Winter Lake, Lac de Gras, and Aylmer Lake map sheets (Figure 2.1; Dredge et al., 1995; Kerr et al., 1996; Ward et al., 1997). In this thesis the Winter lake region refers to the Winter Lake map area. Recently larger scale mapping (Haiblen et al., 2018; Sacco et al., 2018) provides detailed surficial geology and glacial history of smaller areas surrounding Lac de Gras. These maps and accompanying reports provide a framework for the interpretation of the regional surficial geology and glacial history.

During the LGM, the LIS covered a significant portion of Canada and parts of the northern United States. The LIS grew in three major sectors: Labrador, Keewatin, and Baffin (Dyke, 2004). The Keewatin Sector covered the Winter Lake region, and the Keewatin ice divide controlled the direction of ice flow (Dalton et al., 2020; Dyke, 2004). During deglaciation, the position of the Keewatin Ice Divide evolved (Dyke and Prest, 1987), and this led to changes in the direction of ice flow in the Winter Lake region. Radiocarbon and terrestrial cosmogenic nuclide ages indicate that the study area deglaciated between 9.5 and 9 ^{14}C ka BP (Dalton et al., 2020; Dyke, 2004).

Alysworth and Shilts (1989) defined four broad landform assemblage zones within the Keewatin Sector of the LIS. The Winter Lake map sheet is within landform assemblage zones three and four, suggesting that the landform assemblage in the area varies between thick drumlinized drift cover with infrequent eskers to areas of thin to minimal drift cover with significant areas of exposed bedrock.

Regional Quaternary geology research identified three main phases of ice flow history in the Central SGP (Figure 2.2) based on striation sequencing and orientation of streamlined macroforms (Dredge et al., 1994). The first phase is oriented towards the southwest, which is followed by flow to the west and then flow to the west-northwest (Dredge et al., 1994). There is evidence of small local deviations in ice flow after this third phase, with flow to

the southwest in the north-eastern portion of the Aylmer Lake map area and flow to the west in the northern portion of the Winter Lake map area (Dredge et al., 1994). The third phase of ice flow is thought to be the dominant ice flow direction in the region in terms of its ability to transport sediments and shape the landscape (Dredge et al., 1994; Ward et al., 1997).

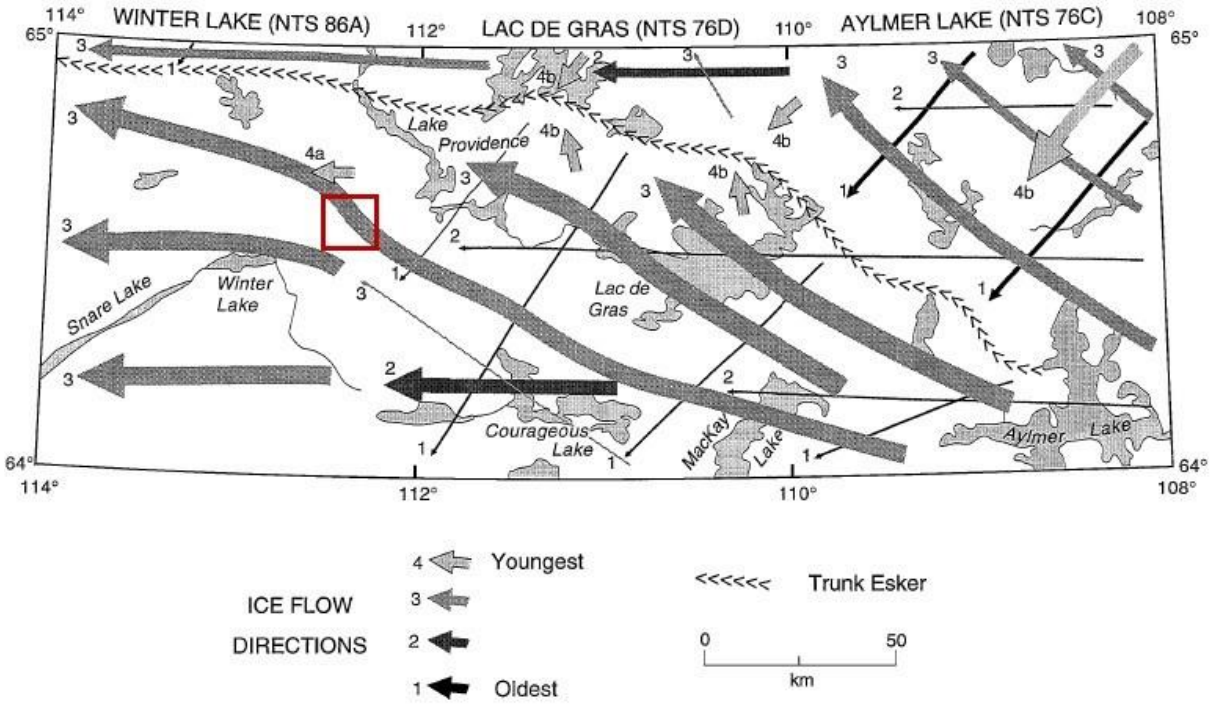

Figure 2.2: Generalized ice flow diagram for the Lac de Gras Region (Dredge et al., 1994), the red box highlights the study area. Flow directions are numbered and the thickness of each arrow denotes the relative effect of the flow on sediment transport and landscape modification.

2.3.2. Subglacial Meltwater Corridors

Subglacial meltwater corridors are elongated, sublinear geomorphic features that contain sediment and landform assemblages resulting from meltwater erosion and deposition by meltwater in subglacial environments. Erosion and reworking by meltwater have been observed worldwide in a wide range of glaciated environments (e.g, Peterson and Johnson, 2018; Peterson et al., 2018; Rampton, 2000; St Onge, 1984) and subglacial meltwater corridors are common in the SGP (Dredge et al., 1985; Dredge et al., 1995; Haiblen, 2016; Kerr et al., 1996; Kerr et al., 2014a; Kerr et al., 2014b; Knight, 2018; Sacco et al., 2018; St Onge and Kerr, 2014; Ward et al., 1997). These features have also been

observed in southern Sweden, where subglacial meltwater corridors are referred to as tunnel valleys or hummock corridors (Ojala et al., 2019; Peterson and Johnson, 2018; Peterson et al., 2018).

Subglacial meltwater corridors include areas of glaciofluvial material occurring as veneers of sand and gravel, boulder concentrations, reworked till and scoured bedrock. Landforms including eskers, deltas, and hummocks are common. Hummocks and mounds have been found within subglacial meltwater corridors in many of the locations where these corridors are described (Campbell et al., 2013; Dahlgren, 2013; Dredge et al., 1995; Haiblen, 2016; McMartin et al., 2020; Rampton, 2000; Rampton and Sharpe, 2014; Sacco et al., 2018; Utting et al., 2009; Ward et al., 1997). In older literature these hummocks are mapped as kames and ribbed moraines (Aylsworth and Shilts, 1989; Dredge et al., 1995; Kerr et al., 1996; Ward et al., 1997). These hummock landforms were targeted for investigation to better understand their genesis.

There are multiple hypotheses regarding the formation of subglacial meltwater corridors. One hypothesis is that subglacial meltwater corridors formed from outburst floods associated with the drainage of large subglacial lakes (Rampton, 2000). Corridors formed when multiple sustained pulses of high energy, subglacial meltwater travelled long distances across the SGP at the ice-bed interface (Rampton, 2000). Another hypothesis is that subglacial meltwater corridor formation is a time transgressive process, with relatively short segments of the corridor forming through time as the margin of the LIS retreated (Campbell et al., 2013; St Onge, 1984; Utting et al., 2009). In this hypothesis the source of meltwater is supraglacial with meltwater reaching the ice-bed interface as it approaches the margin (Campbell et al., 2013; St Onge, 1984; Utting et al., 2009). A third hypothesis that combines aspects of both previously mentioned genesis models suggests that subglacial meltwater corridors formed in a time transgressive manner from high energy sheet-type meltwater flows originating supraglacially which evolved into channelized drainage systems (Haiblen, 2016). Regardless of how subglacial meltwater corridors form it is evident that they lead to erosion, reworking and deposition of remobilized surficial sediments (Haiblen, 2016; Rampton, 2000; Utting et al., 2009).

2.3.3. Bedrock Geology

The bedrock geology of the mapping area includes supracrustal units of the Winter Lake Supracrustsal belt and younger igneous plutons (Figure 2.3). Bedrock mapping in the area was completed in the mid to late 90's by the GSC (Hrabi and Grant, 1999; Thompson et al., 1994). The Winter Lake Supracrustal belt is Archean in age and is made up of three main sequences. In the mapping area the oldest in the sequence is the Newbigging formation, a suite of felsic to intermediate volcanic rocks (Hrabi and Grant, 1999). The second sequence includes mafic volcanics of the Snare and Credit formation and turbidite sedimentary rocks of the Itchen formation (Hrabi and Grant, 1999). The youngest in the sequence is made up of conglomerates and related sedimentary rocks of the Sherpa formation that uncomfortably overlie the rocks of the Itchen formation (Hrabi and Grant, 1999). Younger suites of plutonic rocks ranging from granitic to ultramafic in composition formed during and after deformation of the supracrustal units. In the mapping area these plutonic rocks include the Obstruction suite, Starvation suite, Beauparlant suite, Yamba suite, Terminus suite, and other intrusions.

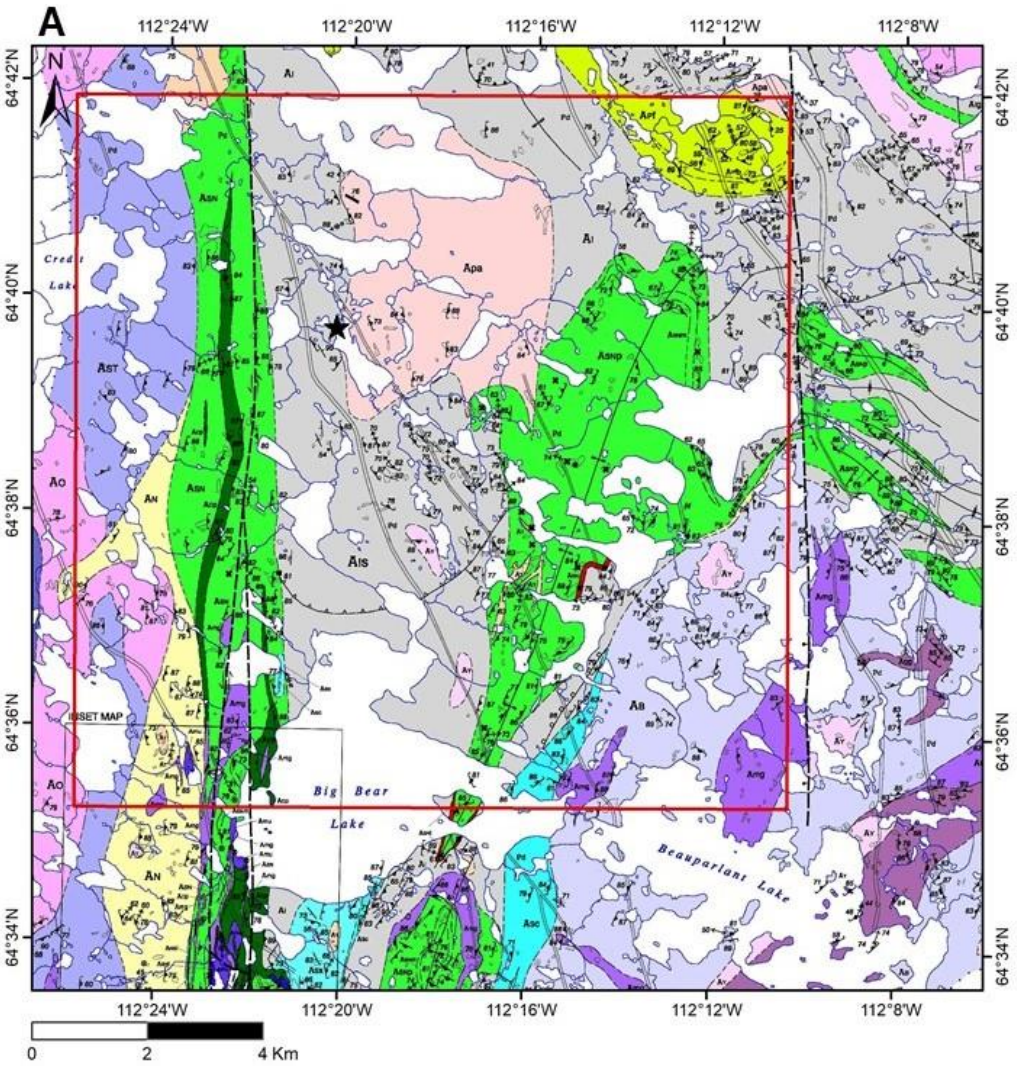
A
N
112°24'W
112°20'W
112°16'W
112°12'W
112°8'W
64°42'N
64°40'N
64°38'N
64°36'N
64°34'N
Credit Lake
Big Bear Lake
Beauparlant Lake
INSET MAP
0
2
4 Km

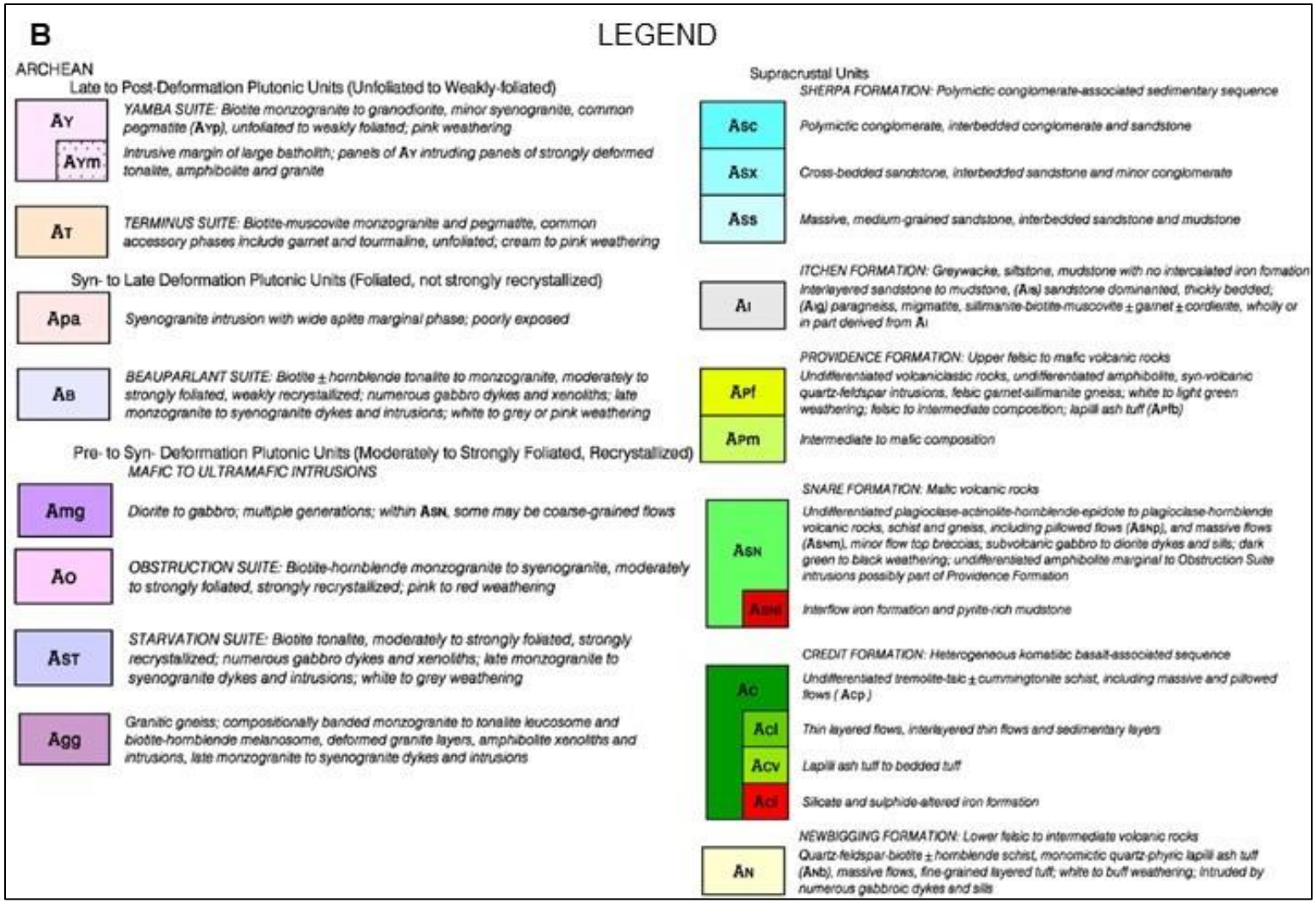

Figure 2.3: A) Bedrock geology of the study area (red box) and the location of our field camp (black star) (modified from Hrabi and Grant, 1999). B) Legend for map displayed in Figure 2.3 A (modified from Hrabi and Grant, 1999).

2.4. Methodology

2.4.1. Field

A field program was completed to characterize and sample surficial materials and measure the orientation of ice-flow indicators. The field program was based from an existing mineral exploration camp located in a central location of the mapping area (Figure 2.3 A). Foot traverses from camp were completed and included stations for ground truthing, mapping, measurement of ice-flow indicators and collection of sediment samples. Helicopter support allowed for a fly over of the entire mapping area to make remote observations from the air, and the collection of samples further from camp. Pits were dug with hand tools and used to characterize the composition of surficial materials, confirm preliminary interpretations, and investigate complex landforms. At sampling sites descriptions of sediment composition, sedimentary structures, clast contents and colour were recorded. General observations of the surface expression and surrounding area were recorded, and photographs of the sediments and surrounding area were taken. Orientation of Ice flow indicators were measured using a compass. The compass view finder was lined up with the trend of striations and the azimuth recorded. Field notes and a table with UTM coordinates of sample locations and descriptions are available in Appendix B.

2.4.2. Mapping

Surficial geology mapping was completed through remote interpretation using digital air photos and the ArcticDEM (Porter et al., 2018) and viewed using three-dimensional (3D) software (Summit Evolution™). A set of 1:35 000 digital air photos of the map area were processed by a photogrammetrist for viewing in 3D. A preliminary draft of surficial geology interpretations was completed at a scale of 1:15 000, and potential field sites were identified. The focus of mapping was delineating the distribution of surficial materials and landforms, and identification of subglacial meltwater corridors for investigation in the field. Following the characterization of sediments in the field the mapping was updated to reflect observations.

This mapping project was completed following surficial mapping standards of the GSC (Deblonde et al., 2018). This standard was modified to include deltas as a distinct

glaciofluvial unit given the observed sediment composition and characteristics in these landforms. Given the scale of mapping the minimum polygon size is ~2 hectares. The primary surficial material accounts for at least 50% of the material in each polygon. Some polygons contained more than one surficial material type; secondary surficial materials are included in the surficial geology label when they occupy between 10 and 50%; they are not included if less than 10%.

The interpretations of the nature, distribution, and genesis of surficial materials in the Beauparlant Lake area is limited by the quality, resolution, and coverage of the available digital air photos used to complete this mapping project. The air photos were taken in 1954, are black and white and in some photos, there is partial cloud coverage. These air photos also do not provide stereo viewing in all areas as they are a compilation of two sets of air photos flown at different times. This means that interpretations are more approximate in a thin section along the middle of the map area in areas of poor photo overlay.

2.5. Surficial Materials and Landforms

Each mapping unit is defined below, including generalized descriptions of each surficial material type, their associated surface expressions and any significant geomorphic processes affecting the unit. Distinguishing characteristics of each mapping unit are specified, and examples provided. Landforms identified on the map are also defined and described. Definitions of the surface expressions used in the mapping area are provided in Table 2.1.

Table 2.1: Definitions of observed surface expressions, providing context for the mapping unit descriptions in the following sections.

Surface Expression	Definition
Veneer (v)	A thin layer of material <2m thick, that does not cover underlying surface irregularities and conforms to underlying topography.
Blanket (b)	A layer of material >2m thick, enough to cover underlying surface irregularities while still conforming to underlying topography; outcrops of bedrock are rare.
Plain (p)	A planar surface of variable thickness, creating an expression that does not conform to the underlying topography. The level surface is a function of material genesis.

Delta (d)	A constructional form resembling a fan >2 m thick, transported by meltwater and deposited in a glacial lake, typically consists of flat (topset) and sloping (foreset) beds.
Hummocks (h)	Groups of mounds of variable height with rounded, sometimes elongated tops, typically associated with subglacial meltwater systems.
Esker (r)	Ridged sediments of variable thickness deposited subglacially, englacially, or supraglacially by meltwater.
Ice-contact (c)	Complexes of hummocks and discontinuous ridged sediments of variable thickness deposited in association with glacial ice.

2.5.1. Organics (Ov)

Organic deposits and consist of plant material in varying stages of decomposition. In general, decomposing organic deposits are dark grey to black in colour, commonly develop over silt and clay and contain plant materials including grasses, sedges, and lichens (Figure 2.4). Organics are commonly very wet and have poor cohesion. They commonly occur in low lying wet areas. It is common for the active layer to be thin in these areas, and therefore, frozen organic material is encountered in the shallow subsurface. Organics are found exclusively as veneers in the area and commonly found as secondary materials with glaciolacustrine sediments and till. In some areas, the organic veneers are found overlying till or glaciolacustrine sediments.

Figure 2.4: Organic materials A) Aerial view of organic veneer proximal to a lake. B) A pit in organic deposit; groundwater is commonly encountered. C) A pit with organics overlying silty sediments and groundwater table near surface. D) A wetland area containing tuffs of organics.

2.5.2. Alluvial sediments (Ap)

Alluvial sediments are uncommon in the mapping area and at the scale of mapping difficult to identify. Upon investigation in the field, active fluvial systems transporting and depositing sediments were identified. Alluvial sediments are mainly composed of sands and gravels and contain concentrations of cobbles and boulders. Many of these larger boulders may not have been transported by water in fluvial systems, rather some of these clasts form a lag at the surface of the alluvial sediments (Figure 2.5). These sediments are sorted and stratified. Generally alluvial sediments are sub-rounded to rounded, commonly more rounded than other material types. Alluvial sediments occur as plains in the mapping area, are always proximal to an active river channel and found spatially associated with glaciofluvial materials.

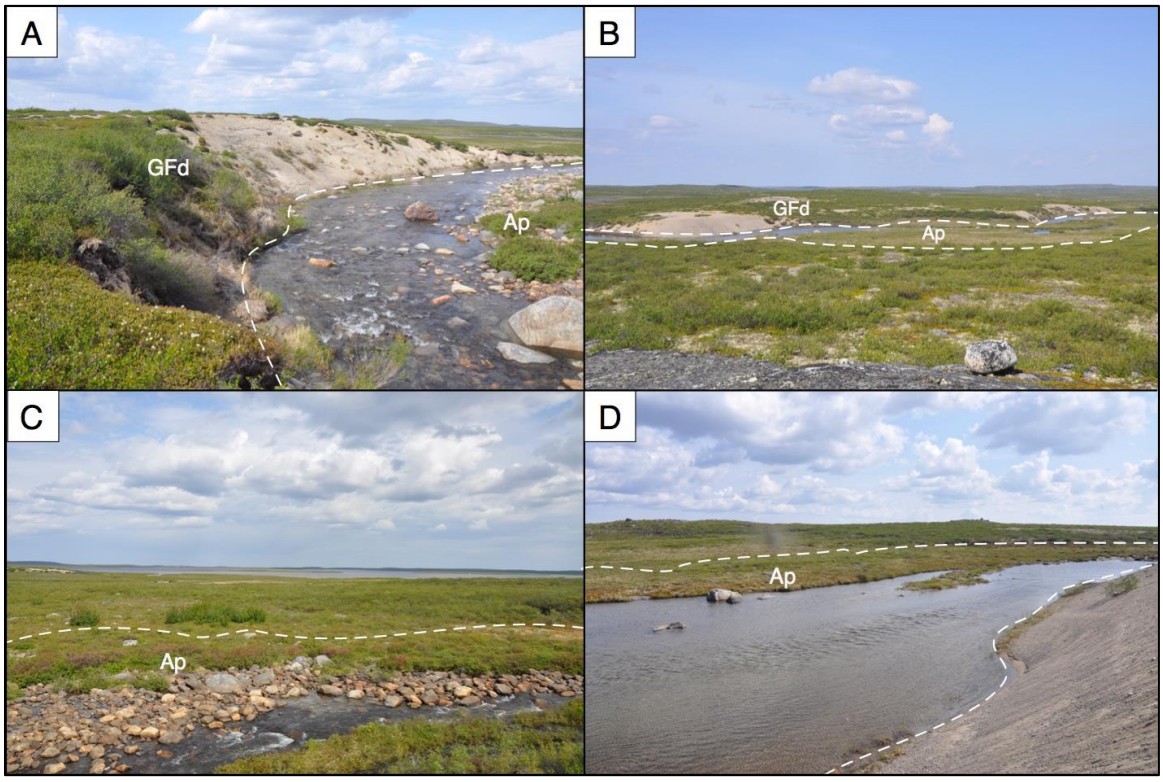

Figure 2.5: Alluvial sediments. A) Active river channel and associated alluvial plain, cutting into a glacifluvial delta. B) Active river channel and associated alluvial plain. C) Concentrated lag of boulders. D) Active river channel cutting into glaciofluvial materials.

2.5.3. Glaciolacustrine Sediments (GLv, GLp)

Glaciolacustrine materials represent sediments deposited into glacial lakes and are uncommon in the area. They occur as plains and veneers. Glaciolacustrine sediments generally range from clay to fine sand with rare clasts; silt is the dominant grain size. These deposits are found proximal to lakes at elevations near that of present lake levels or on islands within lakes.

2.5.4. Glaciofluvial sediments (GFv, GFh, GFc, GFr, GFd)

Glaciofluvial sediments are most commonly observed in extensive linear zones that trend northwest – southeast across the map. Generally, these linear zones include discontinuous esker segments. The linear distribution of glaciofluvial sediments in the area

aid in the delineation of subglacial meltwater corridors. Glaciofluvial sediments are generally stratified sands and gravels with traces of silt (Figure 2.6 A & B). They are commonly sorted and particles are sub-angular to rounded, generally more rounded than clasts in other material types.

The most common surface expression of glaciofluvial sediments is veneers. They are usually found proximal to esker ridges as well as in association with outcrops of bedrock. Other expressions of glaciofluvial materials include ridges, ice contact esker and hummock complexes and deltas (Figure 2.6 C & D). Deltas were interpreted based on the observation of topset and foreset beds and identified as glaciofluvial materials as they are composed of sand and gravels. Some glaciofluvial materials contain ice wedge polygons, which are denoted on the map with the patterned ground overlay or the patterned ground on-site symbol.

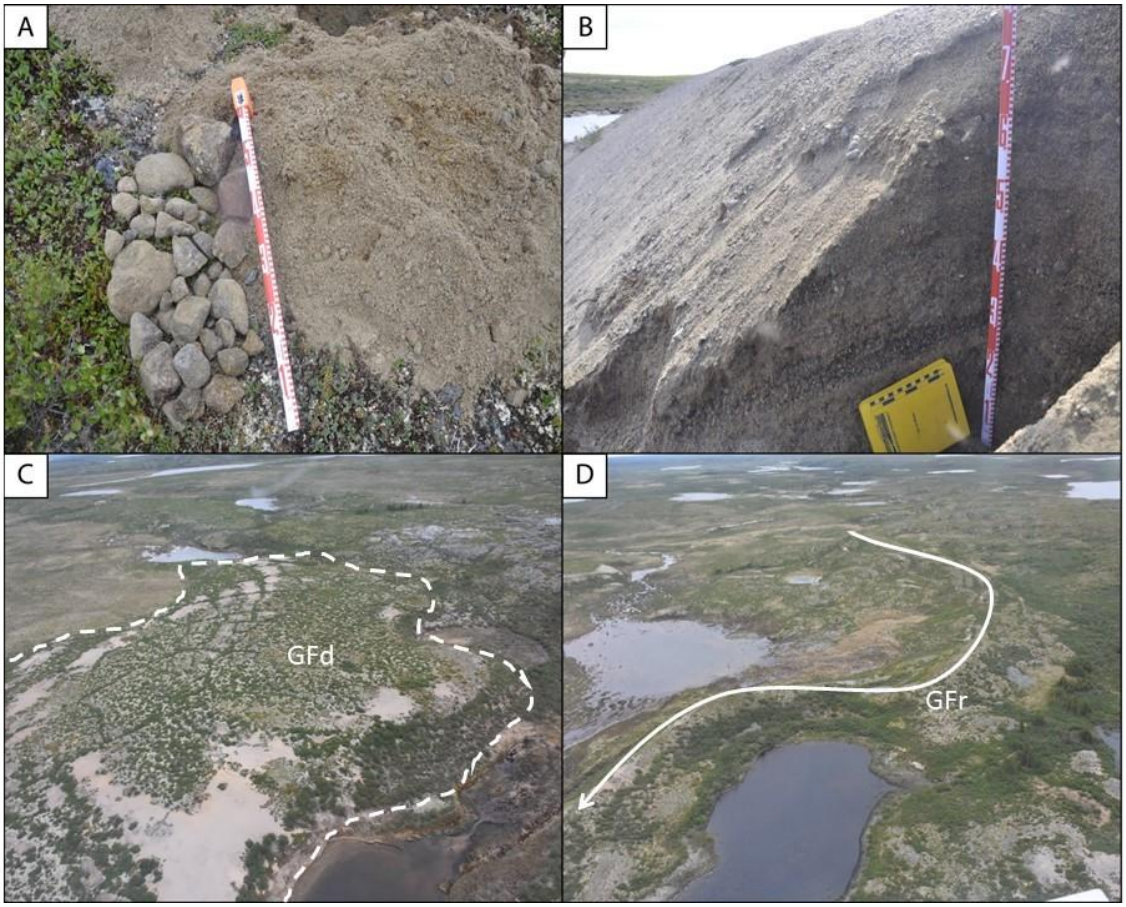

Figure 2.6: Glaciofluvial materials. A) Glaciofluvial sediments dominated by sands and containing pebbles and cobbles. B) Glaciofluvial delta with dipping beds. Material is dominantly sand and gravel. C) Aerial photo of a glaciofluvial delta with ice wedge polygons (dark lines). D) Aerial photo of an esker ridge and surrounding glaciofluvial veneers.

Glaciofluvial Hummocks (GFh)

Glaciofluvial hummocks and their related sediments occur within subglacial meltwater corridors (Figure 2.7). The material in these areas range in grain size distribution from sand and gravel to sandy diamicton (Figure 2.8). Generally, the hummock sediments are dominated by sand and contain less silt and clay than till in the area. They contain a large portion of clasts which are variable in terms of both shape and roundness. Generally, clasts make up ~30% of the material, range from angular to sub-rounded and blocky to tabular in shape. Mound-related sediments usually lack in either fine matrix (silt and clay) or specific ranges of clast sizes such as granules. Hummocks commonly have a pebble and cobble lag and concentration of sub-angular to angular boulders at their surface. In

the area between individual hummocks the material ranges between sandy diamicton and glaciofluvial sands.

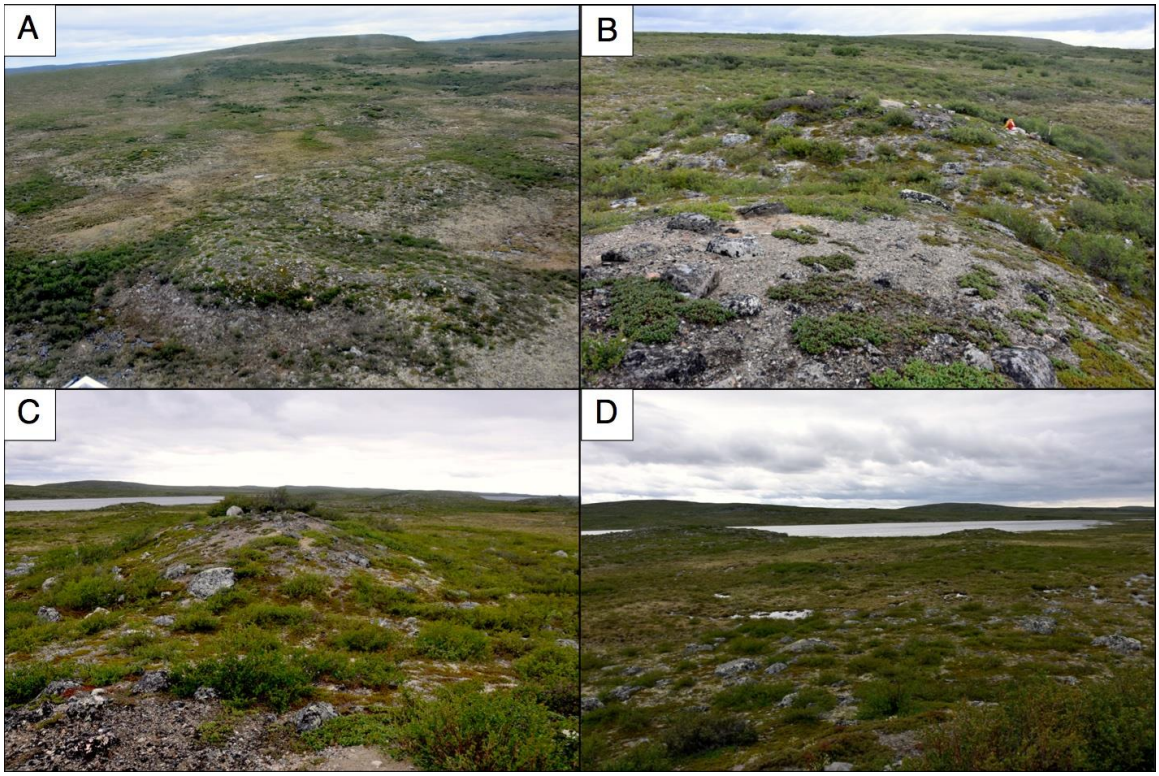

Figure 2.7: Glaciofluvial hummocks. A) A group of glaciofluvial hummocks viewed from the air. B) Two glaciofluvial hummocks with an elongated footprint, person for scale. Boulders are commonly concentrated on the surface of the hummocks. C) A glaciofluvial hummock with a round horizontal footprint. D) Overview of a sampling transect containing multiple glaciofluvial hummocks of various shapes and sizes.

Figure 2.8: Glaciofluvial hummock sampling and grain size investigation. A) Sampling site. B) Glaciofluvial hummock displaying weakly stratified sandy nature of the sediment. C) Glaciofluvial hummock displaying the sandy diamicton with in situ boulders and cobbles.

2.5.5. Till (Tv, Tb)

Till is the most common surficial material. Till described in this project is consistent with the definition of Dreimanis (1989) as there is no evidence that these sediments have been transported, deposited, or sorted by water. It is interpreted that the majority of till in the study area is subglacial.

Till generally occurs as a silty sand matrix supported diamicton. Although variable, till matrix is dominantly silty and sandy and contains ~25% sub angular to sub-rounded clasts ranging from pebbles to boulders (Figure 2.9 C & D). Pebbles are the most abundant clast size. The matrix commonly displays a vesicular texture colloquially known as “aerobar” texture. It is speculated that this texture is the result of freeze thaw processes. The active

layer is being constantly cryoturbated so classic traits such as fissility and over consolidation were not observed.

Till is expressed as blankets and veneers and uncommonly as streamlined crag and tail features. Veneers are the most common primary surficial material unit on the map. An important distinguishing feature used to differentiate between till blankets and veneers is the presence of frost boils, which are very common in till blankets and less commonly in veneers (Figure 2.9 A & B). Another important characteristic in differentiating between till blankets and veneers is whether the bedrock topography and structure are visible in stereo imagery. It is common for till veneers to contain small patches of bedrock outcrops or be proximal to larger bedrock outcrops. Till can be reworked by meltwater or wave action as denoted by the reworked overlay; these instances commonly coincide with the presence of meltwater channels or subglacial meltwater corridors. Ice wedge polygons are rare and found in sandier till. They are denoted using the patterned ground on-site symbol.

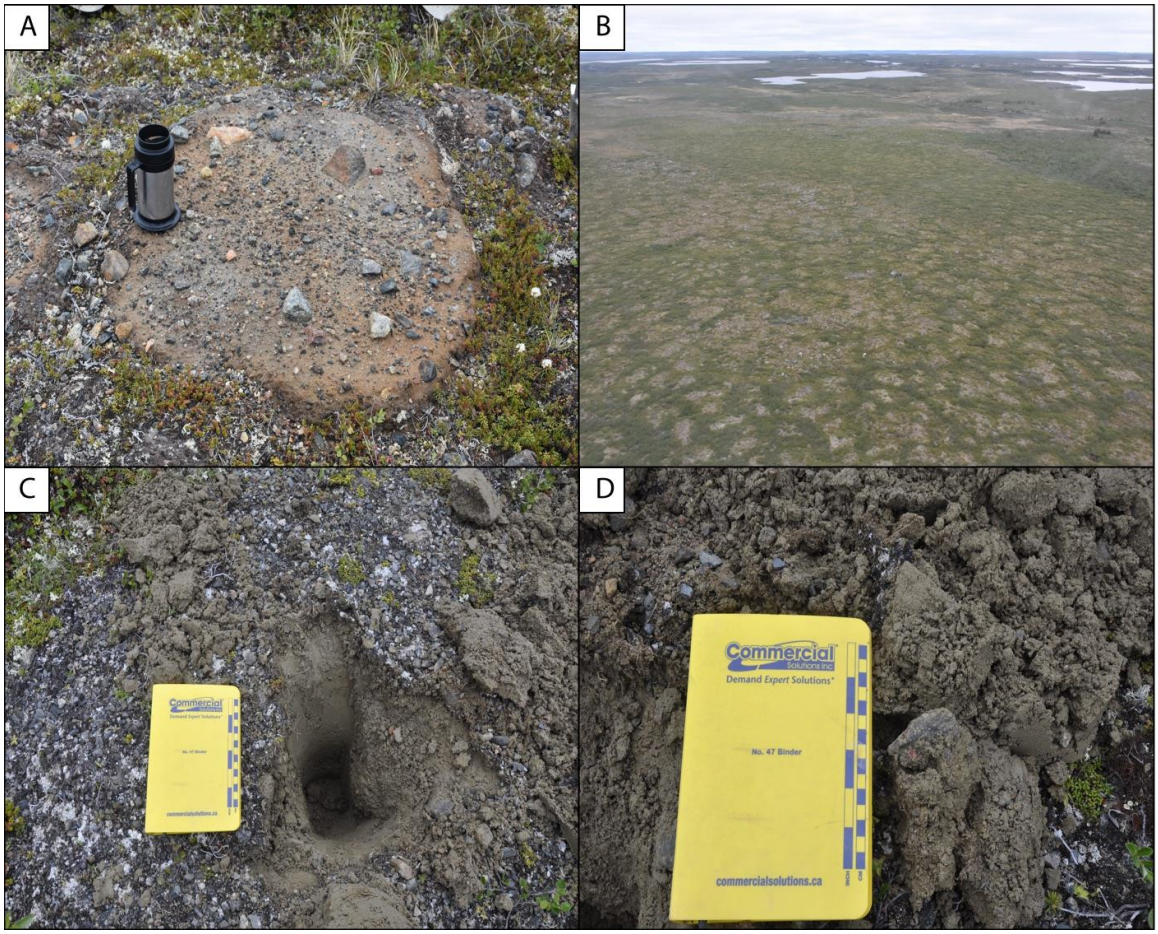

Figure 2.9: Till. A) An active frost boil in a till blanket. B) Aerial photo of a till blanket, displaying characteristic frost boiling pattern. C) Small pit dug from an inactive frost boil, material is silty diamicton with granules and pebbles concentrated on the surface. D) Till collected for analysis showing a silty diamicton containing pebbles.

2.5.6. Bedrock (R)

Bedrock in the mapping area is not commonly the primary surficial material; it is common as a secondary surficial material in areas dominated by both till and glaciofluvial material. In accordance with GSC standards, surface expression was not included for bedrock polygons. However, the most common expressions of bedrock observed in the area are ridges and hummocks. Bedrock ridges commonly represent large mafic dyke systems, they are resistant to erosion. Bedrock hummocks likely represent the highest knobs of the uneven bedrock surface in the area. (Figure 2.10). Bedrock is not differentiated by lithology on the map as most bedrock outcrops were identified using remote sensing methods and not investigated during the field program.

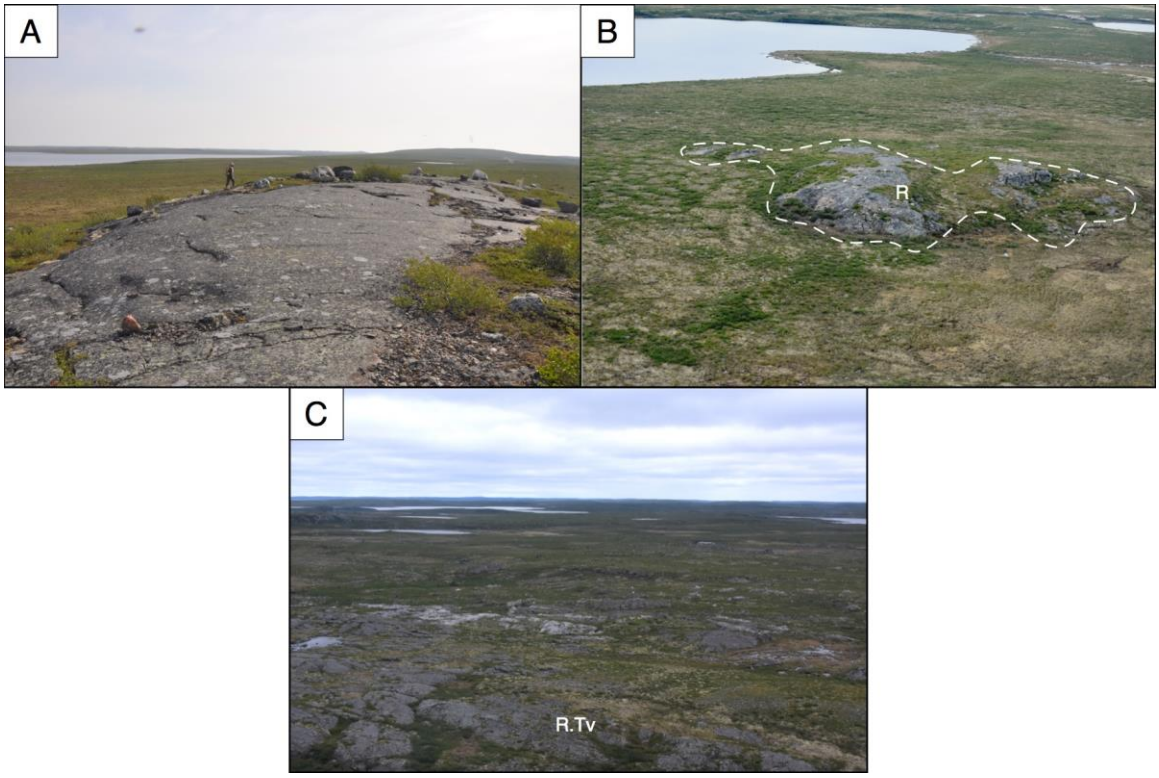

Figure 2.10: Bedrock. A) Glacially smoothed bedrock outcrop investigated for striations. B) An aerial view of a bedrock outcrop surrounded by till blankets and veneers. C) Aerial view of bedrock with lessor amounts of till veneers.

2.6. Landforms

The following sections consist of tables that include the symbology and descriptions of linear features (Table 2.2), point features (Table 2.3), and geomorphic processes (Table 2.4) observed in the mapping area and included on the surficial geology map (Appendix A).

2.6.1. Linear Features

Table 2.2: Linear Geomorphic features observed in the mapping area.

Esker ridges	An esker is a ridge of stratified glaciofluvial sediments with steep sides and can have a sharp, rounded or flattened top. Eskers are commonly deposited subglacially in meltwater channels that ablate up into the ice rather than down into the substrate. Esker ridges are found within subglacial meltwater corridors; the direction of the arrows on the esker ridge symbol denotes the paleo-flow direction of meltwater that formed the esker.
Beach Crest	Beach crests represent the interface between water and land at a single point in geological time. This symbol is utilized to mark the location of paleo-shorelines. Beach crests are best developed in glaciofluvial material, usually eskers, proximal to current lakes and represent higher than present lake levels.
Meltwater Channels	Meltwater channels are identified as areas where glacial meltwater has eroded surficial material forming a channel. They form both subglacially and subaerially. The arrow indicates the paleo-flow direction. Meltwater channels are commonly found leading into the margin of subglacial meltwater corridors or within the corridors. Meltwater channels are found in glaciofluvial material, bedrock and infrequently in till.

Subglacial Meltwater Corridor Margins 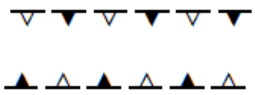	Subglacial meltwater corridor margins represent the approximate boundary between surficial materials affected by subglacial meltwater flow and those that are not. The location of these features is approximate with many boundaries gradational over tens of metres. These corridors are distinguished by their rough microtopography in the digital elevation model, glaciofluvial materials, meltwater associated landforms, bedrock stripped of surficial material, and the presence of many small ponds.
Crag and Tail	A crag and tail is made up of streamlined glacial sediments on the leeside of a small bedrock knob. The streamlined sediments taper away from the bedrock in the direction of ice flow. crag and tails are relatively common and are made up of till.

2.6.2. Point Features

Table 2.3: Geomorphic point features observed in the mapping area.

Hummock 	This onsite symbol denotes a single glaciofluvial hummock. Features denoted as glaciofluvial hummocks are thought to have formed subglacially by meltwater.
Small outcrops 	The small outcrop symbol represents exposed bedrock that is too small to be a separate polygon. This symbol is used in thicker surficial material, such as till blanket, where exposed bedrock may not be expected. These locations are useful for detailed bedrock mapping and measuring ice flow indicators.

Striation measurements	Striation measurement symbols represent a location where a striation was measured. The directionality of the symbol denotes the trend of the striation at that location.
	
Patterned ground	The patterned ground symbol denotes a small area of ice-wedge polygons. This symbol is used when only a portion of the polygon has ice-wedge polygons. If the entire polygon has an ice-wedge polygon expression the extensive patterned ground overlay is used.
	

2.7. Geomorphic Processes

Table 2.4: Geomorphic processes observed in the mapping area.

Patterned ground, extensive	The patterned ground overlay is used to denote when the entirety of a polygon contains ice-wedge polygons. Extensive patterned ground is typically associated with glaciofluvial, glaciolacustrine and organic deposits. Glaciofluvial deltas commonly have extensive patterned ground.
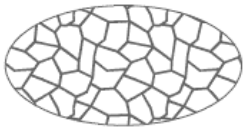	
Reworked by meltwater	The reworked by meltwater overlay is used to signify when the entirety of a till polygon has been reworked by meltwater or modern drainage. This commonly results in the loss of fine-grained matrix, sometimes resulting in a gravel lag or discontinuous sorted deposits. Till reworked by meltwater is commonly found in subglacial meltwater corridors and low-lying areas surrounding lakes outside of meltwater corridors.
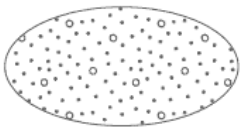	

2.8. Distribution of Mapped Surficial materials

The distribution of surficial materials in the Beauparlant Lake area (Appendix A) has been broken down into percentage of total mapping area covered, based on primary surficial materials. Percentages of primary surficial materials are compared to the previous mapping at 1:125:000 scale. (Table 2.5).

Table 2.5: The area of the map covered by each primary surficial material. The third column shows the distribution of primary surficial materials as interpreted from the Winter Lake mapping (Kerr et al., 1996)

Surficial Material	Percentage of Map Area	Previous Mapping (Kerr et al., 1996)
Till	66.5	76
Glaciofluvial	21.3	9.8
Organics	7.5	1
Bedrock	2.8	12.8
Glaciolacustrine	1.3	0
Alluvial	0.6	0.4

Till is the dominant surficial material in the mapping area and is expressed as blankets and veneers, with veneers being the most common. Till is found extensively throughout the area and accounts for 66.5% of the map, 10% less than previous mapping. Glaciofluvial material makes up 21.3% of the mapping area, an increase of over 10% compared to the previous mapping. Glaciofluvial materials mostly occur within three northwest trending subglacial meltwater corridors and commonly expressed as veneers. Organics account for 7.5% of the mapping area, a significant increase compared to previous mapping. This is likely due to the difference in mapping scale as many of the organic deposits are too small to include at the previous 1: 125 000 scale. Organics occur as veneers and occur in low lying areas, commonly proximal to lakes and ponds. Bedrock makes up 2.8% and occurs within subglacial meltwater corridors and uncommonly as smaller bedrock outcrops throughout the area. This marks a 10% decrease in bedrock compared to previous mapping. This is likely due to differences in the quality of imagery that allowed for more complex surficial geology labels used for this project (i.e, Tv.R). Glaciolacustrine sediments account for 1.3%. Glaciolacustrine material exists as plains

and uncommonly as veneers. Alluvial sediments account for the lowest percentage, making up 0.6% of the total. Alluvial sediments occur as plains and are found connecting lakes with one another and near glaciofluvial sediments.

2.9. Glacial History

2.9.1. Local Ice Flow History

Ice flow indicators were identified in the field and mapped with 3D imagery (Figure 2.11). In the field, bedrock outcrops were investigated at 18 sites, and 22 striation azimuths were measured. Plucked surfaces on the lee side of glacially smoothed and striated bedrock indicated ice flow directionality for some of the observed ice flow indicators. crag and tails were identified from the stereo imagery and ArcticDEM. Ice flow direction of macroforms was interpreted based on the direction of the sediment tails on crag and tail features. Directionality of striations without field indicators were interpreted based on the regional ice flow data (Dredge et al., 1994; Dyke, 2004). Relative ages of some striations could be determined through the preservation of older striations on the lee side of striated bedrock. Others required comparison with regional ice flow history data to interpret the relative ages (Dredge et al., 1994; Dyke, 2004).

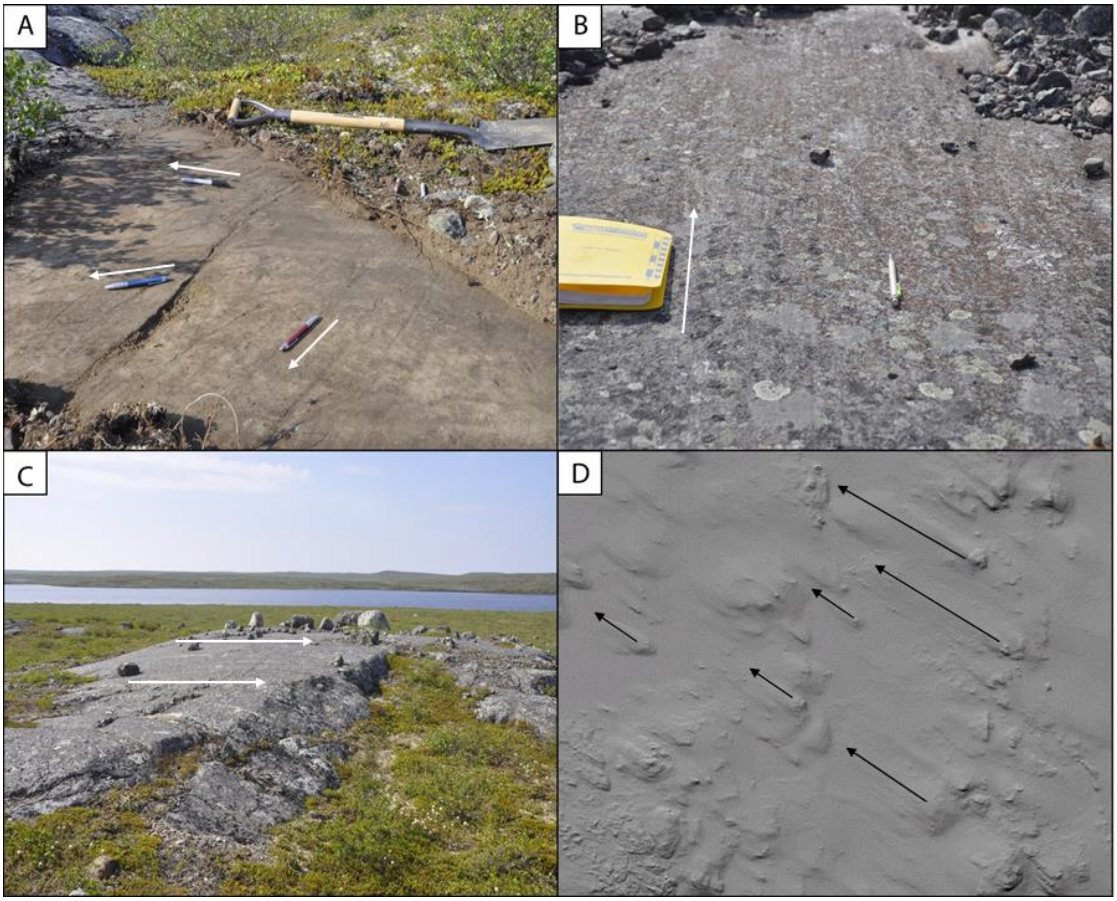

Figure 2.11: Field and remote sensing examples of ice flow indicators. A) Striations on a bedrock surface in mutiple directions. Pens aligned with striation directions. B) Striations in the direction of dominant ice flow. C). A glacially smoothed bedrock outcrop. D) The ArcticDEM (Porter et al., 2018) within mapping area displaying ice flow macroforms. Linear traces are overlain to show directionality of features.

Striation measurements were plotted on a rose diagram to determine the trends in ice flow directions observed in the area (Figure 2.12). Groupings of striations with similar azimuths were interpreted as different phases of ice flow and relative ages for flows with no field indicators were interpreted based on the regional framework (Dredge et al., 1994; Dyke, 2004). An average value was applied to each group to give a generalized direction for each phase of ice flow.

The first ice flow direction recorded in the Beauparlant Lake area is to the southwest. This is followed by a second, stronger ice flow direction to the west-northwest. The third and final ice flow direction is to the northwest and is also the predominate direction of crag and tail landforms.

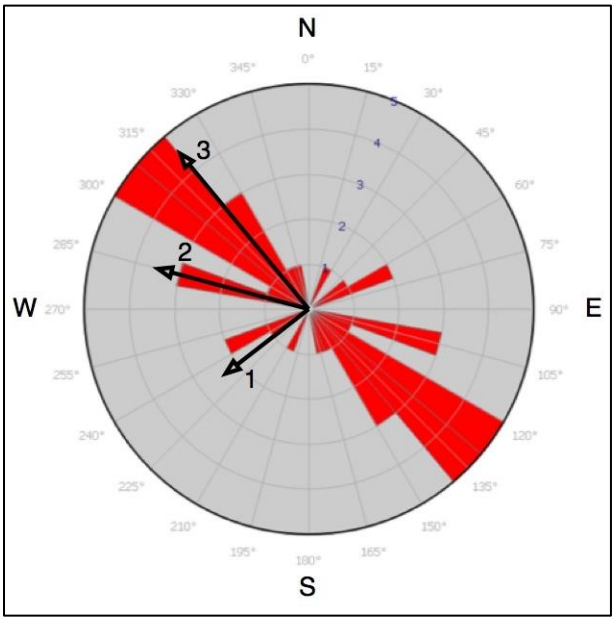

Figure 2.12: A rose diagram of striation orientations. The interpreted average flow directions are overlain on the data and numbered from oldest to youngest (1-3).

The orientation of striations from this project are different than the regional Winter Lake data (Dredge et al., 1994; Figure 2.2). In the regional Winter Lake striation data, the first and second ice flow directions were not observed. However, these earlier phases of ice flow were observed in the Lac de Gras and Aylmer Lake map areas to the east. This suggests that the Winter Lake region may have a more similar ice flow history to the Lac de Gras and Aylmer Lake map areas than previously thought. The observation of these early ice flow indicators suggests that they may exist elsewhere in the Winter Lake region and have yet to be observed.

2.9.2. Depositional History of Glacial Materials

The distribution and genesis of sediments are a function of the glacial history. The local glacial history is of particular importance when considering these sediments for drift prospecting applications. The following section outlines the interpreted depositional history of sediments observed in the study area.

During the advance phase of the Late Wisconsinan glaciation, till began forming at the base of the LIS. This led to the deposition of a widespread layer of till, in the form of

blankets and veneers. Ice flow direction was initially to the southwest, which has been recognized throughout the region (Dredge et al., 1995; Ward et al., 1997). As this flow direction is undated, it is unclear if this represents an early phase of the Late Wisconsinan, or an older glaciation (Dredge et al., 1994). If the former, the intermediate ice flow to the WNW therefore represents a shift in the ice divide axis, as the Keewatin Sector of the LIS evolved during the Late Wisconsinan. The dominant ice flow direction to the northwest is indicated by streamlined bedforms including crag and tails and striations and represents ice flow from the final configuration of the ice divide. During deglaciation, glaciofluvial and glaciolacustrine sediments were deposited. Meltwater was focused in corridors oriented NW, slightly more northward than regional streamlined bedforms, indicating a late-stage change in ice flow direction. Subglacial meltwater eroded till and deposited eskers, hummocks, and veneers of sand and gravel. These corridors are indicated on the map by sublinear assemblages of glaciofluvial deposits, bedrock and discontinuous till deposits that have been modified by meltwater. It is interpreted that meltwater corridor features represent the combined result of episodic meltwater events, occurring in a time-transgressive manner, as the glacier retreated. The following landform relationships indicate that the hummocks formed first and that eskers and flanking glaciofluvial veneers formed after. In some locations eskers crosscut through groupings of glaciofluvial hummocks, with hummocks located on either side of the esker. It is suggested that these landforms could not be preserved proximal to one another if the eskers had formed first. In addition, the high energy turbulent meltwater, interpreted to be required for glaciofluvial hummock formation, would erode away previously emplaced landforms. Some mounds were partially buried by glaciofluvial veneers associated with the eskers.

At the margin of the ice sheet, transient glacial lakes deposited rare glaciolacustrine sediments. However, as these sediments are commonly covered by organic deposits with shallow active layers, more glaciolacustrine deposits could have been missed in the mapping. The relatively common occurrence of shorelines formed in eskers, indicate that many lakes were higher during deglaciation. Holocene deposits are dominantly organics that form in poorly drained areas and rare alluvial deposits in small creeks. Permafrost is ubiquitous and has modified all existing surficial materials to various degrees.

2.10. Applications

The applications of surficial mapping and interpretation of the glacial history range from building our understanding of the Late Wisconsinan glaciation in northern Canada to refining mineral exploration techniques through drift prospecting in the area.

The local glacial history can be fitted into the larger picture of the history of the last glaciation in the SGP. This work adds further data to corroborate the broader history of ice-flow, glacial sediment deposition and landform genesis. The high-resolution mapping completed in the area can be used as a guide for carrying out further drift prospecting by taking into consideration the locations of subglacial meltwater corridors and reworked till. This new mapping can also be used as a reference for re-interpretation of previously completed mineral exploration work in the area.

2.11. Conclusions

The surficial geology and glacial history were interpreted and a 1:15 000 scale surficial geology map was produced, covering a 144 km^2 section of map sheet NTS 86A09. Surficial geology interpretations were based on 3D imagery viewed in Summit Evolution™, the ArcticDEM and sediment characterizations made in the field. Six types of surficial materials were identified in the mapping and occur in a range of surface expressions. In order of most to least prevalent sediments the area consists of till, glaciofluvial, organics, bedrock, glaciolacustrine and alluvium. Linear landforms identified using as on-site symbols include beach crests, eskers, meltwater channels, crag and tails, and subglacial meltwater corridor margins. Landforms identified as point features in the mapping include small bedrock outcrops, glaciofluvial hummocks, patterned ground, and striations.

The glacial history of the mapping area is interpreted through the distribution and genesis of surficial materials and observed ice flow indicators, which generally correlate to regional ice flow records (Dredge et al., 1994). Depositional history was interpreted based on constructive landforms and understanding of glacial and deglacial processes. There were three phases of ice flow in the mapping area, from oldest to youngest: southwest, west-northwest, and northwest. The final flow direction is responsible for the majority of streamlined bedforms, with crag and tails oriented in this direction. It is interpreted that till was deposited throughout the Late Wisconsinan glaciation, followed by the deposition of

glaciofluvial and glaciolacustrine sediments during deglaciation of the area. Finally post glacial sediments including organics and alluvial sediments were and continue to be deposited in the area.

Chapter 3.

Surficial Material Analysis: Granulometry, and Clast Lithology in Subglacial Meltwater Corridors

3.1. Introduction

Drift prospecting in glaciated terrains requires an understanding of the genesis of sampling materials. Subglacial till is an optimal sediment for drift prospecting programs as it is common and widely distributed in glaciated terrains, is derived directly from a bedrock source and transport histories can be interpreted (McClenaghan, 2005; Spirito et al., 2011). Geochemical and mineral anomalies in subglacial till can create large exploration targets as these anomalies are significantly larger than their bedrock source (Levson, 2001). However, the effects of deglacial meltwater processes that may rework and erode till are commonly overlooked or misidentified during exploration programs.

Subglacial meltwater corridors are elongated, sublinear geomorphic features that contain sediment and landform assemblages resulting from meltwater erosion and deposition by meltwater in subglacial environments. Erosion and reworking by meltwater have been observed worldwide in a wide range of glaciated environments (Peterson and Johnson, 2018; Peterson et al., 2018; Rampton, 2000; St Onge, 1984) and subglacial meltwater corridors are common in the SGP (Dredge et al., 1985; Dredge et al., 1995; Haiblen, 2016; Kerr et al., 1996; Kerr et al., 2014a; Kerr et al., 2014b; Knight, 2018; Sacco et al., 2018; St Onge and Kerr, 2014; Ward et al., 1997). These features have also been observed in southern Sweden, where subglacial meltwater corridors are referred to as tunnel valleys or hummock corridors (Ojala et al., 2019; Peterson and Johnson, 2018; Peterson et al., 2018).

The purpose of this chapter is to evaluate the genesis of glaciofluvial hummocks and provide insight for drift prospecting applications. An understanding of the grain size distribution and transport history of sediments in glaciofluvial hummocks will determine if these sediments should be sampled for drift prospecting purposes and how results should be interpreted. Glaciofluvial hummock and subglacial meltwater corridor sediments are described in detail and granulometry compared. Differences in specific grain size-fractions

and overall grain size distributions are evaluated between unmodified till and samples collected from within the meltwater corridor.

Variability of the grain size distributions between observed sediments will lead to insight on the genesis of meltwater related landforms in the corridors. Differences in grain size distributions between till and meltwater corridor sediments is important for drift prospecting as specific grain sizes are processed for indicator mineral picking and analysis.

3.1.1. Subglacial Meltwater Corridors

Subglacial meltwater corridors include areas of glaciofluvial material occurring as veneers of sand and gravel, boulder concentrations, reworked till and exposed bedrock. Landforms including eskers, deltas and hummocks are common. Hummocks and mounds have been found within subglacial meltwater corridors in many of the locations where these corridors are described (Campbell et al., 2013; Dahlgren, 2013; Dredge et al., 1995; Haiblen, 2016; McMartin et al., 2020; Rampton, 2000; Rampton and Sharpe, 2014; Sacco et al., 2018; Utting et al., 2009; Ward et al., 1997). In older literature these hummocks are mapped as kames and ribbed moraines (Aylsworth and Shilts, 1989; Dredge et al., 1995; Kerr et al., 1996; Ward et al., 1997). These hummock landforms were targeted for investigation to better understand their genesis.

There are multiple hypotheses regarding the formation of subglacial meltwater corridors. One hypothesis is that subglacial meltwater corridors formed from outburst floods associated with the drainage of large subglacial lakes (Rampton, 2000). Corridors formed when multiple sustained pulses of high energy, subglacial meltwater travelled long distances across the SGP at the ice-bed interface (Rampton, 2000). Another hypothesis is that subglacial meltwater corridor formation is a time transgressive process, with relatively short segments of the corridor forming through time as the margin of the LIS retreated (Campbell et al., 2013; St Onge, 1984; Utting et al., 2009). In this hypothesis the source of meltwater is supraglacial with meltwater reaching the ice-bed interface as it approaches the margin (Campbell et al., 2013; St Onge, 1984; Utting et al., 2009). A third hypothesis that combines aspects of both previously mentioned genesis models suggests that subglacial meltwater corridors formed in a time transgressive manner from high energy sheet-type meltwater flows originating supraglacially which evolved into channelized drainage systems (Haiblen, 2016). Regardless of how subglacial meltwater

corridors form it is evident that they lead to erosion, reworking and deposition of remobilized surficial sediments (Haiblen, 2016; Rampton, 2000; Utting et al., 2009).

3.1.2. Glaciofluvial Hummocks

There is not a large body of literature regarding the genesis of glaciofluvial hummocks and given their variability in sedimentology and morphology, interpretations of their genesis differ. In Southern Sweden, stratified hummocks containing sediments of differing ages and material type have been interpreted as erosional landforms, formed by subglacial meltwater during the events responsible for tunnel valley formation (Peterson and Johnson, 2018; Peterson et al., 2018). In the Lac de Gras region hummocks of sandy diamicton with infrequent lenses of sorted stratified materials have been interpreted as depositional landforms, formed during a subglacial non-Newtonian flow event associated with the draining of a supraglacial lake (Haiblen, 2016). In the Walker Lake area of Nunavut, glaciofluvial hummocks of stratified sands and gravels that form transverse ridges are interpreted as depositional landforms (Utting et al., 2009). It is interpreted that these hummocks formed because of increased sediment deposition below cavities in channel ceilings during a single, peak flow subglacial meltwater event (Utting et al., 2009).

3.1.3. Setting

The study area is located north of Beauparlant Lake, Northwest Territories. It is in the central SGP, ~260 km northeast of Yellowknife and ~100 km west of Diavik Diamond mine on Lac de Gras (Figure 3.1). It is part of the Beauparlant Lake map sheet (NTS 86A09), located on the western edge of the 1:250 000 Winter Lake map sheet (NTS 86A). It was chosen because it contains multiple subglacial meltwater corridors, meltwater related landforms, unmodified glacial sediments, and has diamond potential. The study area is 144 km^2, centered around an existing exploration camp. The area has low rolling relief, generally not exceeding tens of metres overall. It has many lakes, small ponds, and small areas of shallow organic wetlands. Small outcrops of bedrock are common, though the dominant surficial materials in the area are glacial sediments, the most common of which is till (Kerr et al.,1996)

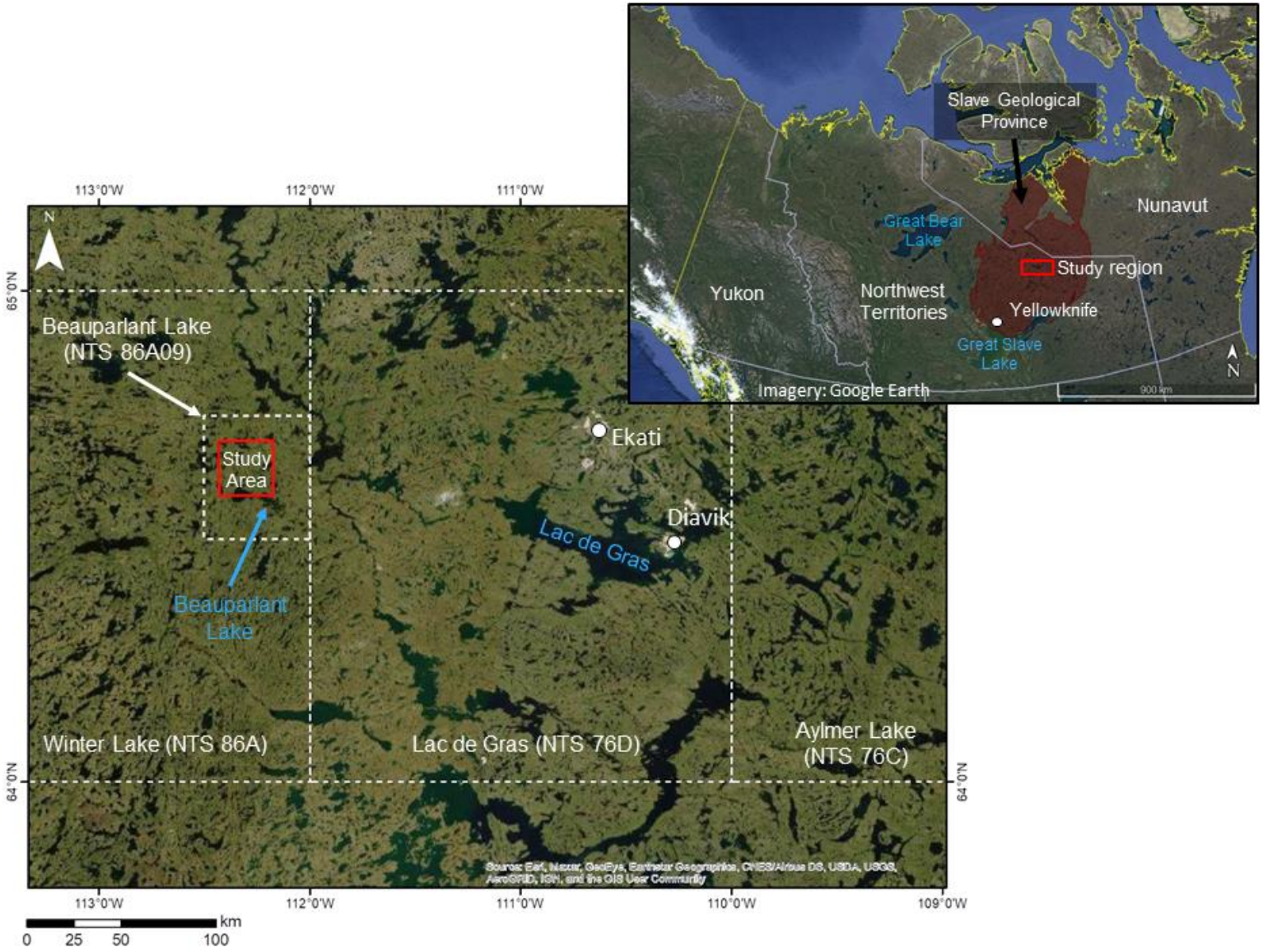

Figure 3.1: Location of the study area with insert map displaying the region in the Northwest Territories. The study area is highlighted in red and relevant locations and NTS map sheets are included.

3.1.4. Regional Glacial History

During the LGM, the LIS covered a significant portion of Canada and parts of the northern United States. The LIS grew in three major sectors: Labrador, Keewatin, and Baffin (Dyke, 2004). The Keewatin Sector covered the Winter Lake region, and the Keewatin ice divide controlled the direction of ice flow (Dalton et al., 2020; Dyke, 2004). During deglaciation, the position of the Keewatin Ice Divide evolved (Dyke and Prest, 1987) and this led to changes in the direction of ice flow in the Winter Lake region. Radiocarbon and terrestrial cosmogenic nuclide ages indicate that the study area deglaciated between 9.5 and 9 ^{14}C ka BP (Dalton et al., 2020; Dyke, 2004).

Alysworth and Shilts (1989) defined four broad landform assemblage zones within the Keewatin Sector of the LIS. The Winter Lake map sheet is within landform assemblage zones three and four, suggesting that the landform assemblage in the area varies between thick drumlinized drift cover with infrequent eskers to areas of thin to minimal drift cover with significant areas of exposed bedrock.

Regional Quaternary geology research identified three main phases of ice flow history in the Central SGP (Figure 3.2) based on striation sequencing and orientation of streamlined macroforms (Dredge et al., 1994). The first phase is oriented towards the southwest, which is followed by flow to the west and then flow to the west-northwest (Dredge et al., 1994). There is evidence of small local deviations in ice flow after this third phase, with flow to the southwest in the north-eastern portion of the Aylmer Lake map area and flow to the west in the northern portion of the Winter Lake map area (Dredge et al., 1994). The third phase of ice flow is thought to be the dominant ice flow direction in the region in terms of its ability to transport sediments and shape the landscape (Dredge et al., 1994; Ward et al., 1997).

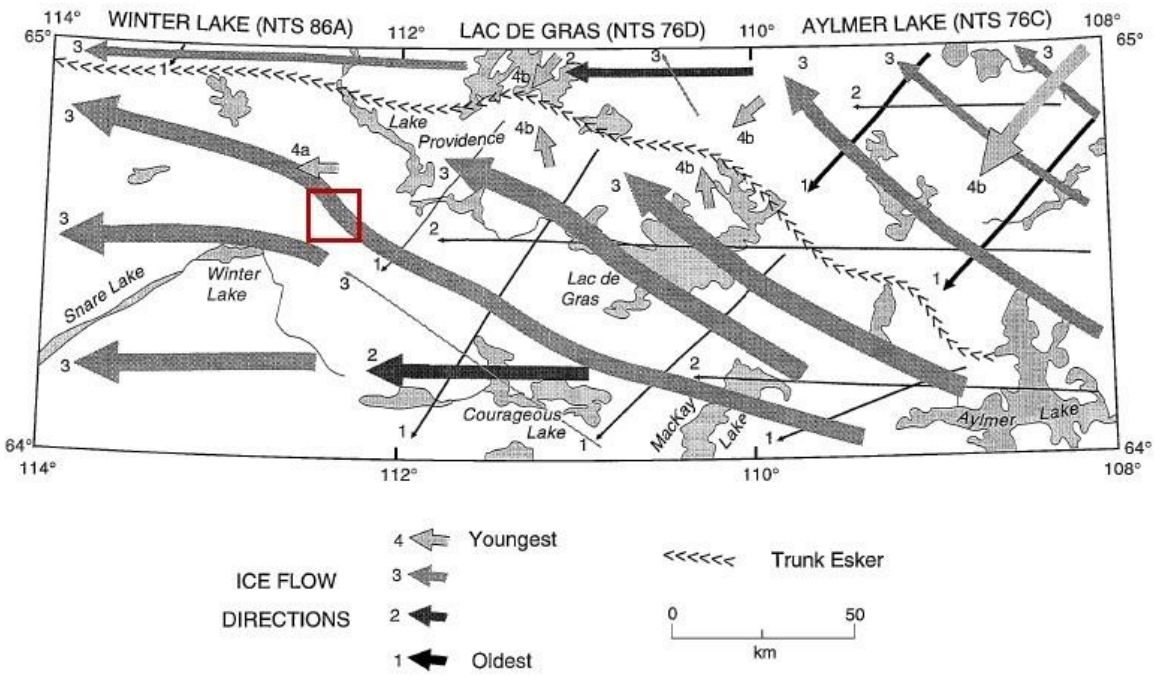

Figure 3.2: Generalized ice flow diagram for the Winter Lake, Lac de Gras, and Aylmer Lake map areas (Dredge et al., 1994). The red box highlights the study area. Flow directions are numbered and the thickness of each arrow denotes the relative effect of the flow on sediment transport and landscape modification.

3.1.5. Bedrock Geology

The bedrock geology of the mapping area includes supracrustal units of the Winter Lake Supracrustsal belt and younger igneous plutons (Figure 3.3). Bedrock mapping was completed in the mid to late 90's by the GSC (Hrabi and Grant, 1999; Thompson et al., 1994). The Winter Lake Supracrustal belt is Archean in age and is made up of three main sequences. The oldest in the sequence is the Newbigging formation, a suite of felsic to intermediate volcanic rocks (Hrabi and Grant, 1999). The second sequence includes mafic volcanics of the Snare and Credit formation and turbidite sedimentary rocks of the Itchen formation (Hrabi and Grant, 1999). The youngest in the sequence is made up of conglomerates and related sedimentary rocks of the Sherpa formation that uncomfortably overlie the rocks of the Itchen formation (Hrabi and Grant, 1999). Younger suites of plutonic rocks ranging from granitic to ultramafic in composition formed during and after deformation of the supracrustal units. These plutonic rocks include the Obstruction suite,

Starvation suite, Beauparlant suite, Yamba suite, Terminus suite, and other intrusions.

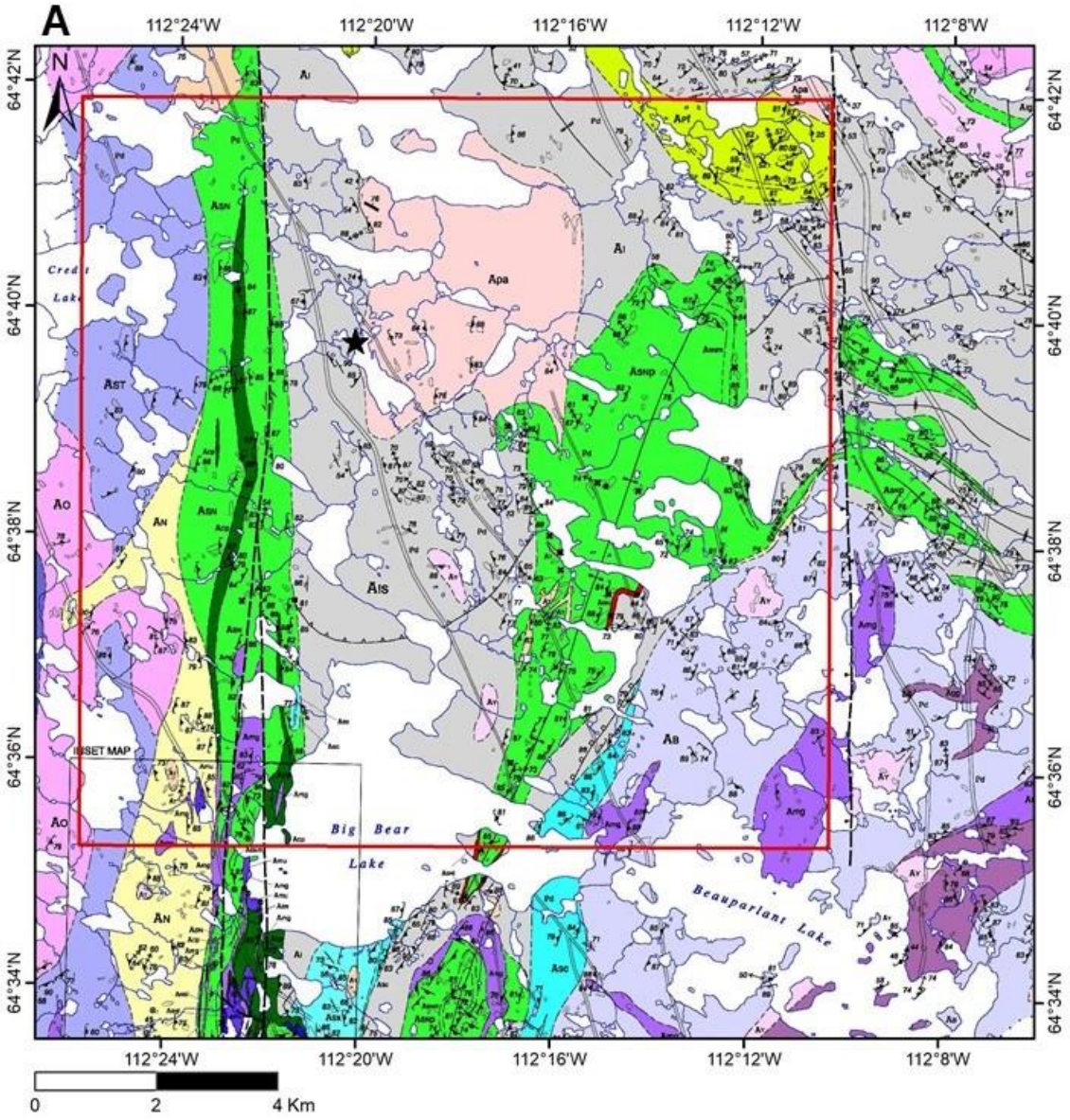

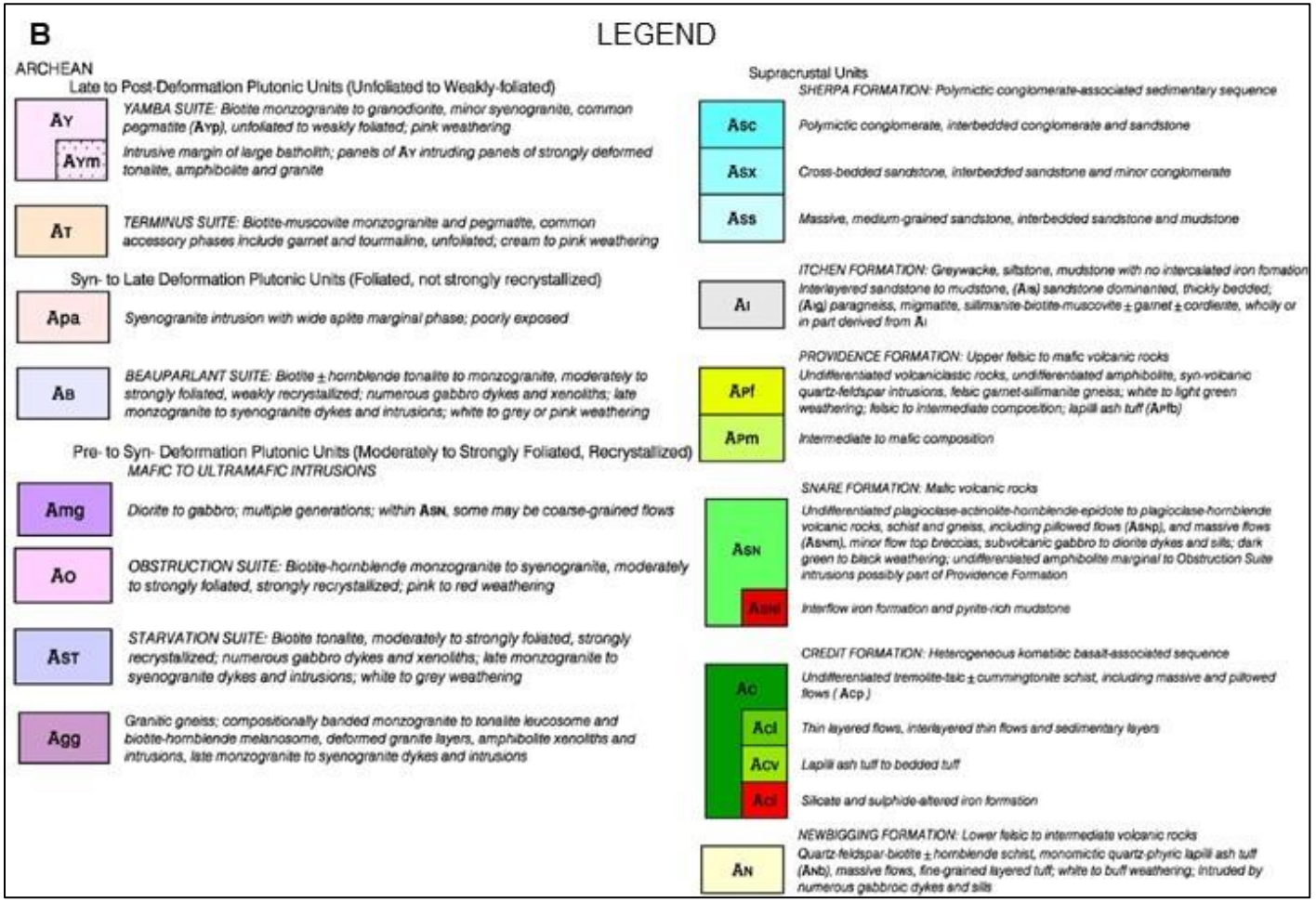

Figure 3.3: A) Bedrock geology of the study area (red box) and the location of field camp (black star) (modified from Hrabi and Grant, 1999). B) Legend for map displayed in Figure 3.3 A (modified from Hrabi and Grant, 1999).

3.2. Methodology

3.2.1. Field Methods

Glacial sediment samples were collected at 46 sites from three discrete areas (transects) (Figure 3.4). The sampling areas were chosen based on the results of preliminary surficial geology mapping. Sampling traverses were planned to transect the contact between unmodified till and modified subglacial meltwater corridor sediments. Samples include unmodified till and sediments collected within subglacial meltwater corridors. Meltwater corridor samples include a range of sediments: reworked till, glaciofluvial sand and gravel and glaciofluvial hummock sediments. Given the focus on glaciofluvial hummocks, samples collected from hummocks have been categorized together. The other meltwater corridor sediment category represents materials ranging from reworked till to glaciofluvial sand and gravel. Sediment descriptions were completed in the field along with other notes regarding general area descriptions. At transects 1 and 2, drone imagery of glaciofluvial hummocks was collected and structure from motion photogrammetry used to create digital elevation models of these features.

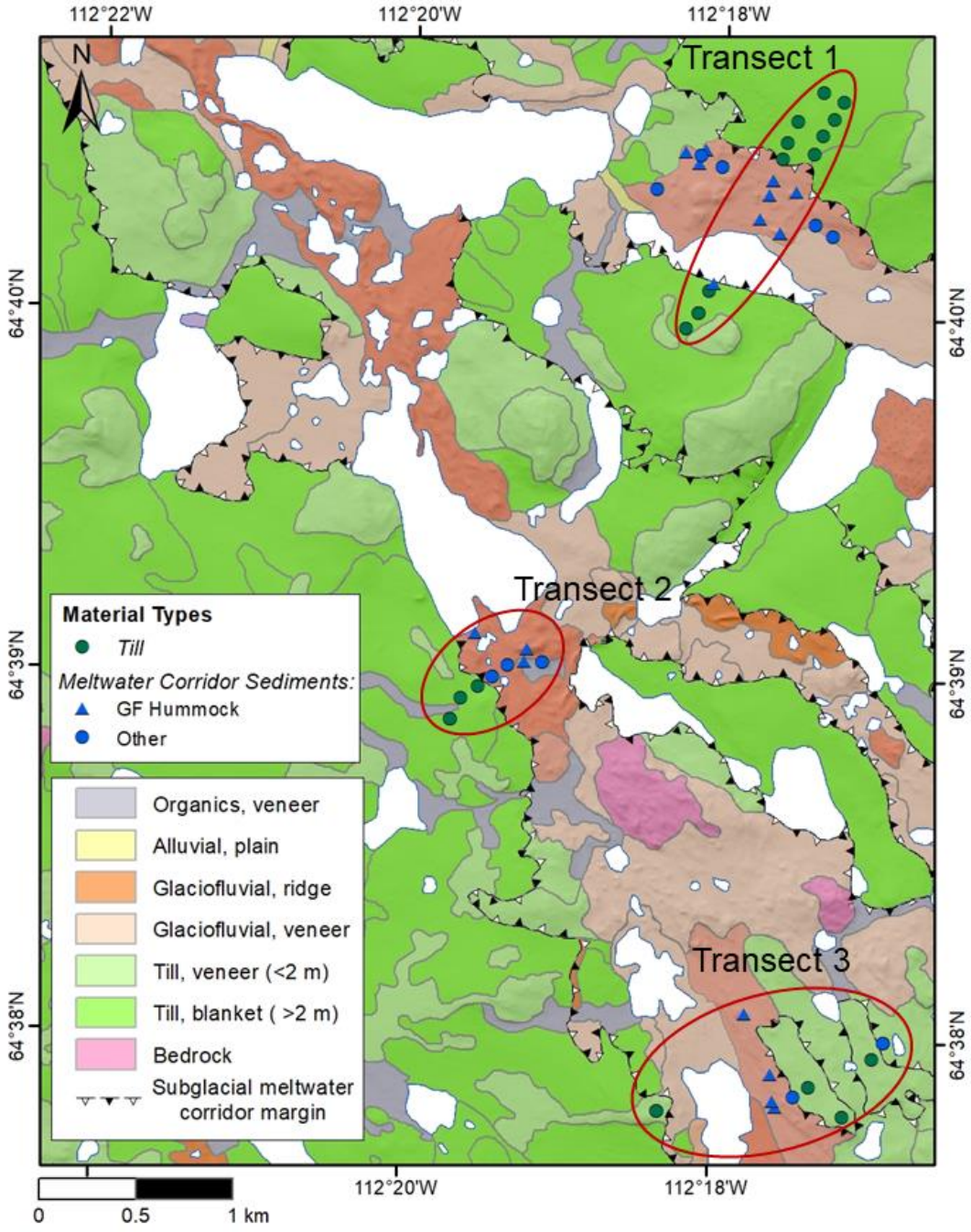

Figure 3.4: Simplified surficial geology overlaying the ArcticDEM of the study area. The location of the three sample transects are highlighted in red.

Each sample transect crosses the margin of a subglacial meltwater corridor from unmodified till into modified corridor sediments, including glaciofluvial hummocks (Figure 3.5). Transect 1 spans the meltwater corridor and includes samples of glaciofluvial

hummocks and unmodified till from each side. Transect 2 spans one side of a meltwater corridor and includes samples of till and a range of reworked meltwater corridor sediments, including three glaciofluvial hummocks. Transect 3 is the most complex, crossing till, glaciofluvial hummocks, other corridor sediments, more unmodified till and then more corridor sediments.

The target sample spacing overall was 100 m, however deviations from this spacing were common due to the distribution of glaciofluvial hummocks and suitable sampling sites, usually active frost boils, in till. Glaciofluvial hummock samples were mainly collected from the tops of individual hummocks. In two instances on large glaciofluvial hummocks along Transect 1 (samples 6, 7 and 15, 16), a second sample from a different location on the hummock was collected. This was completed to determine if there was variability in grain size distribution within individual hummocks. Some samples were taken from lower relief sediments in the corridor, these are indicated as “other” on Figure 3.4.

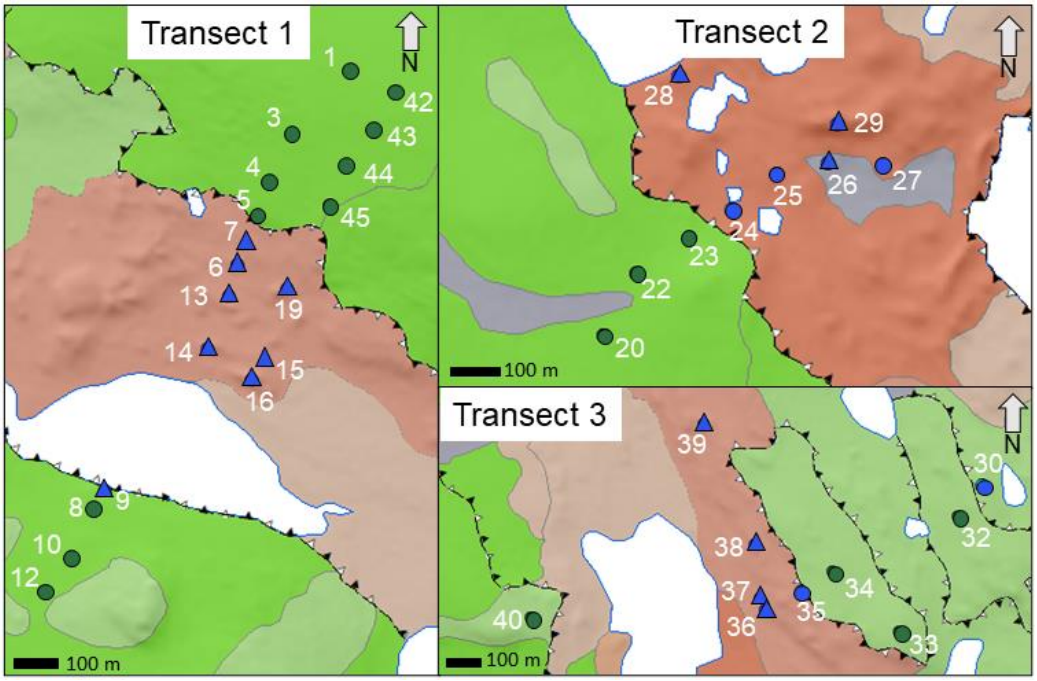

Figure 3.5: Simplified surficial geology maps with transect sample locations, numbers and material type. The legend is consistent with Figure 3.4.

Samples were collected following guidelines set out by the GSC (McClenaghan et al., 2020). At each sampling location, a small hole was dug to between 0.3 to 1 m depth to reach the C-horizon. Sediments were placed in large plastic sample bags. Permafrost activity and cryoturbation in frost boils was targeted when choosing till sampling sites to minimize the pit depth required to reach the C-horizon. At each station three samples were collected: a bulk sample (~10 kg) for KIM and geochemical analysis, a 1 kg sample for grain size analysis and a sample of ≥ 50 pebble sized clasts.

3.2.2. Granulometry

The grain size distribution (Wentworth, 1922) for each sample was determined through a combination of sieving and laser diffraction particle analysis at Simon Fraser University. The mass of sand and granule size-fractions (0.063 - 4 mm) were determined through sieving and compared to the total mass of the sample (<4 mm) to calculate the percentages. Laser diffraction particle analysis was used to determine the proportions of silt and clay (Malvern Instruments, 2007). A sub-sample (~30 g) of silt and clay from each sample was run through a Malvern Mastersizer 2000 to detect the proportion of grain sizes present. The percentage of silt and clay in each sample was then calculated under the assumption that each silt and clay sub-sample is representative of the silt and clay proportions from each 1 kg sample.

Grain size distribution curves were created for each sample using the percentages of each grain size-fraction. Cumulative percentages of specific grain size-fractions are compared amongst samples in each transect to evaluate any differences in composition amongst the samples.

3.2.3. Clast Lithology

Pebble samples were sorted into broad lithological groups (Figure 3.6). The categories used for sorting include: granitoid, meta-volcanic, and meta-sedimentary following the bedrock mapping completed in the region (Hrabi and Grant, 1999; Thompson and Kerswill, 1994). Clasts were sorted based on mineralogy, grain size, cleavage, hardness and the presence of sedimentary structures. The percentage of each lithology type was calculated based on the total number of clasts in the sample. An analysis of clast shape and roundness was assessed as an average value for each sample.

Figure 3.6: An example of a pebble lithology sample (PD19-P47) that has been sorted into the three broad lithology groups. From left to right: granitoids, meta-volcanics and meta-sedimentary.

3.3. Glaciofluvial Hummock Distribution and Composition

Of the 46 samples collected, 18 are from glaciofluvial hummocks. The hummocks are commonly found in groupings of 5 or more individuals of various sizes and shapes and occur exclusively within subglacial meltwater corridors. Observed hummocks ranged in morphology from nearly circular to elongate with multiple rounded tops (Figure 3.7). Elongated hummocks commonly occur as small transverse ridges. Hummocks vary greatly in size, with the smallest observed hummocks having approximately 1 m of relief at its highest point while others were larger with a relief of approximately 4 m. In general, the hummocks observed in the field are composed of a poorly consolidated, matrix supported, sandy diamicton with approximately 15 to 20 % fines (silt and clay). Clasts make up approximately 25-30% of the material and range in size from pebbles to boulders with pebbles being the dominant clast size. Some hummocks are dominated by sand and gravel resembling a material closer to glaciofluvial outwash in composition, these hummocks are commonly found proximal to eskers. Hummock sediments are homogenous, and no stratification was observed. Material between hummocks is similar in composition. Hummocks commonly have a concentration of boulders and pebbles at their surface.

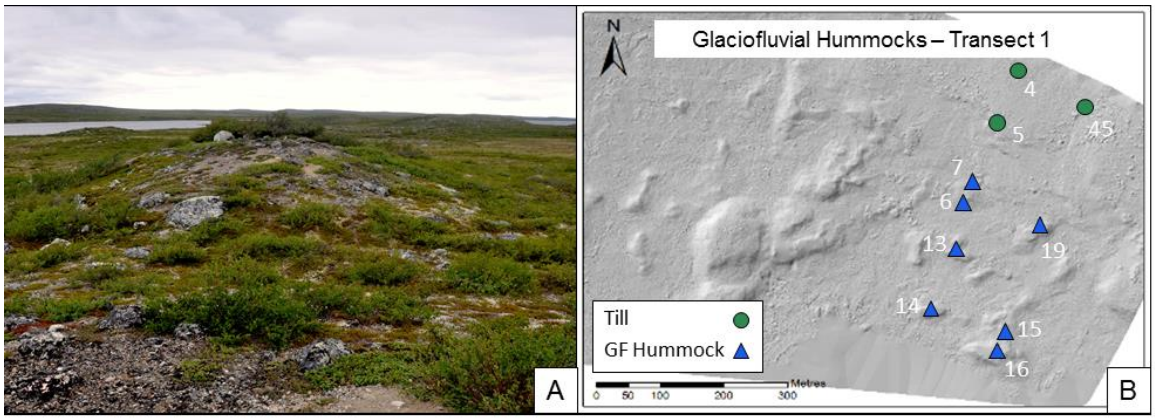

Figure 3.7: Photo of a glaciofluvial hummock (relief is ~2 m), displaying the circular morphology and pebble lag at surface. B) A digital elevation model created from photogrammetry of drone imagery displaying the morphology of glaciofluvial hummocks found in the Transect 1 area.

A large glaciofluvial hummock from Transect 1 had been previously excavated by an animal, creating a hole approximately 80 cm in width and just under 1 m long (Site 19, Figure 3.8). This hole allowed for the examination of the interior sediments of the hummock. This hole was expanded another 60 cm in depth, to reach a total length of 1.6 m, by far the deepest and widest hole dug during the program. The sample collected from this hummock was taken from 1.3 to 1.6 m depth. The sediment at this site is matrix supported and poorly consolidated. The matrix is made up of sand and trace silt. Clasts account for approximately 25% of the material; cobble (6.4 - 25.6 cm) is the most common clast size although the material contains clasts ranging from pebbles to boulders. Clasts are sub-angular to sub-rounded in shape. The material is homogenous and does not display any stratification or sedimentary structures.

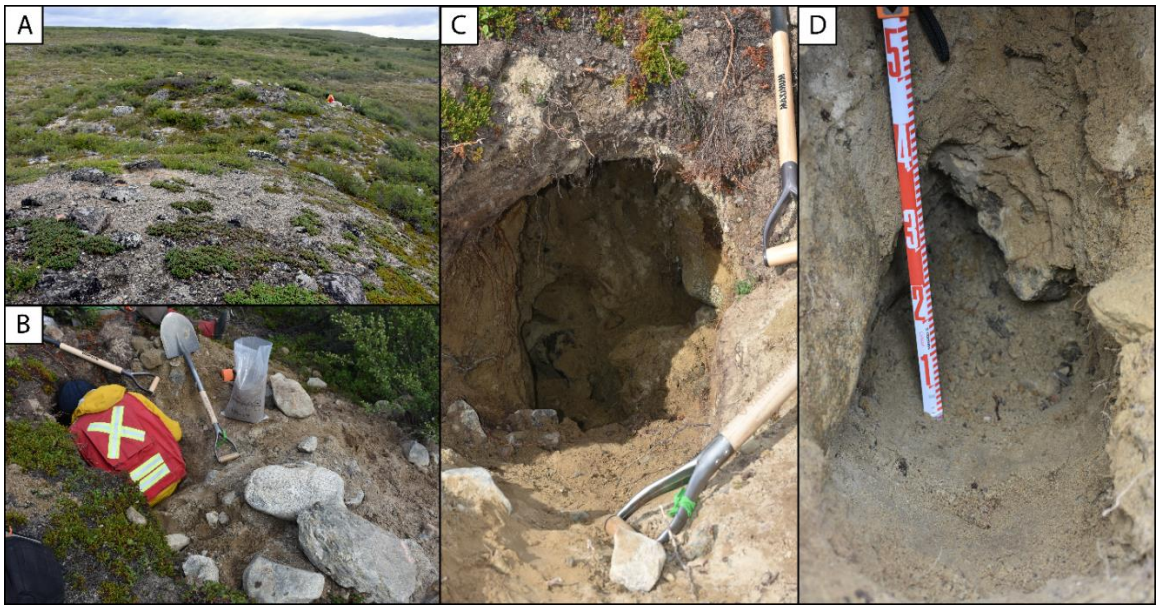

Figure 3.8: A) Two glaciofluvial hummocks at site 19; person for scale. B) Large animal burrow, potentially grizzly, in the largest glaciofluvial hummock appearing in A (where the person is). C) The extent of the hole after further excavation. D) Detailed view of the sediments before sampling.

3.4. Grain size Analysis

The results of grain size analysis include the total weights, cumulative percentages, and differential percentages of each grain size-fraction (Appendix C). Differential percentages are plotted to create a grain size distribution graph for all the samples along the three transects. Cumulative percentages of specific grain size-fractions are plotted along sample transects.

3.4.1. Grain Size Distribution Curves

The grain size distributions of each sample in the three transects are compiled in Figure 3.9. There is variability in the differential percentage of grain sizes that make up the sediment samples collected along the three transects. There are several important trends revealed by the grain size distribution curves. All the till grain size curves share the same general shape, indicating that all analyzed till samples have similar compositions. Therefore, they likely have similar provenance and modes of deposition. All the till samples have a grain size distribution curve with a shallow slope for the coarse grain size-fractions (i.e., granules, very coarse, and coarse sand), that begins to gradually steepen at around

medium sand and finally has a very steep slope at silt. This indicates the till samples all contain a low percentage of granules, very coarse and coarse sand and a high percentage of silt relative to subglacial meltwater corridor sediments.

The grain size curves for the samples collected in the meltwater corridors indicate these samples contain less silt and clay than the till samples. Though there are a few outliers, these curves have a steeper slope in the coarse grain size-fractions than the till samples. Therefore, samples collected in meltwater corridors have a higher percentage of granules, very coarse and coarse sand. There is bimodal variability within the grain size curves of the meltwater corridor sediments, with one grouping of samples immediately below the till sample curves (Group A, Figure 3.9) and another grouping lower on the graph (Group B, Figure 3.9). These two groupings of subglacial meltwater corridor sediments likely reflect the level of meltwater reworking that affected the sediments. Samples in group A (Figure 3.9) have grain size distributions more like till, however their curves still plot lower than all the till samples; this suggests moderate winnowing by meltwater. Samples in group B (Figure 3.9) have a much steeper slope in the larger grain size-fractions, then slope gently through medium sand and finer. This suggests these sediments have been more heavily reworked by meltwater and have compositions more like coarse-grained sandy glaciofluvial material.

Grainsize distribution curves of glaciofluvial hummock samples fall in both group A and group B (Figure 3.9), indicating that the composition of these landforms is variable. Some hummocks have compositions similar to till with less silt and clay (Group A) while others have significantly more coarse-grained sand than till and less silt and clay.

Three of the samples collected from within the same subglacial meltwater corridor are outliers (#24, 28, 29) and have the same shape as the till sample group for at least part of the curve. Two of these samples (#24 and # 29) have a grain size curve like that of till, and this is reflected by field descriptions suggesting these samples are similar in composition to till and may have only been slightly reworked. The third outlier (#28 a glaciofluvial hummock) has steep slopes through the medium to very fine sand size-fractions, suggesting it is closer to a fine-grained sandy glaciofluvial material.

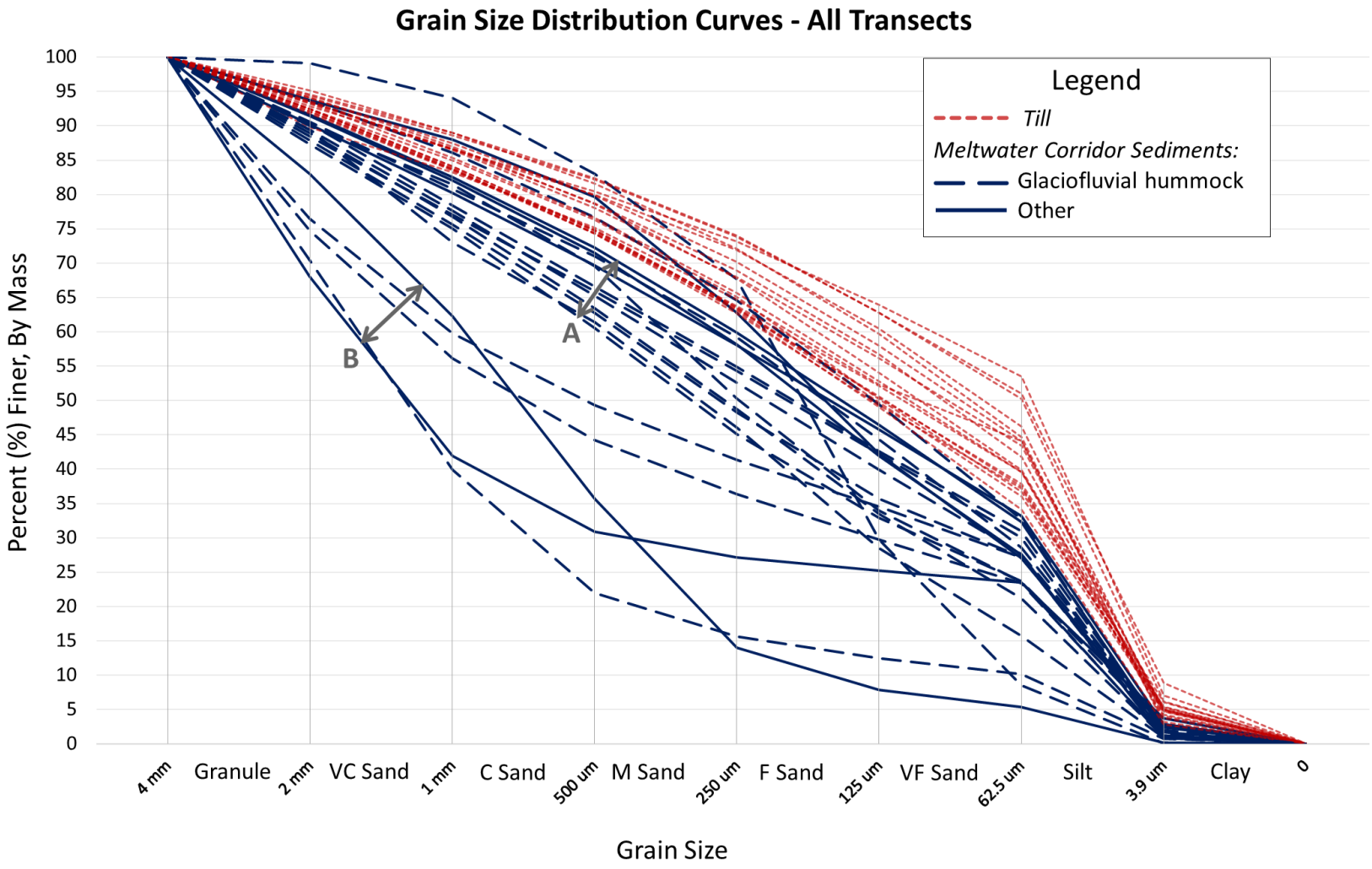

Figure 3.9: Grain size distribution curves of each of the samples collected along all transects symbolized base on material type and landform. The range of meltwater corridor samples in group A and group B are denoted in dark grey.

3.4.2. Silt and Clay Percentages

Specific grain size-fractions were chosen for spatial comparison of cumulative percentages between each sample along the three transects. The silt and clay size-fraction (<62.5µm) were selected for display as field descriptions of sediments suggest that unmodified till sediments are siltier than meltwater corridor sediments. The cumulative percentages of silt and clay across each transect are displayed in Figure 3.10. There is variability in the percentages of silt and clay amongst the samples in each transect. Differences in silt and clay percentages correlate well with the location of the subglacial meltwater corridor margins in all three transects. The till samples have higher percentages of silt and clay than the samples from within the meltwater corridors and there is generally low variability in silt and clay amongst till samples along the same transect. The samples from within the meltwater corridors display lower percentages of silt and clay than the till samples; however, variability in silt and clay amongst meltwater corridor samples is higher. Along sample Transect 2 and 3 where subglacial meltwater corridor samples include glaciofluvial hummocks and other intervening materials, there is not any correlation between silt and clay content and hummock landforms.

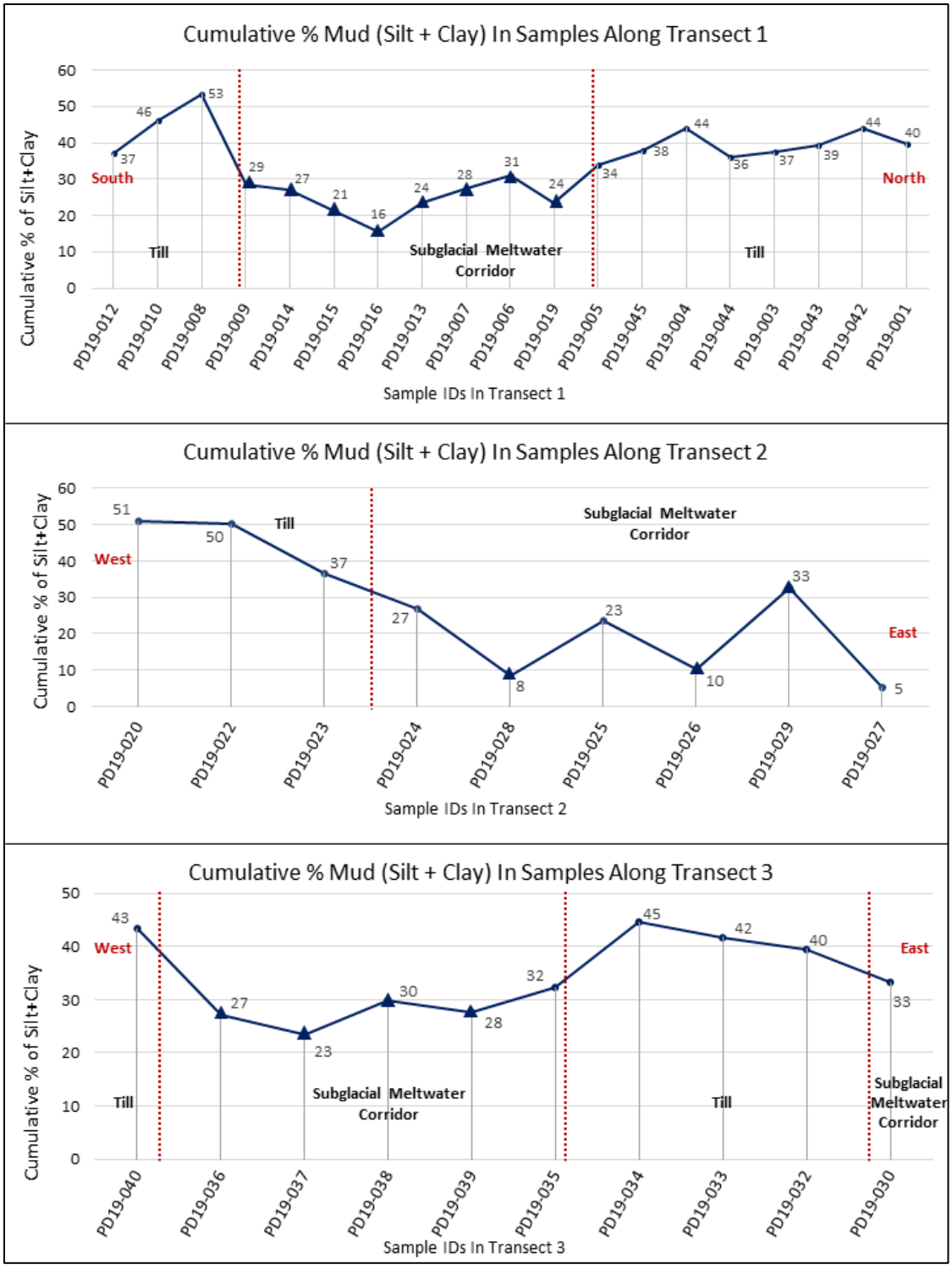

Figure 3.10: The percentage of mud (silt plus clay) present in each sample along the three transects. The X-axis shows sample ID and the Y-axis shows percentage of mud. Red dashed lines indicate the approximate location of meltwater corridor margins. Triangles indicate glaciofluvial hummock samples.

The medium to very coarse sand (0.25-2 mm) size-fractions were selected for display as this is the range of grain sizes picked for KIMs, with medium sand (0.25-0.5 mm) typically containing most KIMs (McClenaghan, 2005; McClenaghan et al., 2000). Till samples in each transect have lower percentages of medium to very coarse sand fractions than subglacial meltwater corridor samples and show relatively low variability (Figure 3.11). Samples collected within the meltwater corridor have higher percentages of medium to very coarse sand compared to the till samples, and differences in medium to very coarse sand contents amongst meltwater corridor sediments are moderately low. These trends are best observed in Transect 1 and Transect 3 (Figure 3.11).

Differences in medium to very coarse sand contents along Transect 2 is higher. Some of the meltwater corridor samples have similar (though slightly higher) percentages of medium to very coarse sand to till samples along the transect. The variability in medium to very coarse sand amongst meltwater corridor samples along Transect 2 does not correlate with samples collected from hummocks. Two samples from Transect 2 that were collected within the meltwater corridor have the highest cumulative percentages in medium to very coarse sand of all three transects (#26-27).

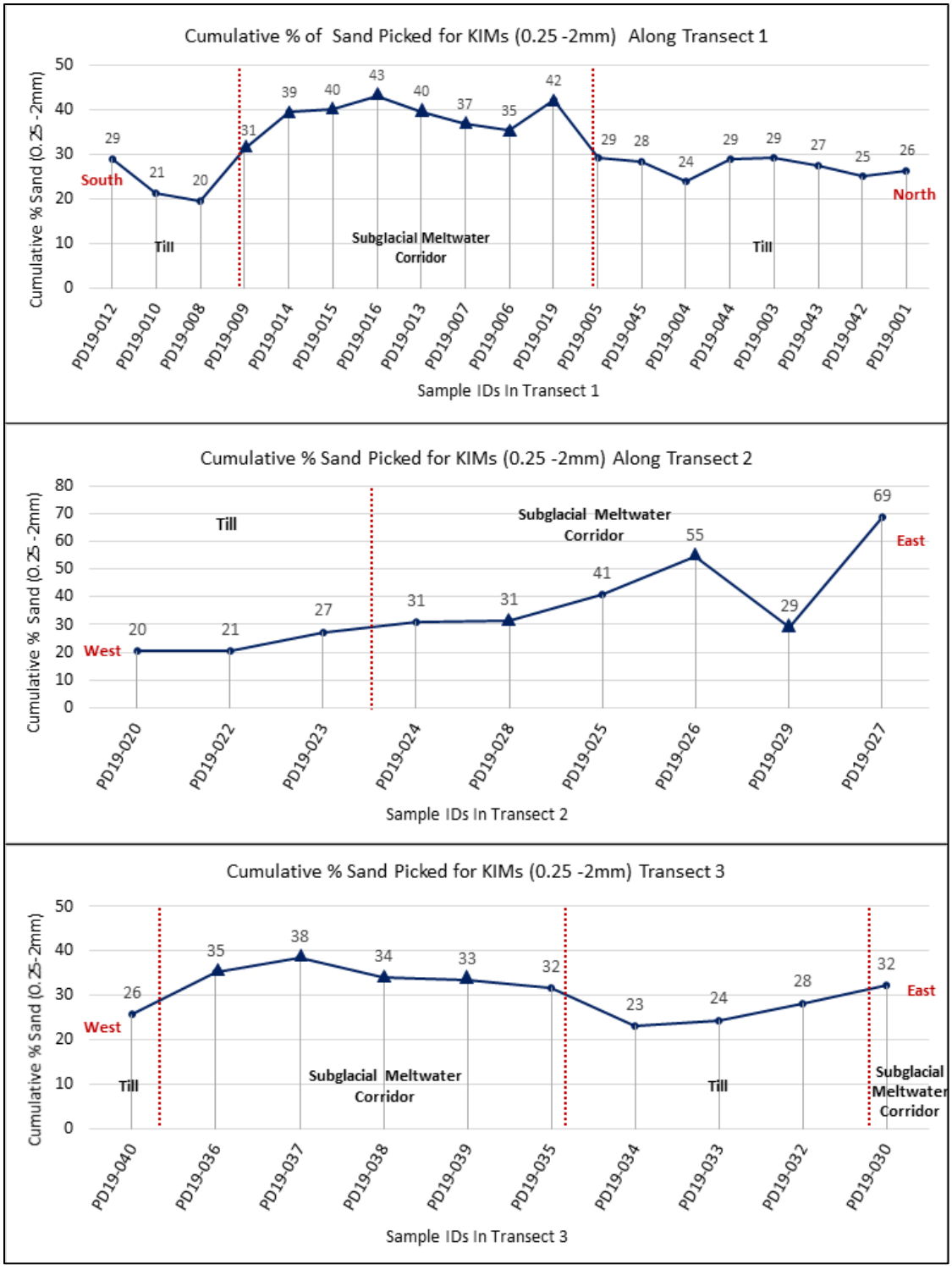

Figure 3.11: The percentage of medium to very coarse sand contents along all sample transects. The X-axis shows sample ID and the Y-axis shows the percentage of coarse sand. Dashed red lines indicate the approximate location of meltwater corridor margins. Triangles indicate glaciofluvial hummock samples.

3.4.3. Discussion

The low range in variability of grainsize distributions and specific grain-size fractions amongst till samples suggests that they have a similar genesis, provenance, and mode of deposition. Under the assumption that all meltwater corridor sediments are initially derived from till, the composition of meltwater corridor sediments can be compared to that of the till samples to determine the degree of meltwater reworking. Samples that deviate in composition the furthest from the till samples suggest the highest degrees of reworking.

Variability in grain size distributions and specific grain size-fractions is common amongst the samples collected from within subglacial meltwater corridors. Differences in silt and clay content amongst these samples is interpreted to represent varying degrees of meltwater reworking due to the evolving nature of meltwater flow in subglacial meltwater corridors through time. Differences in flow regime and sediment transport related to material genesis likely contribute to the large range of compositions observed in meltwater corridor sediments. As the grain size distribution curves of group B are furthest from the till group of samples, (Figure 3.9) it is proposed that meltwater corridor samples in group B have undergone a higher degree of reworking than samples in group A.

The observed trends in the grain size data allow for several important interpretations with regards to both landform genesis and mineral exploration. In terms of landform genesis, it is suggested that the decrease in silt and clay present within meltwater corridor sediments is likely the product of a geological process altering the composition of till. It is proposed that the meltwater responsible for the formation of subglacial meltwater corridors is also responsible for winnowing of silt and clay. In terms of mineral exploration, this removal of silt and clay has led to a relative increase in medium and coarse sand compared to a 10 kg sample of till, and these fractions are the grain size-fractions picked for indicator minerals. This could lead to an inflated concentration of indicator minerals in meltwater corridor samples when compared to unmodified till samples. Therefore, KIM concentrations in till and samples collected within subglacial meltwater corridors should not be directly compared.

3.5. Clast Analysis

At each of the 46 sampling sites, a sample of pebbles was collected. A table of all pebble lithology counts, average shape, and roundness for each clast sample can be found in Appendix D. The bedrock geology differs between the three sampling areas, so the results of clast analysis are interpreted separately for each sampling area. Visual trends were investigated, as the low number of samples in each area (n <30) makes a statistical approach not robust. Visual trends were investigated spatially by looking at the proportions of each lithology type and compared to the local bedrock geology. Figure 3.12 displays the results of clast lithology proportions in the samples collected along each of the three transects.

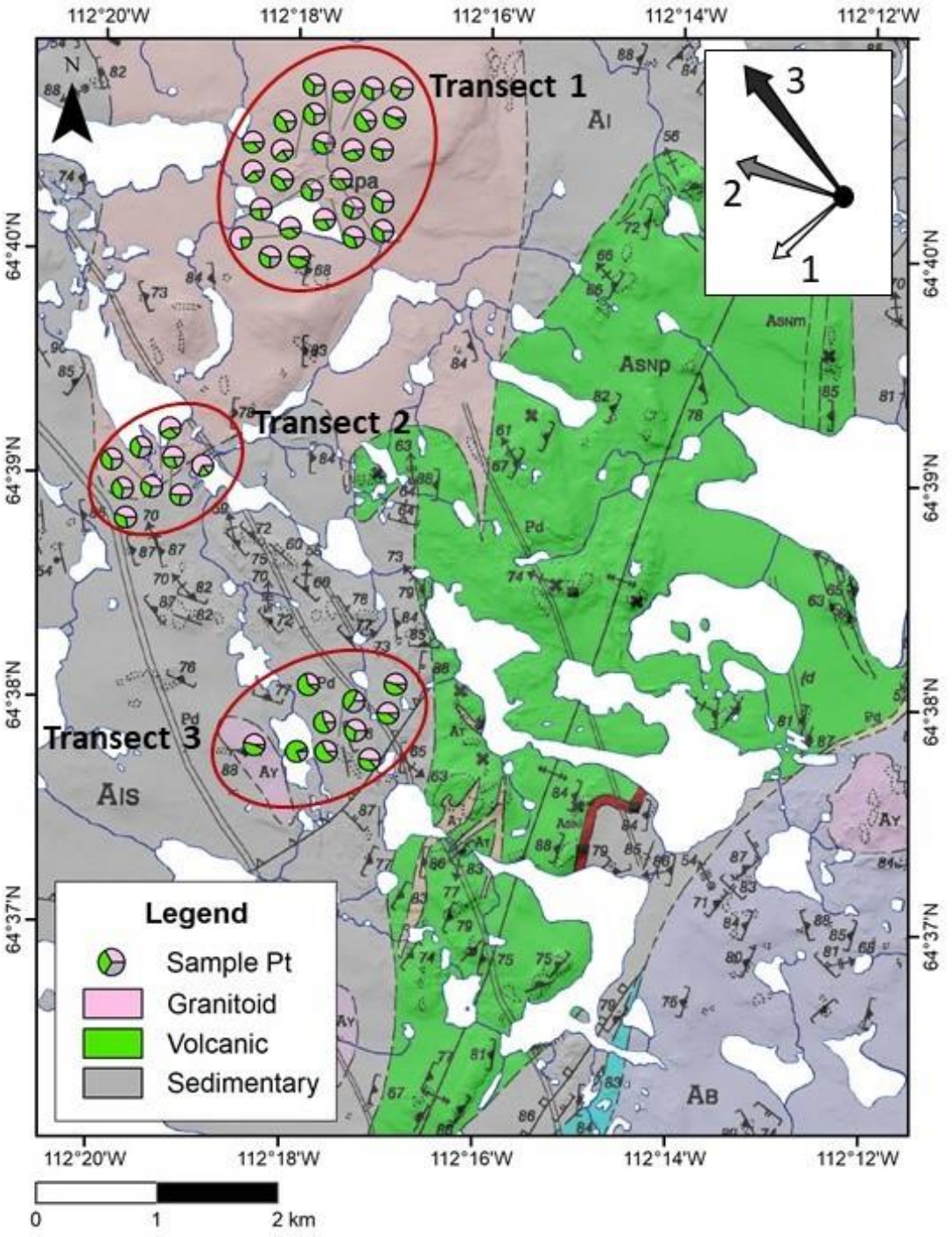

Figure 3.12: Pebble lithology analysis for samples along each transect overlain on a modified version of Hrabi and Grant's (1999) Bedrock map. Pie chart proportions represent the percentage of each lithology group. Arrows display local ice flow directionality and history.

Along sample Transect 1 the lithology proportions within clast samples of till are like those collected within subglacial meltwater corridors. In each sample, meta-sedimentary pebbles make up the lowest percentage of collected clasts and in most samples, granitoid pebbles make up the highest percentage of collected clasts. It should be noted that the bedrock in the area immediately surrounding Transect 1 is a granitoid, potentially explaining why granitoids are the most prevalent clast type in these samples. There are a few outliers in samples taken from till and glaciofluvial hummocks where the percentage of meta-volcanics is either greater than or nearly equal to the percentage of granitoid pebbles. There are no observed trends between material type and clast percentages.

Along Transect 2 the results of pebble analysis are similar to those from Transect 1, showing little variability amongst samples from materials with different genesis. The lowest proportion of clasts is meta-sedimentary and the highest is granitoids, with some exceptions where granitoids and meta-volcanics are found in equal proportions. Pebble samples collected from Transect 2 do not display any trends between clasts lithology proportions and material type. The bedrock underlying Transect 2 is also a granitoid unit and this may explain why granitoids are the dominant clast lithology.

Pebble lithology proportions along Transect 3 are different than the other two transects. However, lithology proportion amongst samples within Transect 3 are similar. In each of the samples, meta-sedimentary pebbles make up the lowest percentage of collected clasts and volcanic clasts make up the highest proportion of recovered clasts. There are a few instances where volcanic and granitoid clasts account for nearly equal proportions of recovered clasts. Pebble samples collected from Transect 3 do not display any trends between clasts lithology proportions and material type. The bedrock underlying Transect 3 is meta-sedimentary suggesting that the meta-volcanic and granitoid clasts must be sourced from further away.

3.5.1. Discussion

The goal of clast analysis was to determine if there were differences in the clast lithologies observed between till samples and samples collected from subglacial meltwater corridors (including glaciofluvial hummocks). Any differences could suggest the provenance of the materials may be different, indicating a difference in transport histories of the materials.

Based on the results of the clast lithology analysis, there is no significant variability in the clast lithologies found in till and adjacent samples collected within meltwater corridors. This outcome can be explained in two ways. The first is that the number of clasts collected in each sample is too small to rigorously show any differences that may exist between these two material groups. If it is assumed that the samples accurately represent all till and subglacial meltwater corridor materials in the area and that there are regional differences in till clast lithologies; similar clast lithologies suggest that meltwater corridor sediments are derived from till with the same provenance as adjacent till samples. If meltwater corridor sediments are derived from local till, then it is suggested that meltwater corridor sediments must have a relatively short transport history; otherwise, it would be expected that they contain different clast lithologies than the local till.

3.6. Genesis of Glaciofluvial Hummocks

The interpreted genesis model of glaciofluvial hummocks observed during this study is presented in the following section. These interpretations do not aim to discredit the possible genesis models of authors that have encountered similar landforms in other areas, but rather that these interpretations provide an explanation for the genesis of observed hummocks.

The observed glaciofluvial hummocks are composed of a sandy diamicton with less silt and clay than till; signifying the material is distinct from both glaciofluvial sand and gravel and local till. The observed glaciofluvial hummocks are poorly sorted and no stratification was observed. This suggests that steady state sustained meltwater flow that leads to sorting and stratification are not responsible for the formation of these landforms.

However, it is proposed that other subglacial meltwater processes are responsible for the formation of glaciofluvial hummocks as the spatial distribution of these landforms is limited to within the bounds of subglacial meltwater corridors. Observed glaciofluvial hummocks are interpreted as depositional landforms. This is interpreted based on the difference in composition and surface expression between glaciofluvial hummocks and unmodified till. If the glaciofluvial hummocks were erosive landforms we would expect them to have the same composition as adjacent unmodified till.

The surficial geology of the area as interpreted in Chapter 2 indicates that subglacial meltwater corridors are made up of glaciofluvial veneers of sorted sand and gravel, reworked till, scoured bedrock and landforms including eskers, deltas and glaciofluvial hummocks. In the map area, the spatial distribution of glaciofluvial hummocks, scoured bedrock, and thin reworked till in subglacial meltwater corridors are correlated (Figure 3.13). Hummocks are located down-flow from areas of scoured bedrock and thin reworked till located within subglacial meltwater corridors. It is suggested the till previously deposited on top of these areas represent a potential source for the sediments that make up glaciofluvial hummocks. This eroded till would be transported and deposited as glaciofluvial hummocks in the down flow direction within the meltwater corridor.

The interpretation that observed glaciofluvial hummocks in the study area are depositional landforms does not negate the idea that similar landforms in other areas formed by subglacial meltwater could also be erosive landforms. For example, hummocks observed in the tunnel valleys and “hummock corridors” of southern Sweden are thought to be erosive remenants (Peterson and Johnson, 2018; Peterson et al., 2018). A key difference between these areas and the Beauparlant Lake area is the substrate overridden by glacial ice. In southern Sweden, the substrate is thick drift from previous glaciations overlying sedimentary bedrock; whereas in the SPG the drift is relatively thin and the crystalline bedrock of the Canadian Shield is more difficult to erode. Similar subglacial meltwater processes could yield very different results depending on the thickness of previously deposited sediments and the hardness of the bedrock.

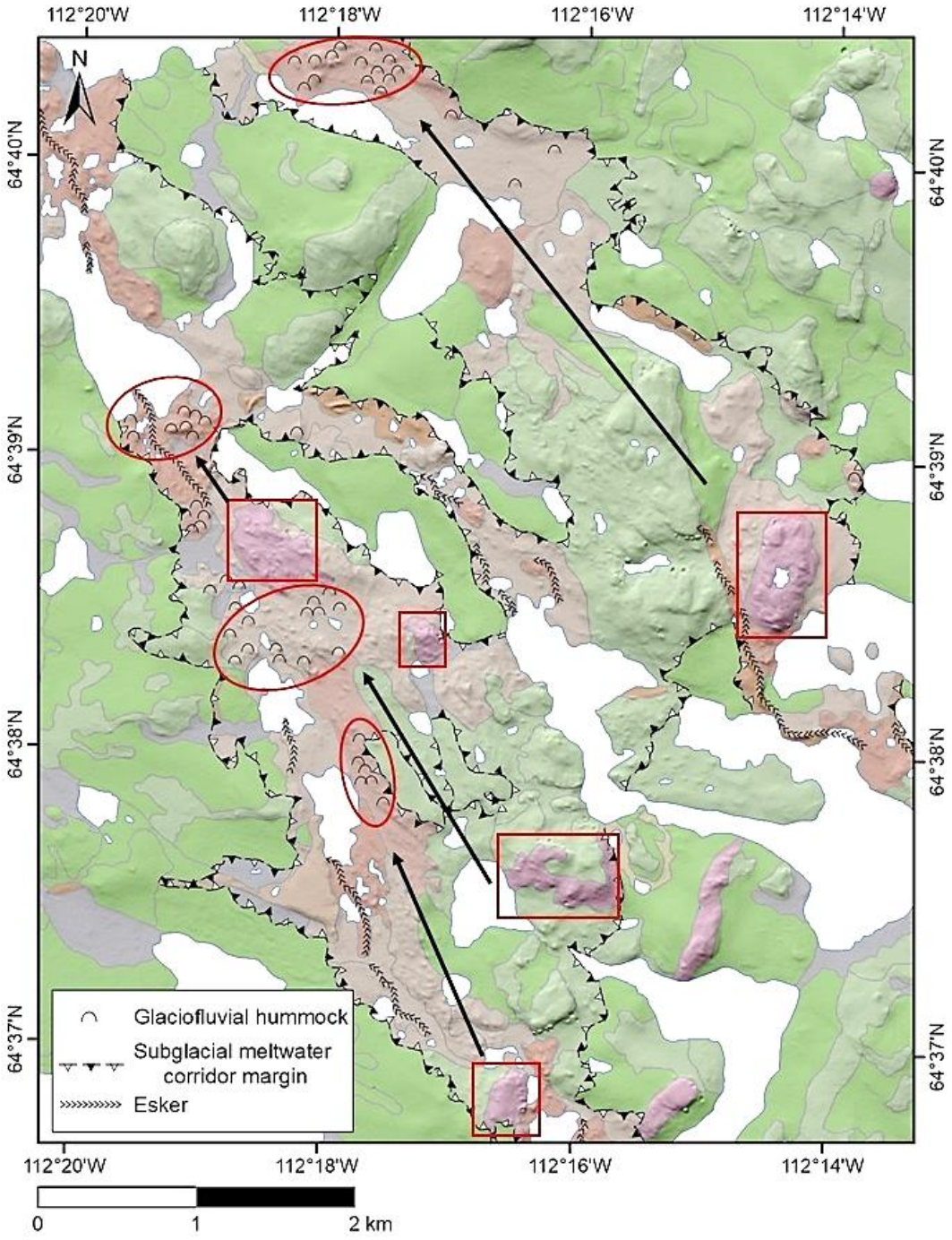

Figure 3.13: Simplified surficial geology displaying subglacial meltwater corridor margins, sediments, and landform assemblages. Surficial geology legend is consistent with Figure 3.4. Red ovals indicate groups of hummocks and red boxes indicate scoured bedrock. Black arrows indicate interpreted paleo-flow direction and potential connections between bedrock and hummocks.

Glaciofluvial hummock grain size analysis indicates that these landforms on average have less slit and clay and a higher proportion of coarser grain size-fractions than the adjacent till. For the observed sediment properties to occur in these hummocks (sandy diamicton, poor sorting, lack of stratification) it is likely that turbulent high energy flow and rapid deposition was responsible for their formation. Otherwise, these sediments would have similar compositions to other glaciofluvial sand and gravel found nearby.

One possible explanation is that a large volume of meltwater reached the ice-bed interface, eroding and transporting existing glacial sediments in a slurry-like mixture as it traveled along the subglacial drainage system (Figure 3.14). The hard bedrock resisted erosion and most of the energy of the turbulent flow was directed up into the ice, providing accommodation space for sediment transport and then deposition and winnowing of silt and clay as flow waned. This process must have had enough energy to transport the observed boulders and be rapid enough to inhibit sorting or stratification during deposition.

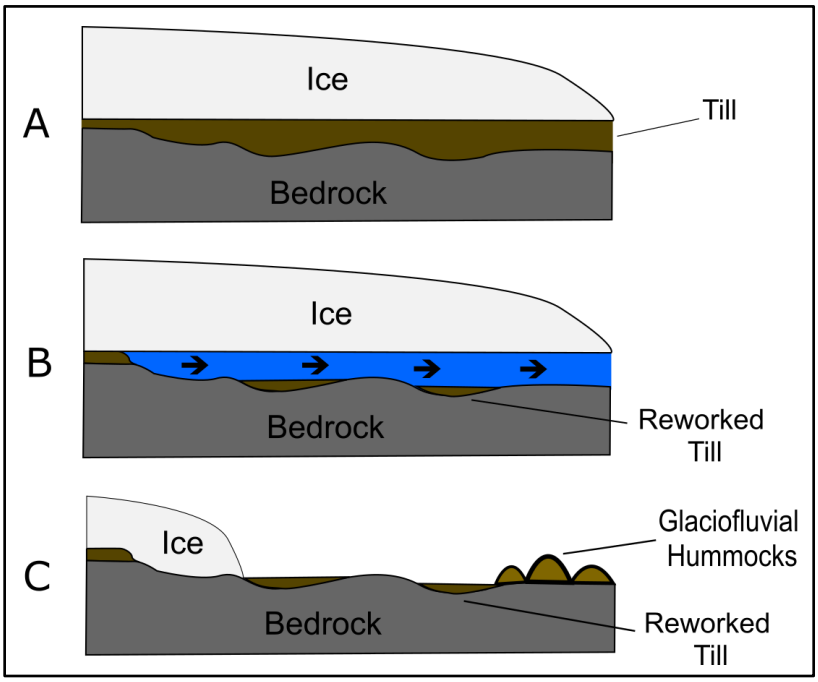

Figure 3.14: Schematic diagrams of subglacial meltwater drainage and the formation of glaciofluvial hummocks through time. A) A widespread layer of till forms at the base of the LIS. B) A large volume of subglacial meltwater drains along the ice-bed interface, eroding and reworking till and scouring bedrock. C) Eroded till is deposited downstream as glaciofluvial hummocks. Reworked till and scoured bedrock is exposed as the glacier retreats.

There are two main hypotheses on the source of water responsible for the formation of subglacial meltwater corridors and glaciofluvial hummocks (e.g. Campbell et al., 2013; Haiblen, 2016; Rampton, 2000; St Onge, 1984; Utting et al., 2009). One hypothesis is that the source of the meltwater is supraglacial. Haiblen (2016) suggests that supraglacial lakes and rivers would act as basins and conduits for water melted from the ablation zone at the surface of the glacier. This surface water would drain, in a potentially cyclical and recurrent nature through moulins and crevasses to the ice-bed interface. The subglacial meltwater would travel in channelized conduits, forming subglacial meltwater corridors in a time transgressive manner. These corridors grow in length as the Ice margin retreats and the meltwater events recur; creating the long linear corridors we see in the SGP today. The other water source hypothesis is that meltwater originates from subglacial lakes. Rampton (2000) suggests that large subglacial reservoirs could periodically drain leading to subglacial floods. These floods would be responsible for the formation of subglacial meltwater corridors and much of the sediment and landform assemblages found within them. The results of this thesis do not provide evidence to support or refute either of the hypotheses on the source of the water responsible for the formation of subglacial meltwater corridors.

Both types of meltwater drainage events related to lakes have been documented on, and under modern day ice sheets. Supraglacial lake drainage events have been observed on the Greenland Ice Sheet (e.g. Box and Ski, 2007; Stevens et al., 2015). At the western margin of the Greenland Ice Sheet, drainage from supraglacial lakes and streams has been documented and correlated with changes in discharge at the margin (Chu, 2014; Cowton et al., 2013). Subglacial lakes have been identified under the Antarctic Ice Sheet (e.g. Siegert, 2000). Ice surface elevation changes over these lakes has been recorded and interpreted to represent subglacial lake drainage (Smith et al., 2017; Wingham et al., 2006). However, subglacial lakes generally require significant subglacial topography to form (e,g. Wingham et al., 2006); topography which is lacking up ice of meltwater corridors in the SGP. These modern-day examples of supraglacial lake and subglacial lake drainage events may illustrate processes that led to the formation of subglacial meltwater corridors and glaciofluvial hummocks in the SGP during deglaciation of the LIS.

3.7. Implications

3.7.1. Mineral Exploration

The results of grain size analysis can be applied to drift prospecting in the SGP. The higher proportion of sand in glaciofluvial hummocks can have an influence on the normalization of KIM results. KIMs are picked from the sand size-fractions so, normalizing counts to a 10 kg sample would result in a higher concentration when compared to till with more silt and clay. This could create a potential false concentration of KIMs recovered from samples modified by these meltwater processes. Given the potential difference in transport histories between till and meltwater corridor sediments, KIM counts from meltwater corridor and hummock samples should not be directly compared to adjacent till samples.

The potential for variable concentration of indicator minerals caused by grain size differences in meltwater corridor sediments should be taken into consideration when planning and interpreting the results of drift prospecting campaigns. In the planning stages the sampling area should be mapped by a reputable Quaternary geologist at a resolution suitable to the sampling density. Close attention should be paid to the location of subglacial meltwater corridors due to the reworking and secondary transport that can occur. This mapping should inform the targeted areas and materials selected for sampling. When executing the sampling program, either all the samples should be collected from unmodified materials (till for example) or the results of indicator mineral analysis standardized with an approximate correction based on the level of sediment modification. However, even with a correction for meltwater modification, samples with different transport histories cannot be directly compared.

In a scenario where subglacial meltwater corridors and meltwater modification are widespread through the sampling area, samples collected from within subglacial meltwater corridors may be necessary. In this case these samples transport histories should be treated like esker sediments when vectoring back to a potential source area. Subglacial meltwater corridor sediments, including glaciofluvial hummocks are a second derivative of bedrock and can be used as a vector towards mineralization by sampling upstream within subglacial meltwater corridors. The furthest upstream anomalies can be used as an indication of where further investigation in the till should begin.

At the interpretation stage of a drift prospecting campaign, it would be useful for grain size analysis to be completed on all samples. This analysis will aid in calibration of the initial surficial mapping and quantify the range of grain size distributions present in different surficial materials. Grain size analysis may also reveal the location of contacts between sediment types at higher resolution than mapping. The completion of grain size analysis will ensure that only similar sediments are compared when reviewing indicator mineral counts. Specific percentages of grain size-fractions may also allow for a standardized adjustment to be made to indicator mineral counts in sediments with the same transport history so that samples with differing sand contents may be compared more equally.

3.8. Conclusions

Grain size analysis and pebble lithology analysis were completed on 46 sediment samples collected over three sample areas. Sample materials include unmodified till and samples collected from within subglacial meltwater corridors, including glaciofluvial hummocks. Sampling areas focused on the transition between in-situ till blankets to remobilized sediments in subglacial meltwater corridors. The grain size analysis revealed that the till and corridor-sediments have different grain size distributions. Till samples on average have more silt and clay than glaciofluvial hummocks and other sediments in subglacial meltwater corridors. It is suggested that the difference in grain size distribution between these sediment types is due to the deglacial meltwater processes responsible for the formation of subglacial meltwater corridors and the landforms that occur within them.

Based on the morphology and sedimentology of observed glaciofluvial hummocks, it is proposed that they are depositional landforms. It is hypothesized that a large volume of highly pressurized meltwater draining at the ice-bed interface would erode and transport existing glacial sediments in a turbulent slurry like mixture as it evacuates along the channelized drainage system. The bedrock resists erosion and most of the energy of the turbulent flow is directed up into the ice, providing accommodation space for sediment transport and then rapid deposition and winnowing of silt and clay as flow wanes. These meltwater flow events occur as part of the time transgressive meltwater processes responsible for the formation of subglacial meltwater corridors.

Differences in grain size distribution between subglacial meltwater corridor sediments and till should be considered during drift prospecting programs. A sample containing

significantly less silt and clay than till could have relatively higher KIM concentrations as the percentage of size-fractions containing indicator minerals will be relatively higher in a standardized 10 kg silt and clay poor sample.

Chapter 4.

Surficial Material Analysis: Mineral Chemistry and Matrix Geochemistry

4.1. Introduction

Successful mineral exploration in the SGP of the Northwest Territories depends on effective drift prospecting methods and an understanding of the genesis of sampling materials. Subglacial till is an optimal sediment for drift prospecting programs as it is common and widely distributed in glaciated terrains, is derived directly from a bedrock source and transport histories can be interpreted (McClenaghan, 2005; Spirito et al., 2011). Geochemical and mineral anomalies in subglacial till can create large exploration targets as these anomalies are significantly larger than their bedrock source (Levson, 2001) and can be used as a vector back to mineralization given an understanding of the glacial history (McClenaghan et al., 2002). Post-depositional modification of till by meltwater processes is commonly overlooked and can mislead exploration programs by obfuscating the primary dispersal patterns.

The purpose of this chapter is to examine an area where deglacial meltwater processes have affected till and assess the effects of these processes on KIM concentrations, chemistry, and distributions. The deglacial meltwater processes targeted for this project are those that formed subglacial meltwater corridors and reworked the sediment within them. These complex depositional environments can produce sediments that have similar characteristics to till but have different transport histories and compositions. This chapter aims to determine if sediments modified by meltwater have different KIM concentrations and distributions than those in unmodified till. This question was addressed through the determination of KIM concentrations, matrix geochemistry, and KIM chemistry in till and sediment samples collected within subglacial meltwater corridors. Analytical results are investigated to evaluate relationships based on material genesis and material provenance is investigated through matrix geochemistry and KIM chemistry comparison between material types.

The hypothesis is that meltwater modified sediments will have higher concentrations of KIMs because meltwater reworking leads to a decrease in the silt and clay fraction of the sediments (see Chapter 3).

4.1.1. Drift prospecting in the Slave Geological Province

Diamond bearing kimberlites were discovered in the Lac de Gras region of the Northwest Territories in 1991 when exploration across the region led to the discovery of the point lake kimberlite (Fipke et al., 1995). Since then, significant effort has been placed on developing methods for diamond exploration in glaciated terrains. Drift prospecting guidelines and best practices have been released and are continuously revised by the GSC (McClenaghan et al., 2013; McClenaghan et al., 2020; Spirito et al., 2011).

Kimberlites have a distinct mineral and geochemical signature (Sparks et al., 2006) and are usually relatively soft compared to the surrounding bedrock. When glaciers flow over kimberlites or other mineral deposits they can easily erode and deposit them in the till down ice (McClenaghan 2005; McClenaghan et al., 2002; Miller, 1984); this creates patterns of anomalous indicator mineral concentrations, referred to as dispersal trains. Once a dispersal train has been discovered, vectoring in the up-ice direction can lead to the kimberlite source. These dispersal train anomalies can be an extremely useful exploration tool for vectoring towards kimberlites in the SGP (Dredge et al., 1994; McClenaghan et al., 2002,).

The process of vectoring can be complicated by non-linear dispersal due to multiple ice flow directions as is the case in the SGP; the complex ice flow history can produce non-linear, palimpsest dispersal trains (McClenaghan et al., 2000). The formerly linear, almost cigar shaped anomaly can be smeared out into a fan shape or even more complex forms depending on the different directions of ice flow (McClenaghan et al., 2000). Therefore, it is important to understand the glacial history when interpreting surficial exploration datasets.

Esker sediments can also be used for KIM sampling. Usually, glaciofluvial sediments are sampled during regional scale reconnaissance exploration (e.g, Cummings et al., 2011; Henderson, 2000; Parent et al., 2004; Tremblay et al., 2009). Esker sediments are generally further travelled from their source and represent a second derivative of bedrock

because they are commonly derived from till (Cummings et al., 2011). Esker sediments may also be derived directly from bedrock. The most likely transport history of KIMs in glaciofluvial material is that subglacial meltwater intersects and erodes a KIM dispersal train in till and deposits it further downstream (Cummings et al., 2011). The derivative nature of glaciofluvial sediment transport history must be considered when sampling any subglacial meltwater corridor sediments and the secondary meltwater transport considered when vectoring towards mineralization.

4.1.2. Subglacial Meltwater Corridors

Subglacial meltwater corridors are elongated, sublinear geomorphic features that contain sediment and landform assemblages resulting from meltwater erosion and deposition by meltwater in subglacial environments. Erosion and reworking by meltwater have been observed worldwide in a wide range of glaciated environments (Peterson and Johnson, 2018; Peterson et al., 2018; Rampton, 2000; St Onge, 1984) and subglacial meltwater corridors are common in the SGP (Dredge et al., 1985; Dredge et al., 1995; Haiblen, 2016; Kerr et al., 1996; Kerr et al., 2014a; Kerr et al., 2014b; Knight, 2018; Sacco et al., 2018; St Onge and Kerr, 2014; Ward et al., 1997). These features have also been observed in southern Sweden, where subglacial meltwater corridors are referred to as tunnel valleys or hummock corridors (Ojala et al., 2019; Peterson and Johnson, 2018; Peterson et al., 2018).

Subglacial meltwater corridors include areas of glaciofluvial material occurring as veneers of sand and gravel, boulder concentrations, reworked till and scoured bedrock. Landforms including eskers, deltas, and hummocks are common. Hummocks and mounds have been found within subglacial meltwater corridors in many of the locations where these corridors are described (Campbell et al., 2013; Dahlgren, 2013; Dredge et al., 1995; Haiblen, 2016; McMartin et al., 2020; Rampton, 2000; Rampton and Sharpe, 2014; Sacco et al., 2018; Utting et al., 2009; Ward et al., 1997). In older literature these hummocks are mapped as kames and ribbed moraines (Aylsworth and Shilts, 1989; Dredge et al., 1995; Kerr et al., 1996; Ward et al., 1997). These hummock landforms were targeted for investigation to better understand their genesis.

There are multiple hypotheses regarding the formation of subglacial meltwater corridors. One hypothesis is that subglacial meltwater corridors formed from outburst floods

associated with the drainage of large subglacial lakes (Rampton, 2000). Corridors formed when multiple sustained pulses of high energy, subglacial meltwater travelled long distances across the SGP at the ice-bed interface (Rampton, 2000). Another hypothesis is that subglacial meltwater corridor formation is a time transgressive process, with relatively short segments of the corridor forming through time as the margin of the LIS retreated (Campbell et al., 2013; St Onge, 1984; Utting et al., 2009). In this hypothesis the source of meltwater is supraglacial in origin with meltwater reaching the ice-bed interface as it approaches the margin (Campbell et al., 2013; St Onge, 1984; Utting et al., 2009). A third hypothesis that combines aspects of both previously mentioned genesis models suggests that subglacial meltwater corridors formed in a time transgressive manner from high energy sheet-type meltwater flows which evolved into channelized drainage systems (Haiblen, 2016). Regardless of how subglacial meltwater corridors form it is evident that they lead to erosion, reworking and deposition of remobilized surficial sediments (Haiblen, 2016; Rampton, 2000; Utting et al., 2009).

4.1.3. Setting

The study area is located north of Beauparlant Lake, Northwest Territories. It is in the central SGP, ~260 km northeast of Yellowknife and ~100 km west of Diavik Diamond mine on Lac de Gras (Figure 4.1). It is part of the Beauparlant Lake map sheet (NTS 86A09), located on the western edge of the 1:250 000 Winter Lake map sheet (NTS 86A). It was chosen because it has multiple subglacial meltwater corridors, meltwater related landforms, unmodified glacial sediments, and has diamond potential. The study area is 144 km^2, centered around an existing exploration camp. The area has low rolling relief, generally not exceeding tens of metres overall. It has many lakes, small ponds, and small areas of shallow organic wetlands. Small outcrops of bedrock are common, though the dominant surficial materials in the area are glacial sediments, the most common of which is till (Kerr et al.,1996).

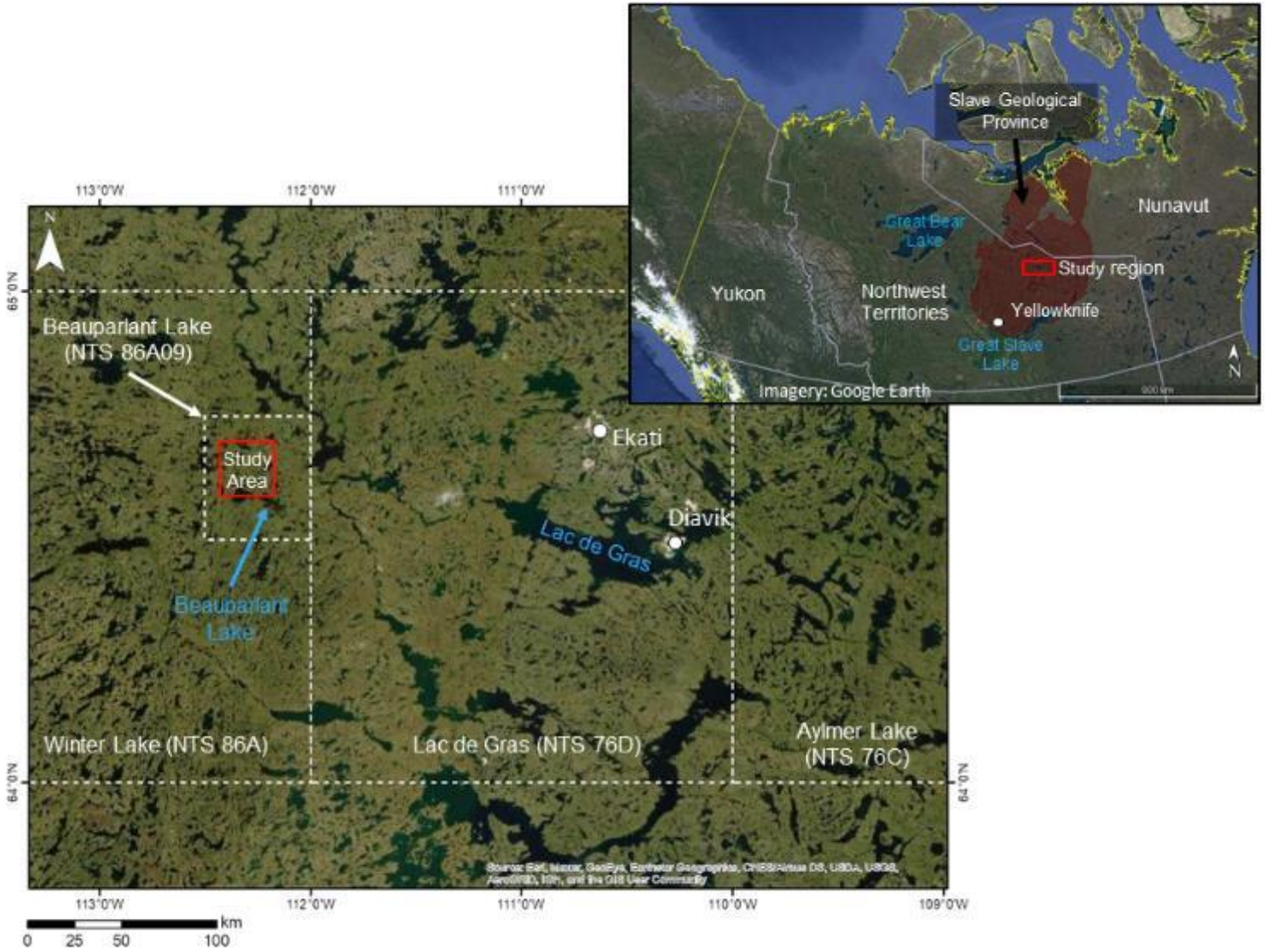

Figure 4.1: Location of the study area with insert map displaying the region in the Northwest Territories. The study area is highlighted in red and relevant locations and NTS map sheets are included.

4.1.4. Regional Glacial History

During the LGM, the LIS covered a significant portion of Canada and parts of the northern United States. The LIS grew in three major sectors: Labrador, Keewatin, and Baffin (Dyke, 2004). The Keewatin Sector covered the Winter Lake region, and the Keewatin ice divide controlled the direction of ice flow (Dalton et al., 2020; Dyke, 2004). During deglaciation, the position of the Keewatin Ice Divide evolved (Dyke and Prest, 1987), and this led to changes in the direction of ice flow in the Winter Lake region. Radiocarbon and terrestrial cosmogenic nuclide ages indicate that the study area deglaciated between 9.5 and 9 ^{14}C ka BP (Dalton et al., 2020; Dyke, 2004).

Alysworth and Shilts (1989) defined four broad landform assemblage zones within the Keewatin Sector of the LIS. The Winter Lake map sheet is within landform assemblage zones three and four, suggesting that the landform assemblage in the area varies between thick drumlinized drift cover with infrequent eskers to areas of thin to minimal drift cover with significant areas of exposed bedrock.

Regional Quaternary geology research identified three main phases of ice flow history in the Central SGP (Figure 4.2) based on striation sequencing and orientation of streamlined macroforms (Dredge et al., 1994). The first phase is oriented towards the southwest, which is followed by flow to the west and then flow to the west-northwest (Dredge et al., 1994). There is evidence of small local deviations in ice flow after this third phase, with flow to the southwest in the north-eastern portion of the Aylmer Lake map area and flow to the west in the northern portion of the Winter Lake map area (Dredge et al., 1994). The third phase of ice flow is thought to be the dominant ice flow direction in the region in terms of its ability to transport sediments and shape the landscape (Dredge et al., 1994; Ward et al., 1997).

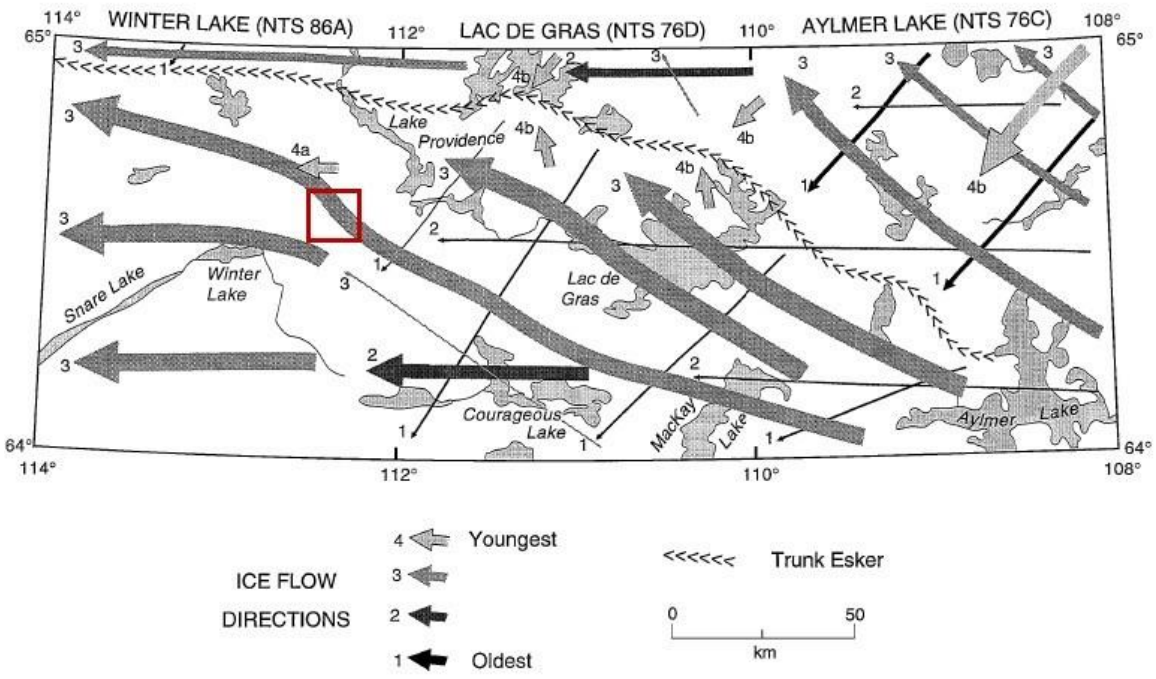

Figure 4.2: Generalized ice flow diagram in the central SPG (Dredge et al., 1994). The red box highlights the study area. Flow directions are numbered and the thickness of each arrow denotes the relative effect of the flow on debris transport and landscape modification.

4.1.5. Bedrock Geology

The bedrock geology of the mapping area includes supracrustal units of the Winter Lake Supracrustsal belt and younger igneous plutons (Figure 4.3). Bedrock mapping was completed in the mid to late 90's by the GSC (Hrabi and Grant, 1999; Thompson et al., 1994). The Winter Lake Supracrustal belt is Archean in age and is made up of three main sequences. The oldest in the sequence is the Newbigging formation, a suite of felsic to intermediate volcanic rocks (Hrabi and Grant, 1999). The second sequence includes mafic volcanics of the Snare and Credit formation and turbidite sedimentary rocks of the Itchen formation (Hrabi and Grant, 1999). The youngest in the sequence is made up of conglomerates and related sedimentary rocks of the Sherpa formation that uncomfortably overlie the rocks of the Itchen formation (Hrabi and Grant, 1999). Younger suites of plutonic rocks ranging from granitic to ultramafic in composition formed during and after deformation of the supracrustal units. These plutonic rocks include the Obstruction suite, Starvation suite, Beauparlant suite, Yamba suite, Terminus suite, and other intrusions.

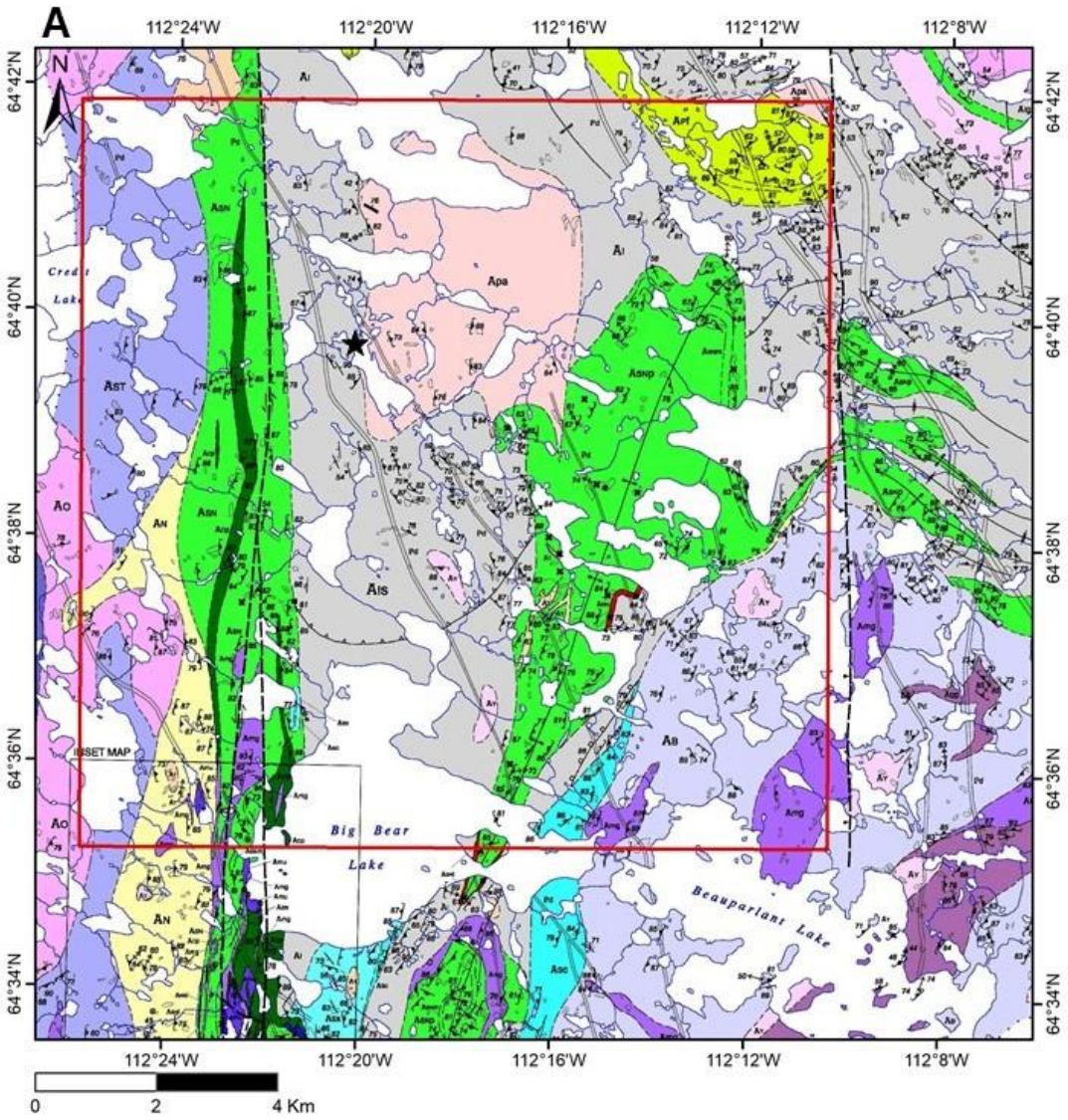
A
N
112°24'W
112°20'W
112°16'W
112°12'W
112°8'W
64°42'N
64°40'N
64°38'N
64°36'N
64°34'N
Credit Lake
Big Bear Lake
Beauparlant Lake
ISSET MAP
0
2
4 Km

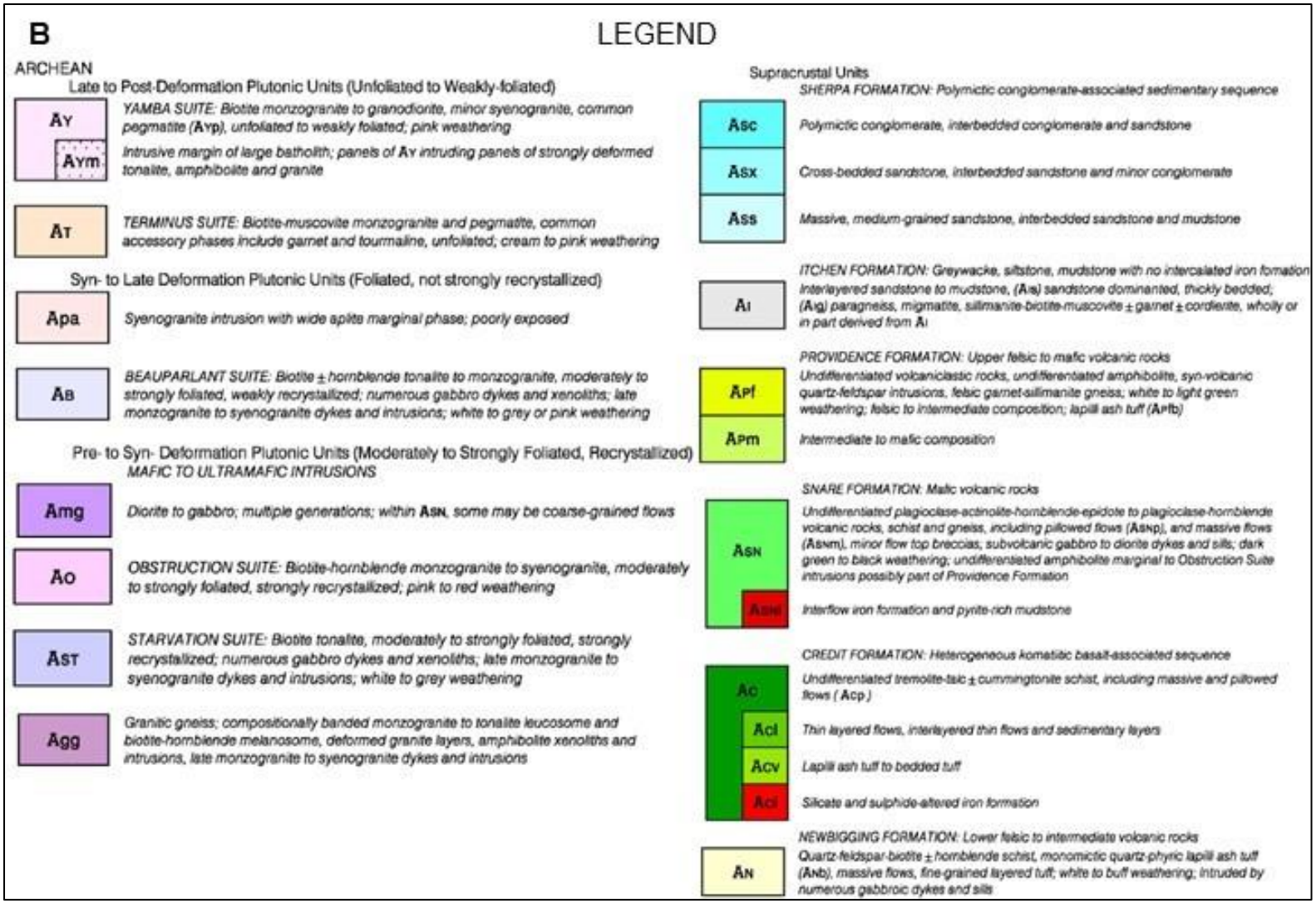

Figure 4.3: A) Bedrock geology of the study area (red box) and the location of field camp (black star) (modified from Hrabi and Grant, 1999). B) Legend for map displayed in Figure 4.3 A (modified from Hrabi and Grant, 1999).

4.2. Methodology

4.2.1. Field

Sediment sampling occurred in three locations (Figure 4.4). The selection of the three sampling areas was based on the results of preliminary surficial geology mapping. Sampling traverses were planned to transect the contact between unmodified till and modified subglacial meltwater corridor sediments. Samples include unmodified till and sediments collected within subglacial meltwater corridors. Meltwater corridor samples include a range of sediments: reworked till, glaciofluvial sand and gravels and glaciofluvial hummock sediments. Sediment descriptions were completed in the field along with other notes regarding general area descriptions. At Transects 1 and 2, drone imagery of glaciofluvial hummocks was collected and structure from motion photogrammetry used to create digital elevation models of these features.

Fifty-two sediment samples were collected for KIM analysis (Figure 4.4). Thirty-nine of these samples make up the three transects. Five samples are field duplicates and a further eight were collected from meltwater corridor sediments in the area surrounding Transect 1. Samples were collected following guidelines set out by the GSC (McClenaghan et al., 2020). Bulk 10-15 kg samples were collected from hand dug excavations between 0.3 to 1 m depth to reach the C horizon of the soil and placed in large plastic sample bags. Permafrost activity and active cryoturbation in frost boils was taken into consideration when choosing specific sampling sites to minimize the depth required to reach the C horizon of the soil. Till sampling sites targeted active frost boils.

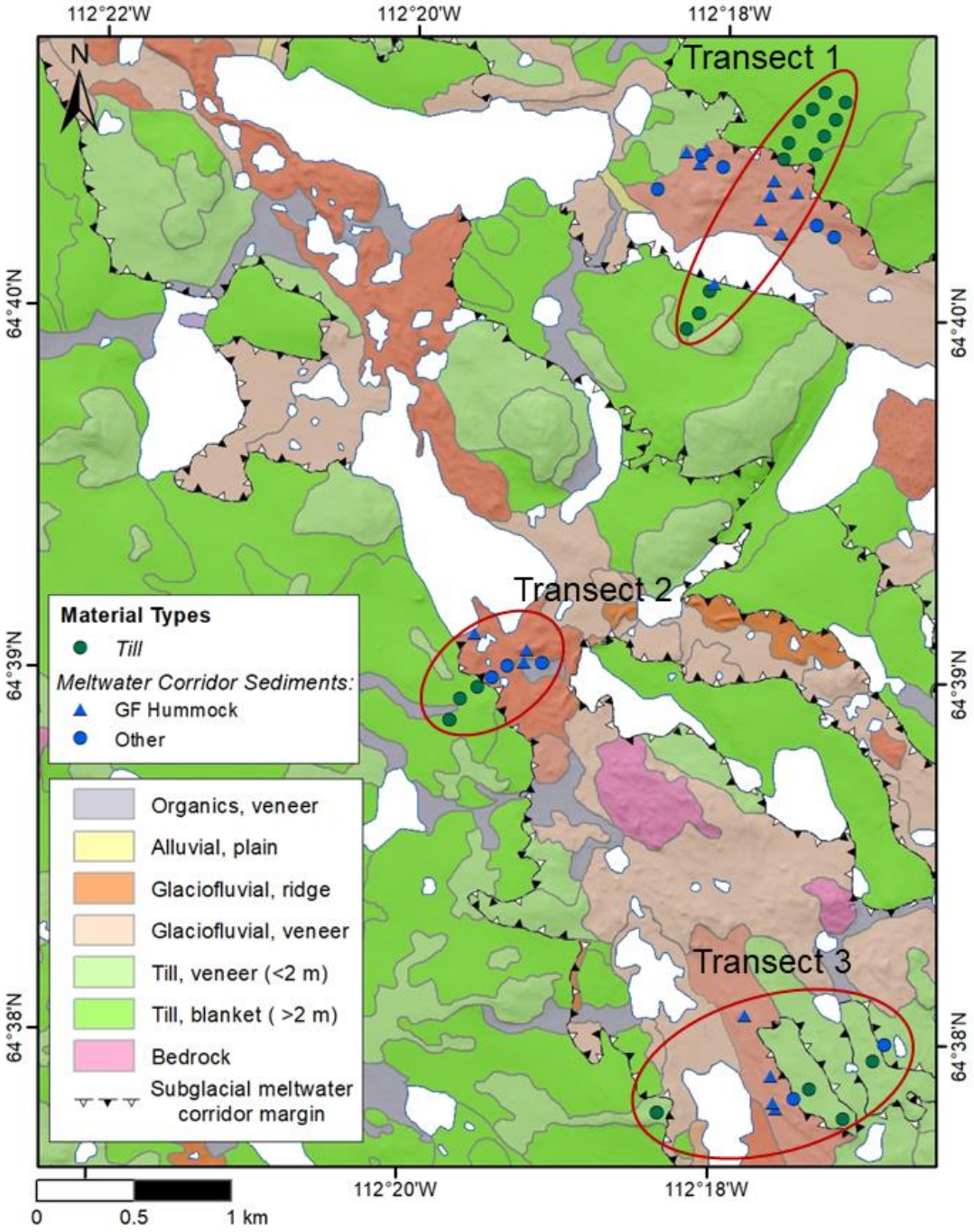

Figure 4.4: Simplified surficial geology map of a portion of the study area. The location of the three sample transects are highlighted in red.

Glaciofluvial hummock samples were collected from the tops of individual hummocks. In two instances on large glaciofluvial hummocks along Transect 1 a second sample from a different location on the hummock was collected. This was completed to determine if there was variability in KIM contents and matrix geochemistry within individual hummocks. The target sample spacing was 100 m, however deviations from this spacing were common due to the distribution of glaciofluvial hummocks and active frost boils in till.

4.2.2. Kimberlite Indicator Mineral Analysis

Several methods of indicator mineral analysis were completed to measure indicator mineral concentrations and chemical composition. These methods of analysis include visual indicator mineral picking and counting, mineral liberation analysis (MLA) and electron microprobe analysis.

Indicator Mineral Separation

Sediment samples were sent to Overburden Drilling Management, Nepean, ON for processing and indicator mineral picking. The separation of the heavy mineral concentrate was completed following the standard protocols recommended by the GSC (McClenaghan et al., 2000; McClenaghan et al., 2013; McClenaghan et al., 2020). The processes to produce the heavy mineral concentrate is as follows. First a 500 g aliquot is taken from each sample and archived. The remaining sample is disaggregated and sieved to < 2 mm. The mass of the < 2 mm size-fraction (Table feed) is recorded and then the < 2 mm size-fraction is fed through a shaker table to begin concentrating the heavy mineral grains. Heavy liquids are then used to separate minerals with a specific gravity > 3.2, which then undergo a ferromagnetic separation to remove any magnetic grains. Finally, the non-ferromagnetic heavy mineral concentrate is dry-sieved into three grain size-fractions: medium sand (0.25-0.5 mm), coarse sand (0.5-1 mm) and very coarse sand (1-2 mm).

KIM grains are then visually identified from each size-fraction of the non-ferromagnetic heavy mineral concentrate. A technician examines the grains under a microscope selecting KIM grains based on colour and habit. The minerals are sorted into vials based on type (pyrope, eclogitic garnet, Cr-diopside, chromite and forsterite) and grain size. The number of picked indicator minerals is recorded for each grain size-fraction. Counts of each indicator mineral type were then normalized to 10 kg based on the mass of the of < 2 mm fraction of the sample. Normalized counts are rounded to the nearest whole number

for each sample. Normalization of the KIM concentration results account for the variability in mass of each collected bulk sample.

Mineral Liberation Analysis

MLA is a proprietary, automated scanning electron microscopy technique that can identify specific mineral grains by shape and characterize mineralogy based on backscatter electron images and x-ray spectra gathered from identified grains (Layton-Mathews, 2014). MLA was completed on pyrope and Cr-diopside as they occur in most samples and were the most abundant KIMs. Pyrope and Cr-diopside grains (0.25 – 2 mm) were mounted in epoxy and then analysed using a scanning electron microscope with field emission gun-based hardware coupled with MLA software. The centroid of each identified mineral grain is bombarded with an electron beam, exciting the atoms, and producing characteristic x-ray radiation (Layton-Mathews, 2014). The x-ray radiation is then measured by an energy dispersive spectrometer to create x-ray spectra for the point analysis. X-ray spectra are then classified using a library of known mineral x-ray spectrums. The final output is a false colour image of each mineral grain characterized based on interpreted mineralogy. The results of this analysis allowed for the identification of mineral grains incorrectly picked and indicator mineral counts were corrected for misidentified grains.

Electron Microprobe Analysis

Major-element mineral chemistry of pyrope and Cr-diopside grains (0.25 – 2 mm) was determined through electron microprobe analysis. Epoxy grain-mounts were placed in the electron microprobe and each grain was bombarded with an electron beam, exciting the atoms, and producing characteristic x-ray radiation and backscatter electrons. The x-ray radiation is then measured by wave and energy dispersive spectrometers. The x-ray spectra intensities from each grain are then compared to the spectra of reference materials of known compositions (standards), producing a chemical composition for a specific spot on the mineral grain. Pyrope and Cr-diopside grains were analysed for weight percentages of SiO_2, Al_2O_3, TiO_2, Cr_2O_3, FeO, MnO, MgO, CaO, Na_2O, and K_2O. At least two points were analysed on each grain, one near the center of the grain and one closer to the edge to determine if there was compositional zonation.

A significant body of work has been completed in determining indicator mineral compositional constraints associated with kimberlites and diamonds (Cookenboo and Grütter, 2010; Crabtree, 2003; Fipke et al., 1989; Grütter et al., 2004; Grütter and Sweeney, 2000; Gurney, 1984; Morris et al., 2002; Quirt, 2004). Chemical compositions of mineral grains were then compared based on sample material type and assessed for kimberlite association and diamond fertility.

4.2.3. Matrix Geochemistry

A split of the fine fraction (silt and clay) of each sample was taken by Overburden Drilling Management and sent to ALS Global Vancouver for geochemical analysis. Concentrations were determined for a suite of 65 elements (Appendix G). Elements selected for analysis include kimberlite pathfinder elements (Ni, Cr, Ba, Co, Sr, Rb, Nb, Mg, Ta, Ca, Fe, K, Ti) (McClenaghan and Kjarsgaard, 2001) and rare earth elements (REE). Determination of elemental concentrations was completed through inductively coupled plasma mass spectrometry and several sample preparation techniques were used to ensure the best dissolution of elements from samples for analysis. An aqua-regia digestion was employed for preparation of most chemical analytes in each sample. A lithium metaborate fusion was used for REE analysis and a four-acid digestion was used for a selected set of kimberlite pathfinder elements.

After the samples have been prepared, they are put into a vacuum and introduced to a plasma which ionizes the material. Ions are then transported in vacuum via an inert carrier gas phase to the mass spectrometer. The ionized material is then accelerated and passes through a quadrupole mass selector where the mass of individual ions is established, and the number of ions counted. By comparing ion counts with the counts of standard reference materials of known compositions, the concentrations of elements in each sample are determined. All matrix geochemistry results are provided in Appendix G.

4.3. Kimberlite Indicator Minerals

KIM counts, including the original number of picked grains, the mass of the table feed (<2 mm size-fraction) and the normalized results are presented in Appendix E. The results of electron microprobe analysis of pyrope and Cr-diopside grains including backscatter

electron images of grains with multiple analysis points and the concentrations of elemental analytes for each analysis point are presented in Appendix F.

4.3.1. Mineral Grain Counts

Pyrope is the most abundant KIM by an order of magnitude making up 84% of all visually identified indicator minerals (Figure 4.5). Cr-diopside is the second most abundant, accounting for 11% of visually identified indicator minerals. Very few ilmenite and chromite grains were recovered, with each of these minerals accounting for only 3% of the total.

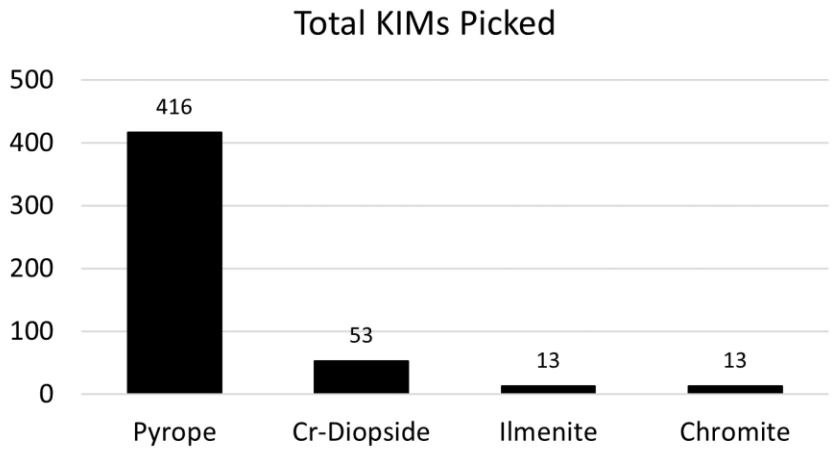

Figure 4.5: Bar graph displaying the total number of KIMs picked across all samples.

KIM counts were evaluated by material type and transect. At each transect samples were divided into two groups, samples collected from within subglacial meltwater corridors and unmodified till collected outside of the subglacial meltwater corridor. Each sample transect crosses the margin of a subglacial meltwater corridor from unmodified till into modified corridor sediments, including glaciofluvial hummocks (Figure 4.6). Transect 1 spans the meltwater corridor and includes samples of glaciofluvial hummocks and unmodified till from each side. Transect 2 spans one side of a meltwater corridor and includes samples of till and a range of reworked meltwater corridor sediments, including three glaciofluvial hummocks. Transect 3 is the most complex, crossing till, glaciofluvial hummocks, other reworked corridor sediments, more unmodified till and then more reworked corridor sediments.

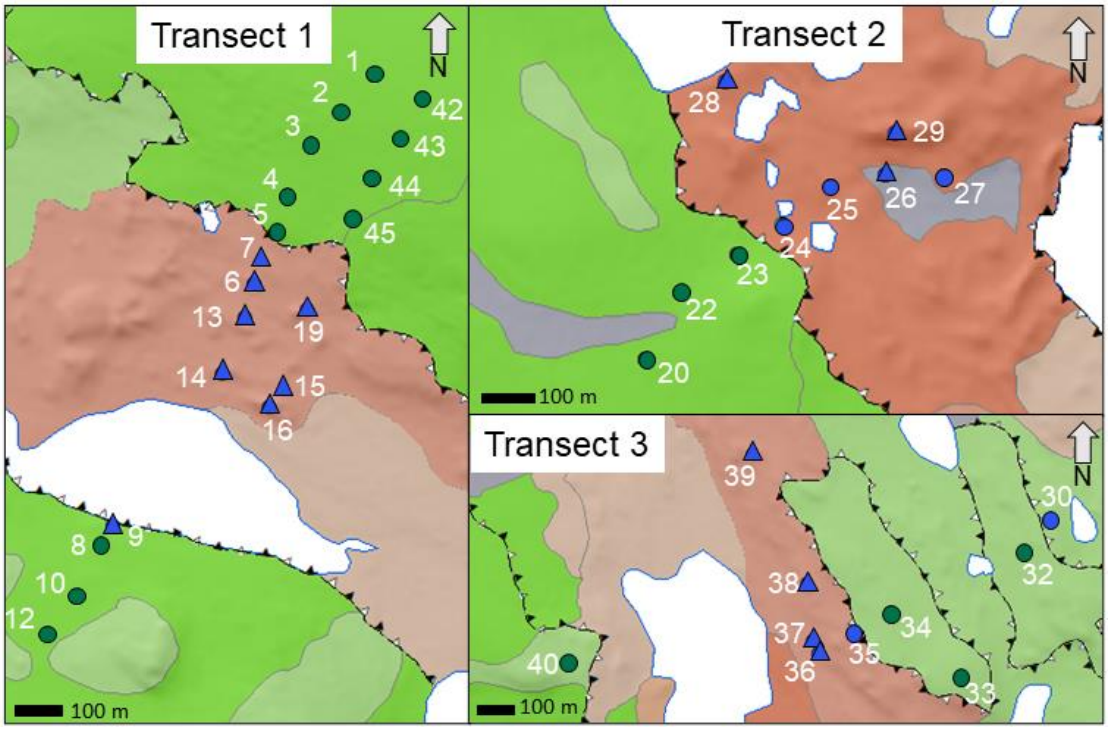

Figure 4.6: Simplified surficial geology maps with transect sample locations, numbers and material type. Legend is consistent with Figure 4.4.

Pyrope grains recovered from the medium-sand size-fraction (0.25-0.5 mm) were selected for presentation as they have the highest counts of all indicator minerals at each grain size-fraction. The counts of other KIMs are too low to identify any trends amongst samples. For each transect, the average and median pyrope grain content is higher in subglacial meltwater corridor sediments than in till (Table 4.1). The range of pyrope counts is also higher in subglacial meltwater corridor sediments than till and the highest pyrope counts are always from subglacial meltwater corridor sediments. These results suggest that in the sampling areas subglacial meltwater corridor sediments contain more pyrope grains than unmodified till and that pyrope grains are less evenly distributed in subglacial meltwater corridor sediments than unmodified till.

Table 4.1: Summary statistics of pyrope concentrations in the medium-sand size-fraction for each material type and transect.

		Normalized Pyrope counts (0.25-0.5 mm)			
Transect #	**Material Type**	**Average**	**Maximum**	**Minimum**	**Median**
Transect 1	**Till**	5.4	10	2	6.5
	Subglacial Meltwater Corridor	8.8	15	1	9.5
Transect 2	**Till**	0.7	1	0	1
	Subglacial Meltwater Corridor	6.3	13	2	6
Transect 3	**Till**	6.5	7	5	7
	Subglacial Meltwater Corridor	9.7	17	2	10

Normalized pyrope contents from the medium-sand size-fraction are compared across each of the three transects (Figure 4.7). The saw-toothed patterns depicted in subglacial meltwater corridor sediments along each transect (Figure 4.7) indicate the variability of pyrope counts amongst subglacial meltwater corridor samples. In general, till samples have more consistent concentrations of pyrope. The till samples collected from the north side of Transect 1 have elevated pyrope counts compared to all other till samples. It is possible that these samples have intercepted a kimberlite dispersal train. However, the average pyrope counts from these till samples is still lower than in the subglacial meltwater corridor samples collected along Transect 1, masking this potential anomaly in the till.

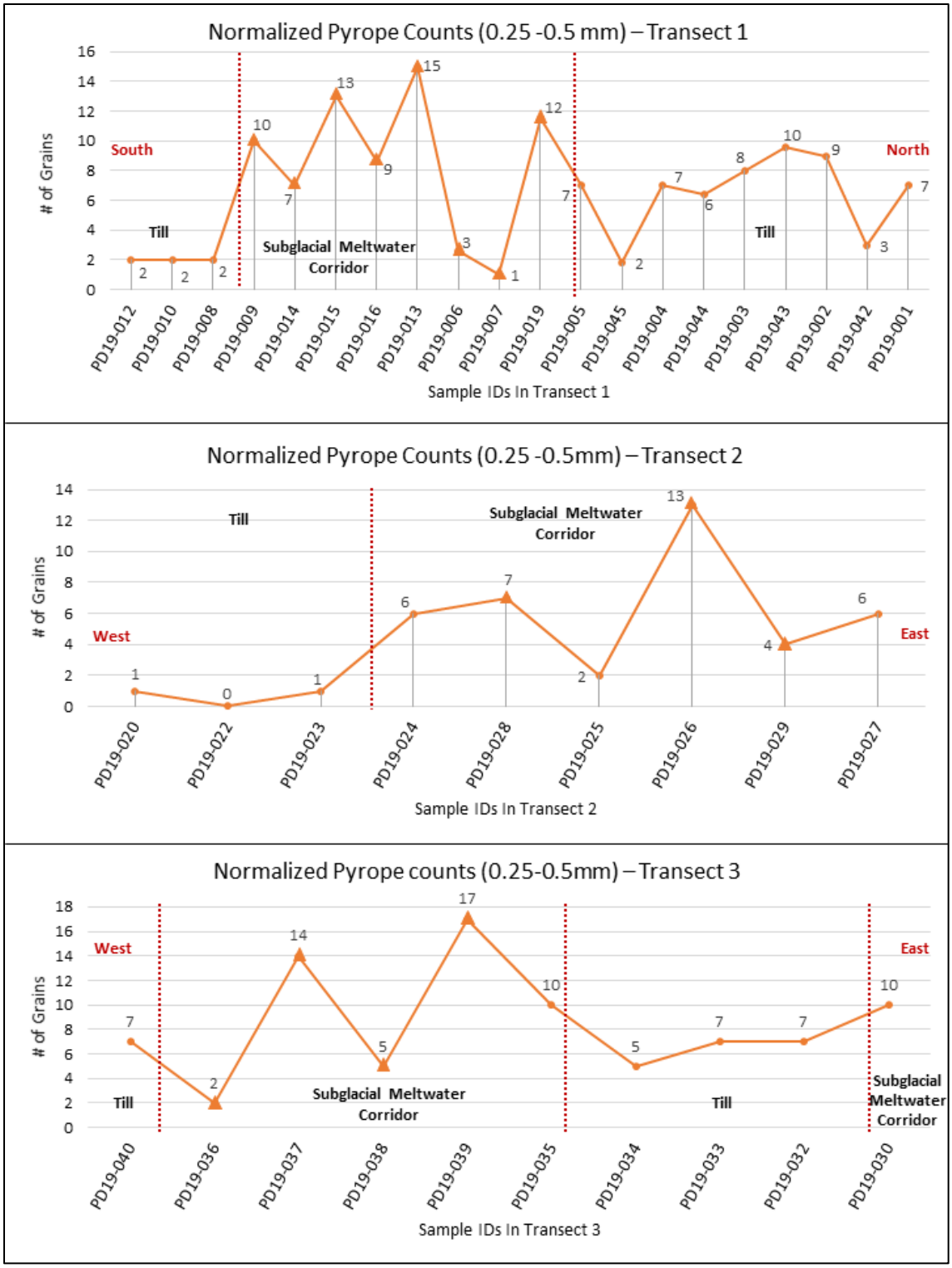

Figure 4.7: Normalized pyrope counts from the medium sand size-fraction along each transect. The X-axis shows sample ID and the Y-axis shows pyrope content. Red dashed lines indicate the approximate location of meltwater corrridor margins.Triangles indicate glaciofluvial hummock samples.

4.3.2. Discussion

There are correlations between pyrope contents and material type (till vs subglacial meltwater corridor sediments) along the three sample transects. There is higher variability amongst the meltwater corridor sediments, and on average, higher pyrope contents. Till samples generally have a lower range and fewer pyrope grains than the meltwater corridor sediments. It could be argued that thin dispersal trains occurring exclusively within the bounds of subglacial meltwater corridors are the reason for these trends. However, given that this trend is observed along all three transects, intersecting separate subglacial meltwater corridors that are several kilometres apart, the thin dispersal train argument is poorly supported. This increase in pyrope counts is likely the result of sediment genesis by deglacial meltwater processes. These meltwater processes rework and erode sediments, removing silt and clay (see Chapter 3) and thereby increase pyrope contents, when compared to a standardized 10 kg till sample.

Glaciofluvial hummock samples along each transect always contain the highest concentrations of pyropes, these samples also have the highest variability, suggesting that KIMs are not evenly distributed in glaciofluvial hummocks. The uneven distribution of pyrope in glaciofluvial hummock samples is likely related to the turbulent meltwater flow responsible for their formation (See Chapter 3). The high variability in pyrope concentrations amongst these samples highlights why it is important to consider groups of samples when evaluating anomalies as opposed to single sample anomalies.

The variability in pyrope counts between subglacial meltwater corridor sediments is interpreted to reflect the complex depositional environments in which these sediments are deposited. The time transgressive deglacial meltwater processes that form subglacial meltwater corridors vary in their capacity to rework and erode previously emplaced sediments based on how long the process is occurring in an area and the energy of the meltwater. This leads to a spectrum of reworking within these corridors from reworked till to glaciofluvial sands and gravels. These processes may lead to an unequal redistribution of KIMs. The range of meltwater reworking produces sediments with different grain size distributions, likely contributing to the variability in pyrope counts in subglacial meltwater corridor samples.

4.4. Mineral Liberation Analysis

Of the 416 visually identified pyrope grains analyzed by MLA, only four of them were determined incorrectly during the visual evaluation. The four misidentified grains were either almandine or zircon (Figure 4.8). Of the 53 visually identified Cr-diopside grains nine were determined incorrectly during the visual evaluation. Nearly all misidentified grains are epidote group minerals. These results suggest that counts of Cr-diopside grains are less reliable and more easily misidentified during the visual picking process, while pyrope grain counts are quite reliable with a lower rate of misidentification during visual picking. It should be noted that this does not consider any errors associated with any KIMs that may have been missed during visual identification.

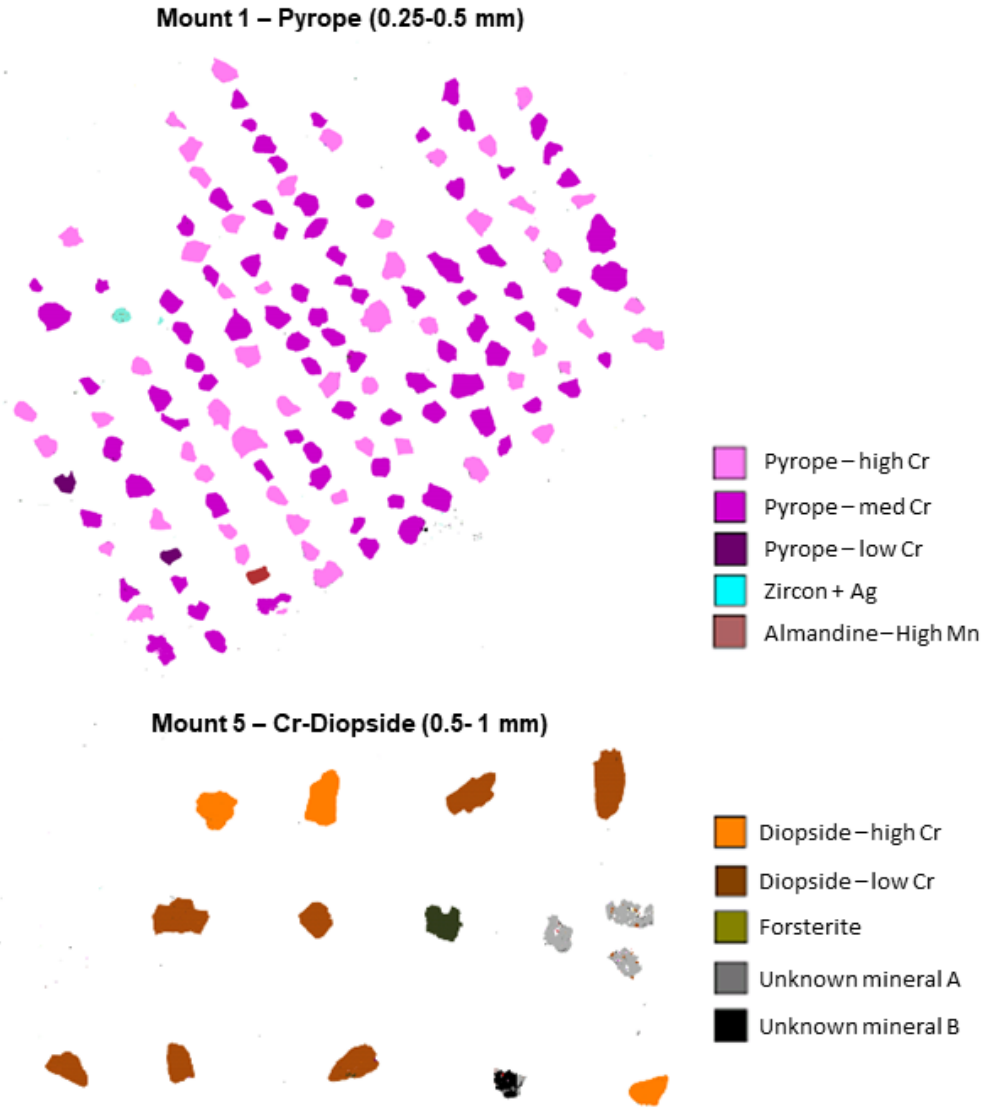

Figure 4.8: Example of false colour images displaying the results of mineralogy identification through MLA. Mount 1 includes visually picked pyrope grains between 0.25-0.5mm, mount 5 includes visually picked Cr-diopside grains between 0.5-1mm.

4.5. Mineral Chemistry

4.5.1. Pyropes

The resulting concentrations of major cations of the two-point analyses for each grain were plotted against one another and the correlation in the data analysed (e.g., Figure 4.9 for Cr_2O_3). For the major cation oxides of Cr_2O_3, MgO, and CaO, the r-squared value for each scatterplot is above 0.99 and these near perfect linear trends suggest that there is no variation in chemical composition of analysed pyropes.

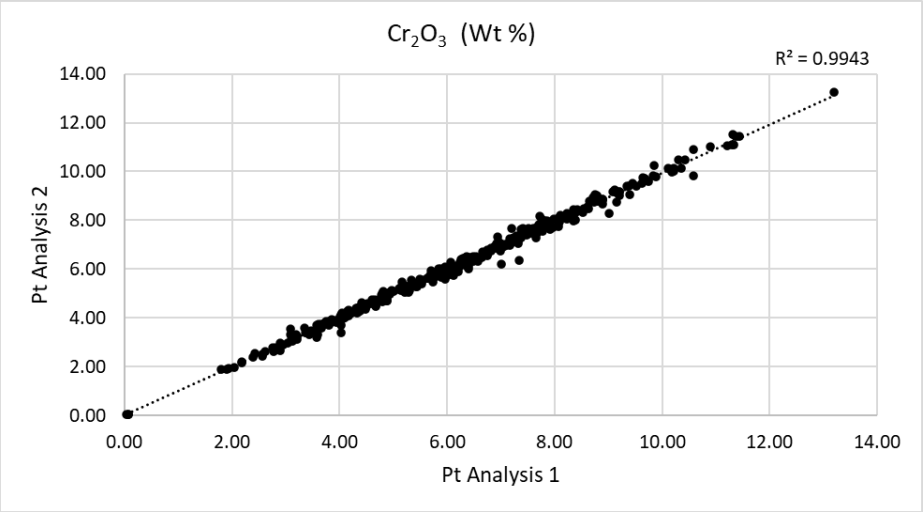

Figure 4.9: Cr_2O_3 weight percent (Wt. %) results from the central and rim microprobe measurements of each grain.

The comparison of the two microprobe measurements from each grain indicates that there is little zonation of composition, and therefore, the average of the two measurements was used for evaluation. The difference in pyrope chemistry was assessed for the samples from different material types and on different transects. Pyrope grains were grouped by transect and whether they were collected from a till sample or a subglacial meltwater corridor sample. Trends in pyrope chemistry by material type or transect may indicate differences in the bedrock source of the material and potentially aid in our understanding of the transport distances of sediments within subglacial meltwater corridors. Table 4.2 displays the average, maximum and minimum concentrations of MgO, CaO, and Cr_2O_3 for each group of pyrope grains. All pyrope chemistry results are provided in Appendix F.

Table 4.2: Summary table of pyrope mineral chemistry displaying the average, maximum and minimum values based on material type and transect.

		MgO (Wt. %)			CaO (Wt. %)			Cr_2O_3 (Wt. %)		
Transect #	**Material Group**	**Avg.**	**Max.**	**Min.**	**Avg.**	**Max.**	**Min.**	**Avg.**	**Max.**	**Min.**
Transect 1	Till (*n* = 91)	19.49	21.11	12.38	5.39	7.72	2.92	6.14	11.20	2.50
	Subglacial meltwater corridor (*n* = 154)	19.20	22.00	4.29	5.53	9.30	1.17	6.36	11.44	0.05
Transect 2	Till (n = 7)	19.78	20.53	18.39	5.56	6.76	4.87	5.65	8.62	3.08
	Subglacial meltwater corridor (n = 38)	19.54	20.83	11.62	5.48	10.59	4.20	5.93	13.23	1.89
Transect 3	Till (n = 50)	19.53	22.63	11.93	5.13	7.52	1.12	5.62	9.84	0.06
	Subglacial meltwater corridor (n = 59)	19.29	21.40	12.35	5.75	12.76	2.49	6.65	11.41	1.83

A Welch's two sample t-test was completed on the average concentrations of major cations for the till and meltwater corridor groups of pyrope grains. These t-tests were completed to determine if there is a difference in pyrope grain chemistry between the material types. The p-values for each of the completed t-tests are not statistically significant given an alpha value of 0.05, except for the major cations in the till and meltwater groups of Transect 3. This means that for the pyrope grains recovered from transect three we can reject the null hypothesis that pyropes recovered from till and meltwater corridor sediments have the same average weight percentage of major cations (Cr, Ca, Mg). For Transects 1 and 2 we cannot reject the null hypothesis that pyropes recovered from till and meltwater corridor sediments have the same average chemistry.

Pyrope grains were characterized based on their Cr_2O_3 and CaO contents following the mantle derived pyrope composition and diamond inclusion studies of Gurney (1984) and Grütter and others (2004) (Figure 4.10). The graph also displays the graphite – diamond constraint of Grütter and Sweeney (2000) that uses Cr_2O_3 concentrations within the G10 pyropes as a barometric constraint for diamond potential. Plotted pyropes are symbolized based on material type and transect. Most pyropes are lherzolitic in composition falling within the compositional constraints of G9. Approximately 5% of recovered pyropes fall within the G12 compositional constraints suggesting they are wehrlitic in origin. Of the wehrlitic pyropes most of them were recovered from meltwater corridor sediments and only one of these pyropes came from a meltwater corridor sample along Transect 2. Approximately 10% of recovered pyropes fall within the G10 compositional constraint making them harzburgitic in composition. Of the G10 pyropes, 8 of them fall above the graphite-diamond constraint meaning that these pyropes have a high potential to be associated with diamond bearing kimberlites. A nearly equal proportion of recovered G10 garnets came from till vs meltwater corridor samples, and only one G10 pyrope was recovered from a meltwater corridor sample along Transect 2.

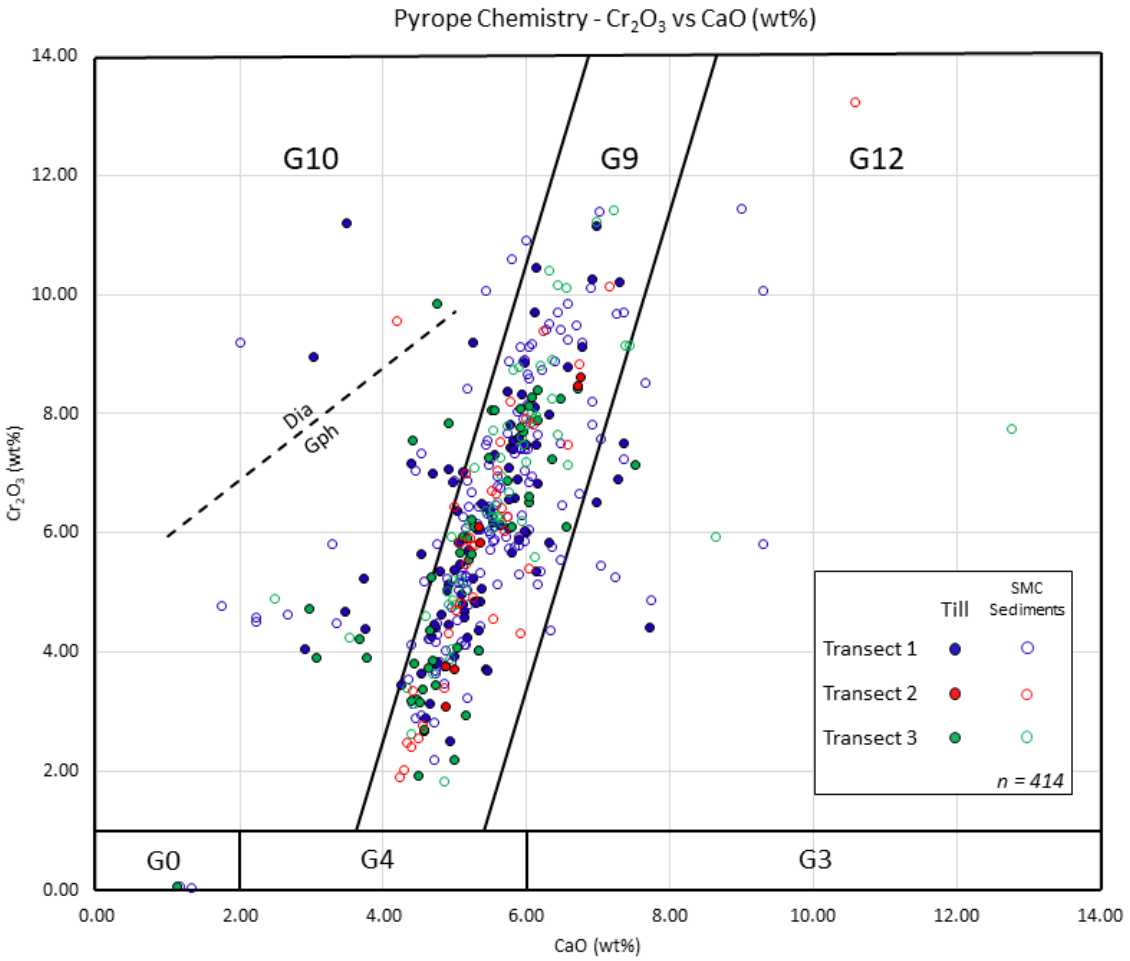

Figure 4.10: Bi-variate pyrope composition plot modified from Grütter et al., 2004. Solid lines indicate the compositional constraints of each "G" type. The dashed line represents the diamond graphite constraint. Pyropes are symbolized based on transect and material type.

Most of the G10 pyropes come from Transect 1 and the surrounding area (Figure 4.11). The relatively high concentration of G10 pyropes from this area, especially given that many were recovered from unmodified till, is worth future investigation. The higher G10 pyrope contents in till and subglacial meltwater corridor sediments collected from Transect 1 suggest these samples are more likely related to kimberlites and targeted sampling in this area may reveal kimberlite dispersal trains.

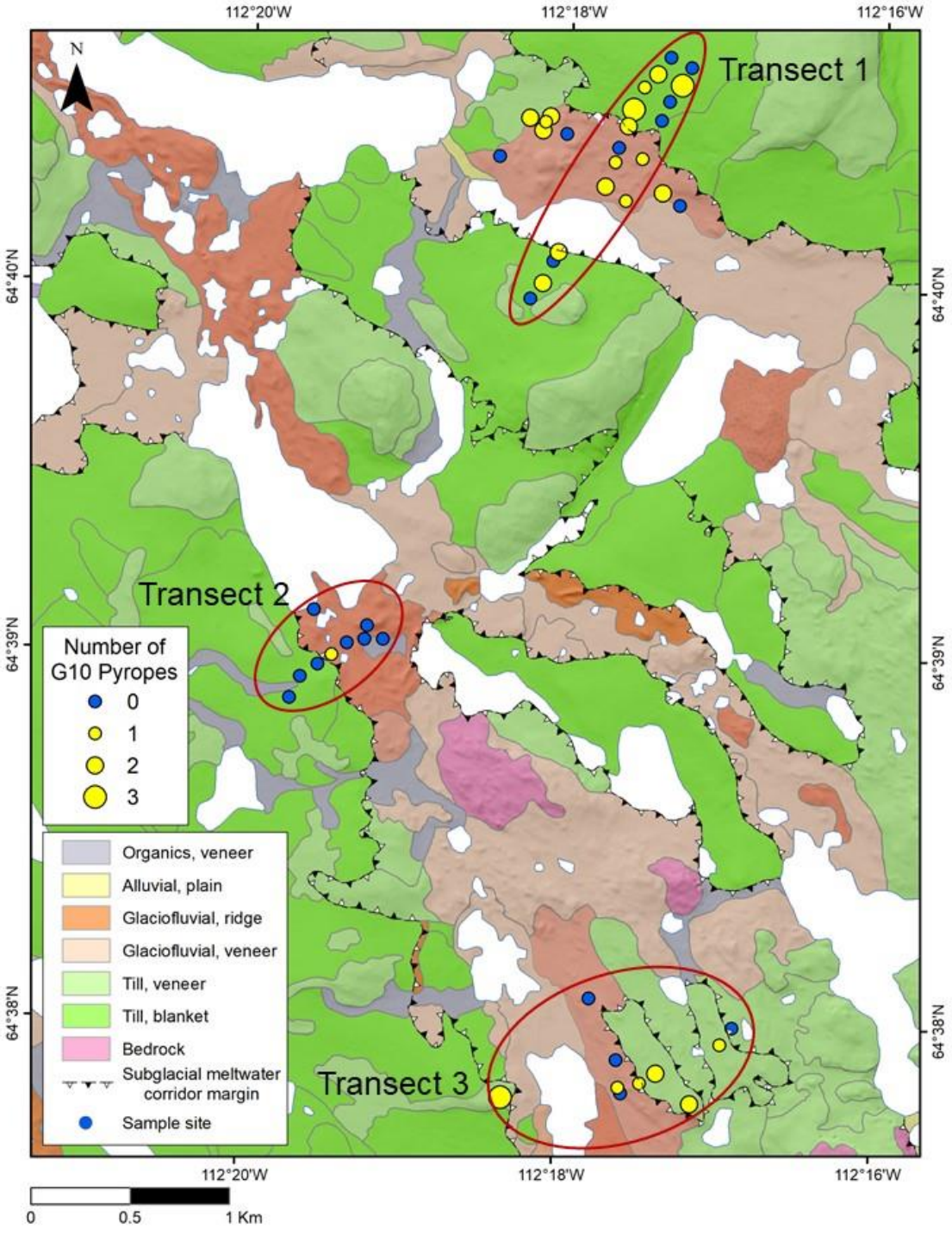

Figure 4.11: Surficial geology map displaying the spatial distribution of G10 pyropes.

Pyropes recovered from Transect 1 have high variability in Cr_2O_3 and CaO compositions (Figure 4.10; Table 4.2). They account for most of the recovered G10 pyropes and 75% of the G10 pyropes plotting above the graphite-diamond constraint (Figure 4.10). These results indicate potential for a diamondiferous kimberlite source associated with these pyropes in the direction inverse to ice flow. Pyropes recovered from Transect two have the least variability in Cr_2O_3 and CaO compositions, with all but two of these pyropes plotting within the G9 compositional constraints.

When looking at variability in Cr_2O_3 and CaO compositions of pyropes collected from till vs meltwater corridor sediments, pyropes recovered from meltwater corridor sediments have a much wider range of compositions than that of pyropes collected from till. This is evidence that meltwater corridor sediments are likely sourced from a wider region than till and include sediments with various provenances. This reflects the derivative nature of meltwater corridor sediments and their more complex transport history.

4.5.2. Cr-Diopside

A minimum of two microprobe analysis measurements were collected from each Cr-diopside grain to determine if there was chemical zonation. As an example, the scatterplot displaying CaO concentrations by point analysis for each Cr-diopside grain is displayed in Figure 4.12. This test was repeated for the major cation oxides of FeO, MgO, and CaO and the r-squared value for each scatterplot is between 0.74 and 0.81. Based on the r-squared value of the relationship there is evidence for zonation in chemistry for two of the Cr-diopside grains.

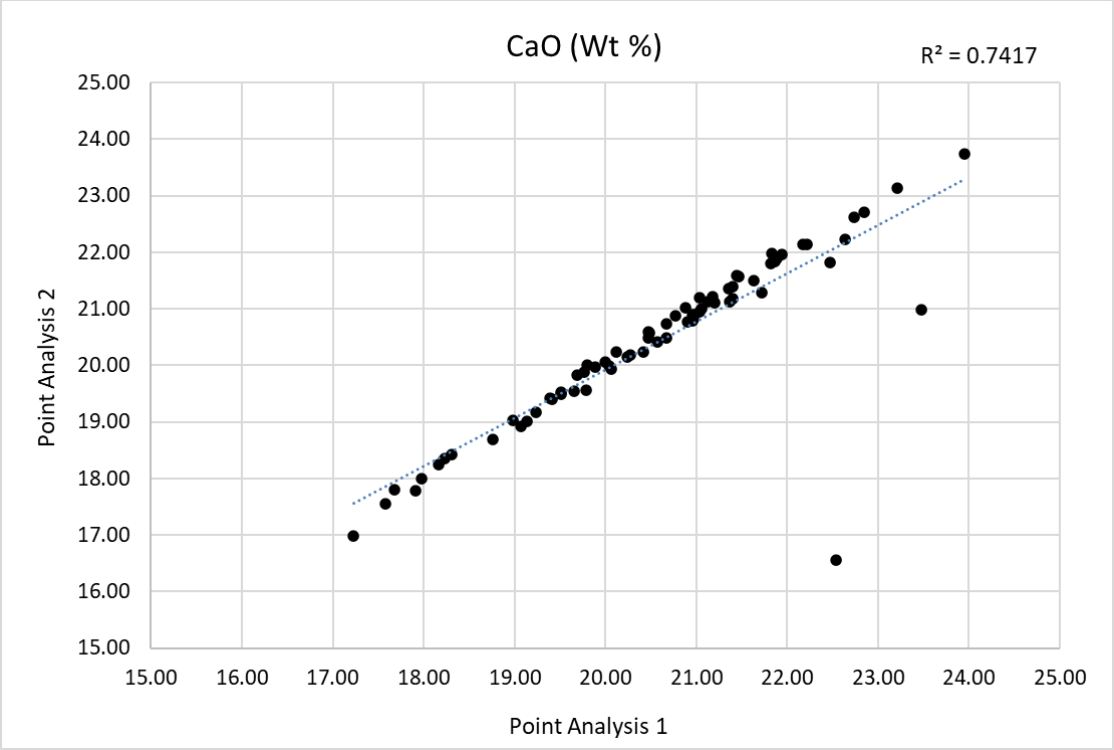

Figure 4.12: Scatterplot with line of best fit for CaO Wt.% for the two electron microprobe point analysis completed on Cr-diopside grains.

Since it was determined that Cr-diopside chemistry is not consistent between point analyses within each grain, each point analysis was used as a data point in analysis of the Cr-diopside mineral chemistry results.

Cr-diopside chemistry was analysed based on material type and transect. Cr-diopside grains were grouped by which transect they were recovered from and whether they were collected from till or meltwater corridor sediments. Table 4.3 displays the average, maximum and minimum concentrations of FeO, MgO, and CaO for each group of Cr-diopside grains. All Cr-diopside chemistry results are available in Appendix F

Table 4.3: Summary table of selected major cation Cr-diopside mineral chemistry displaying the average, max and min values based on material type and transect.

		FeO (Wt. %)			MgO (Wt. %)			CaO (Wt. %)		
Transect #	**Material Group**	**Avg.**	**Max**	**Min**	**Avg.**	**Max**	**Min**	**Avg.**	**Max**	**Min**
Transect 1	Till (n = 42)	2.96	4.63	2.36	17.13	19.43	15.58	20.89	22.74	18.16
	Subglacial meltwater corridor (n = 54)	2.91	3.79	1.75	17.29	19.35	15.26	20.47	23.48	17.79
Transect 2	Till (n = 2)	4.47	4.50	4.45	15.88	15.88	15.88	21.90	21.97	21.84
	Subglacial meltwater corridor (n = 32)	3.14	7.98	2.27	17.44	19.30	15.69	20.04	22.54	16.56
Transect 3	Till (n = 8)	2.80	3.59	2.35	17.27	17.90	16.65	20.90	23.95	18.91
	Subglacial meltwater corridor (n = 12)	2.89	3.84	2.11	17.77	19.68	16.51	19.61	21.13	16.98

There are only two-point analysis for the till group of Cr-diopsides along Transect 2, and therefore, this transect should not be used to make interpretations regarding variability in Cr-diopside chemistry amongst material groups. Otherwise, the average weight percent oxides of major cations (Fe, Mg, Ca) are consistent between till and meltwater corridor groups for Transect 1 and Transect 3 suggesting that there is no difference in Cr-Diopside chemistry between till and meltwater corridor sediments.

To determine if the mineral chemistry of the recovered Cr-diopside grains is consistent with Cr-diopside chemistry from known kimberlite sources, ternary plots of Cr-diopside chemistry were created as a tool for screening the origin of Cr-diopside grains (Crabtree, 2003; Fipke et al., 1989; Morris et al., 2002; Quirt, 2004).

Figure 4.13 displays the relative Wt. % oxides of Ca, Mg, and Fe of each Cr-diopside point analysis plotted on a wollastinite-enstatie-ferrosilite ternary diagram. The compositional range associated with kimberlites as described by Quirt (2004) is displayed by the thick dashed line. Grains are symbolized based on the transect and material type that the grain was recovered from.

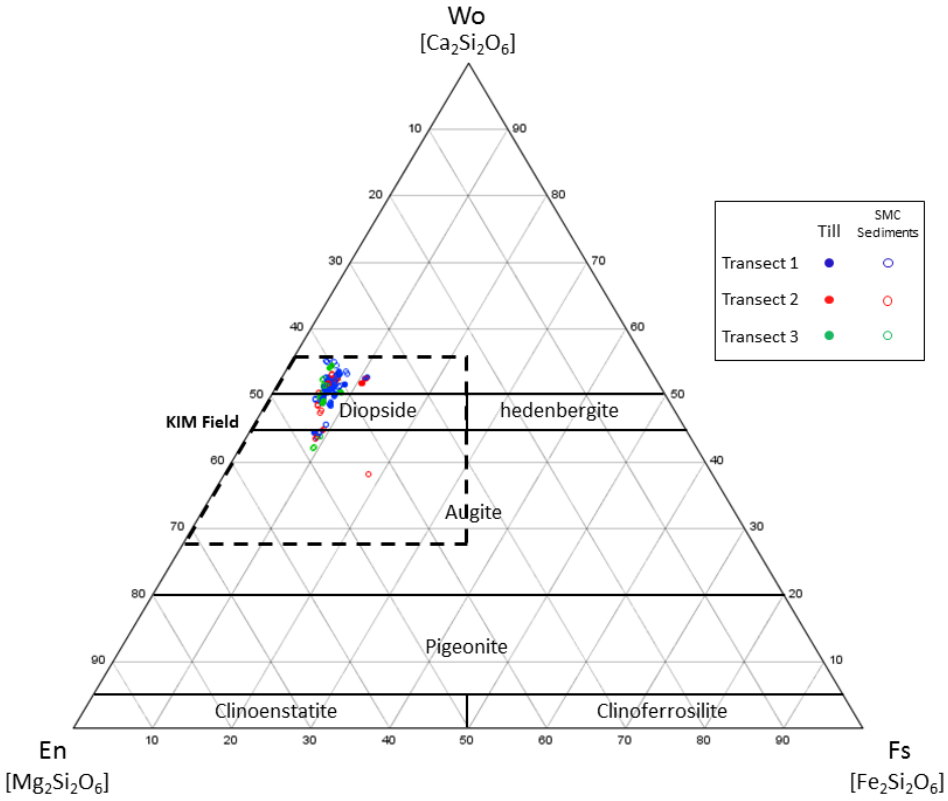

Figure 4.13: Wo-En-Fs composition ranges for Cr-diopside grains. Cr-diopside point analysis are symbolized based on transect and material type. Dashed line represents compositional range associated with kimberlites (Quirt, 2004)

All Cr-diopside grains plot within the compositional ranges consistent with Cr-diopside grains recovered from kimberlite (Figure 4.13). Most of the Cr-diopside compositions plot in a tight grouping centered near the upper boundary of diopside field. The only real outlier is a grain from Transect 2 (#28) that has low Ca and high Fe compared to the other grains and plots within the augite field. Regardless, this grain plots in the KIM field and the second analysis on the same grain has a composition more consistent with other grains. There is no clear variation or groupings of grains based on the material type or transect from which the grains were recovered.

The geochemical composition of Cr-diopside grains was evaluated for consistency with kimberlitic Cr-diopside based on there Cr, Al, and Na concentrations following the methods of Morris et al. (2002). Figure 4.14 displays the Al-Cr-Na ternary cation plot with the kimberlite xenolith and xenocrystal compositional field of Morris et al. (2002). The geochemical compositions of eight Cr-diopside grains along Transects 1 and 2 indicate

they fall outside of the kimberlite xenolith and xenocryst field, suggesting that these grains are not kimberlitic in origin. All Transect 3 Cr-diopside compositions plot within the kimberlite xenolith and xenocryst field.

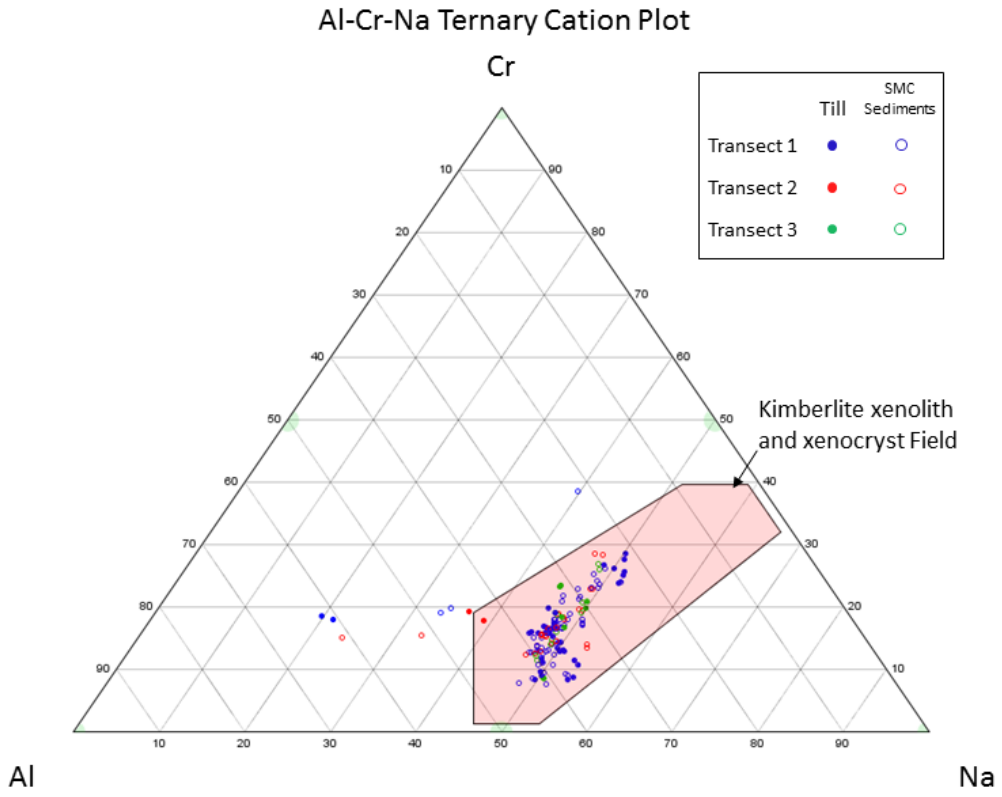

Figure 4.14: Al-Cr-Na ternary cation plot displaying the 85% field for kimberlite xenoliths and xenocrysts of Morris et al., 2002. Cr-diopside point analysis are symbolized based on transect and material type.

Multiple compositional screenings should be used in conjunction with one another to confirm the kimberlitic origin of visually identified Cr-diopside grains. Based on the results of both ternary plots completed as a means of screening Cr-diopside composition for a determination of origin, it is suggested that most if not all Cr-diopside grains are kimberlitic in origin. However, it should be noted that each individual plot is not perfect as it has been shown from other studies that some kimberlitic Cr-diopsides fall outside compositional ranges in kimberlites and many non-kimberlitic Cr-diopsides fall within these ranges (Quirt, 2004).

It is suggested that Cr-diopside contents only be used to assess kimberlite potential following mineral chemistry analysis. The results indicate a higher percentage of

misidentified visually picked Cr-diopside grains and the limits of compositional constraints for kimberlite and diamond inclusion derived Cr-diopside grains.

4.6. Geochemistry

4.6.1. Results

Table 4.4 displays summary statistics of concentrations for a selected set of elements with sample groups defined by transect number. The elements in the summary table include known kimberlite pathfinder elements (McClenaghan and Kjarsgaard, 2001) and four elements that had a high average value and range across the transects. A complete table of geochemistry results is available in Appendix G.

Table 4.4: Concentration (ppm) summary statistics for a selected set of pathfinder and high average and range elements. Summary statistics are sorted based on transect location.

Transect #	Summary Stat	Ba	Co	Cr	Nb	Ni	Rb	Sr	Ta	As	Cu	Sc	V	Zn
Transect 1 (n = 20)	Average	439.65	8	17.56	6.51	20.3	65.42	216.15	0.7	20.41	21.25	6.35	46.7	33.15
	Maximum	533	11	21.5	8.2	27	76.8	246	1.2	37.6	31	7	59	52
	Minimum	386	6	13.75	5.2	15	54.8	188.5	0.5	9.3	11	6	36	26
	Range	147	5	7.75	3	12	22	57.5	0.7	28.3	20	1	23	26
Transect 2 (n = 9)	Average	450.67	13.33	33.72	6.71	33	60.09	220.44	0.59	29.86	58.78	8.44	66.67	52.22
	Maximum	600	34	58.1	8.8	74	74.2	264	1	89.4	225	14	116	125
	Minimum	314	7	12.15	4.8	16	48.7	187	0.4	8.7	15	5	39	20
	Range	286	27	45.95	4	58	25.5	77	0.6	80.7	210	9	77	105
Transect 3 (n = 10)	Average	428.3	12.1	26.475	6.1	30.2	68.03	211.05	0.64	20.66	43.9	7.3	58.8	34.2
	Maximum	487	31	52.3	7.1	88	73	227	0.9	37.3	135	10	82	50
	Minimum	363	6	13.15	5	16	65	173.5	0.4	11.4	23	6	45	24
	Range	124	25	39.15	2.1	72	8	53.5	0.5	25.9	112	4	37	26

4.6.2. Discussion

For each transect, geochemical concentrations in the silt and clay size-fraction of the samples were evaluated to identify correlations related to material type. No correlations were identified for the kimberlite pathfinder elements (Figure 4.15). No correlations between material type and geochemistry of the other elements examined (See Appendix G) were observed along any of the three transects.

Ni, Cr and Co concentrations determined through lithium metaborate fusion and inductively coupled plasma mass spectrometry have low variability across Transect 1 and no trends are observed between elemental concentrations and material type. Ni, Cr and Co concentrations along Transects 2 and 3 also have low variability in the till samples and higher variability in the meltwater corridor samples, with one or two samples having elevated concentrations in the corridors. Samples that have elevated values of Ni, Cr, and Co are sample PD19-026 on transect two and PD19-036 on transect three. It should be noted that PD19-026 also has elevated pyrope counts and sample PD19-036 has a low pyrope count (Figure 4.7), suggesting that there may not be a strong correlation between kimberlite pathfinder element concentrations and pyrope counts. However, the general trends along these transects indicate that there is no correlation between pathfinder element concentrations and material type, beyond outliers being found in meltwater corridor samples.

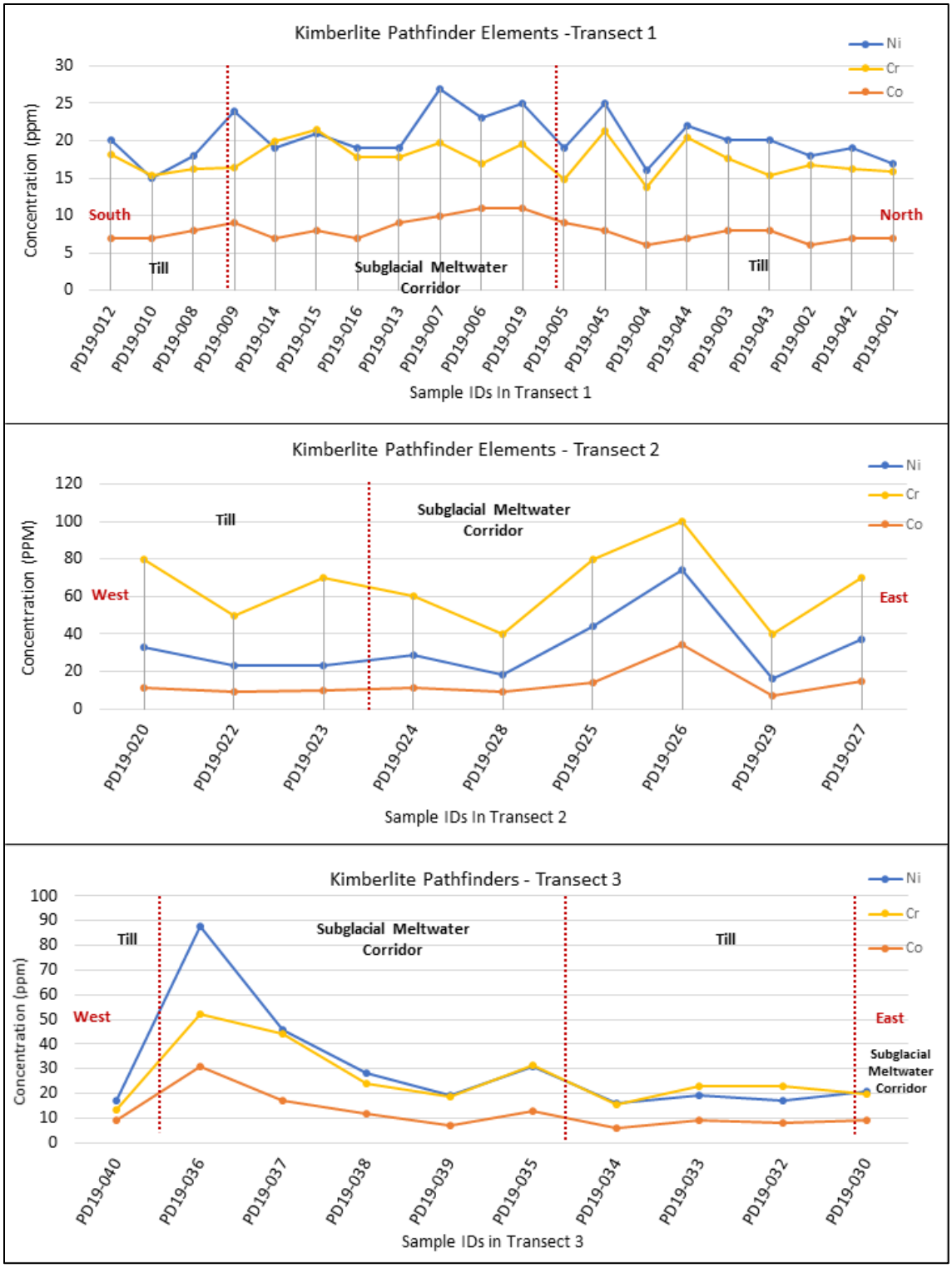

Figure 4.15: The concentration of Ni, Cr, and Co in samples along each of the three transects. The X-axis shows sample ID and the Y-axis shows concentration in ppm. The red dashed lines indicate the approximate location of subglacial meltwater corridor margins.

The similar matrix geochemical compositions of till and subglacial meltwater corridor sediment samples taken from all three transects may indicate that these materials are not from geochemically distinct sources. It is possible that this result indicates that these materials are sourced from similar locations or derived from sediments with a similar provenance. If till and subglacial meltwater corridor sediments are sourced from similar locations, it suggests that the transport distance of subglacial meltwater corridor sediments is relatively short and similar in distance to that of surrounding till.

4.7. Implications for Drift Prospecting

The results of KIM analysis have significant implications for drift prospecting in areas where subglacial meltwater corridors are present. The elevated counts of pyropes in subglacial meltwater corridor sediments with similar characteristics to till could be misinterpreted in a mineral exploration program. These sediments are likely to have elevated counts of KIMs compared to unmodified till as a result of decreased silt and clay content and increased sand content due to deglacial meltwater processes that have winnowed the sediments. Sampling subglacial meltwater corridor sediments and comparing analytical results to till samples should therefore be avoided during exploration in the SGP. Anomalies observed in subglacial meltwater corridors must be properly interpreted, taking into consideration the secondary transport of the materials.

If subglacial meltwater corridors and meltwater modification are widespread through the exploration property, sampling within subglacial meltwater corridors may be necessary. These samples transport histories should be treated similar to esker sediments in the interpretation of KIM results, by considering the secondary transport vector. Subglacial meltwater corridor sediments, including glaciofluvial hummocks, are a second derivative of bedrock and can be used as a vector towards mineralization by sampling upstream within subglacial meltwater corridors. The furthest upstream anomalies can be used as an indication of where alternative exploration such as geophysical surveys or till sampling programs should be initiated.

To avoid misinterpretation of material types and analytical results, Quaternary geologists should complete high-resolution property scale surficial geology mapping before drift sampling campaigns. These maps could be used as sampling suitability guides, showing any areas that should be avoided (eg., Sacco et al., 2018) or where changes in material

types should be evaluated with respect to compositional changes. During drift prospecting campaigns, the individuals collecting sediment samples should be trained to identify material types and changes in grain sizes amongst samples. This would allow for a better analysis of sample results and interpretation of collected materials.

4.8. Conclusions

A sediment sampling program targeting till and sediments collected in subglacial meltwater corridors was completed to determine if there was a difference in KIM concentrations between these materials. KIMs were recovered, matrix geochemistry determined, and indicator mineral chemistry assessed. The data was analysed for trends to evaluate differences in these datasets between material type and spatial distribution of anomalies. Key findings include:

1. Pyrope is the most abundant KIM recovered from the sediment samples in the Beauparlant study area. The high concentrations of pyrope grains, coupled with well defined chemical constraints that allow for prediction of diamond fertility, make the indicator mineral method useful for diamond exploration in the study area and likely in the surrounding region.

2. Sediments within subglacial meltwater corridors, have higher average concentrations of pyrope grains than till samples. This means the delineation of subglacial meltwater corridors is imperative when analysing KIM datasets. The difference in pyrope counts is likely attributed to the removal of silt and clay by meltwater, which results in a relative increase in the sand size-fraction that is picked for KIMs (see chapter 3), as compared to the till samples.

3. Matrix geochemistry of the silt and clay size-fraction of sediment samples is consistent between till and subglacial meltwater corridor sediments. Pyrope chemistry is consistent across till and meltwater corridor sediments except in samples collected from Transect 3. These general trends suggest that meltwater corridor sediments are derived from till with the same mineral chemistry and geochemistry as adjacent unmodified till. This could mean that meltwater corridor sediments are sourced from relatively near-by till and have a relatively short transport distance.

4. Evaluating the chemistry of pyrope grains revealed that 10% of pyrope grains are harzburgitic in composition and fall within the G10 field of Cr_2O_3 and CaO compositions. Most G10 pyropes were recovered from Transect 1 and the surrounding area. Eight of the pyropes plot above the graphite – diamond constraint in the G10 field. These results indicate potential for a diamondiferous kimberlite source associated with these pyropes.

5. Cr-diopside can be mistaken for the epidote group of minerals during visual picking. Mineral chemistry analysis of recovered Cr-diopside grains is required to confirm mineralogy and determine mineral source before assessing spatial distribution of Cr-diopside counts.

The results of this study reveal that there is a difference in KIM concentrations between till and subglacial meltwater corridor sediments. It is imperative that subglacial meltwater corridors be delineated and considered during drift prospecting projects to ensure that results are properly interpreted. KIM chemistry analysis is a critical step in confirming mineralogy and kimberlitic source of recovered mineral grains. Future work into determining transport distances of subglacial meltwater corridor sediments would be useful for interpreting data collected from these sediments.

Chapter 5. Summary and Conclusions

This chapter summarizes the key findings of this project and how they relate to the research question: how do deglacial meltwater processes affect the concentrations of KIMs in meltwater modified sediments? In answering the research question of this thesis, several additional questions have arisen, which are presented in a discussion of future research to build on the knowledge gained from this study. A discussion of the limitations of the findings of this study is also presented.

5.1. Project Summary and Key Findings

To effectively answer the main research question, several smaller research objectives were generated. A summary of key findings of this project are presented and characterized based on the associated research objective.

The research objectives of this project are:

1. Determine the nature, genesis, and distribution of glacial sediments in the area.
2. Refine the glacial history of the area.
3. Quantify sedimentological differences between glacial sediments.
4. Determine concentrations of KIMs.
5. Determine indicator mineral chemistry and matrix geochemistry and compare across material types.

5.1.1. Nature, Genesis, and Distribution of Glacial Sediments

The surficial geology was interpreted at a scale of 1:15 000 to inventory and determine the distribution of surficial materials. Before undertaking this project, the distribution of sediments in the study area were known through the small-scale regional mapping of the Winter Lake map area (Kerr et al., 1996). Our new larger scale mapping reveals a more detailed distribution of sediments. Six surficial materials were identified in the area that occur as a range of surface expressions. In order of most to least prevalent, surficial

materials consist of till, glaciofluvial sediments, organics, bedrock, glaciolacustrine sediments, and alluvial sediments. The mapping reveals subglacial meltwater corridors contain a complex distribution of sediments and landforms: veneers of glaciofluvial sand and gravel, reworked till, bedrock, and meltwater related landforms including eskers, deltas, and glaciofluvial hummocks. In previous mapping, these corridors only included glaciofluvial materials and bedrock, and the reworked till was not identified (Dredge et al., 1994; Kerr et al., 1996; Ward et al., 1997). The identification of these processes has significant importance to surficial mineral exploration program planning and interpretation.

Based on the distribution, sediment-landform associations, and sedimentology determined in the subglacial meltwater corridors, a possible model for the genesis of glaciofluvial hummocks was interpreted. Glaciofluvial hummocks are located downflow from areas of scoured bedrock in subglacial meltwater corridors. Remnants of reworked till that indicate incomplete erosion are also located up-flow from the hummocks. It is suggested that these areas of bedrock represent a potential source area of the sediments that make up glaciofluvial hummocks. It is likely that these areas were covered by till before deglacial meltwater eroded down to bedrock. This material would be deposited as glaciofluvial hummocks in the down flow direction.

The findings of the sedimentological investigation indicate that observed glaciofluvial hummocks in the study area are composed of sandy diamicton with less silt and clay than till, signifying the material is distinct from eskers, glaciofluvial outwash and till. The observed glaciofluvial hummocks are poorly sorted and no stratification was observed. This suggests that steady state sustained meltwater flow that leads to sorting and stratification are not responsible for the formation of these landforms. For the observed sediment properties to occur in these hummocks (sandy diamicton, poor sorting, lack of stratification) it is likely that turbulent high energy flow and rapid deposition was responsible for their formation.

One possible explanation for the genesis of glaciofluvial hummocks is that a large volume of meltwater reached the ice-bed interface, eroding and transporting existing glacial sediments in a slurry like mixture as it travelled along the channelized drainage system. The hard bedrock resisted erosion and most of the energy of the turbulent flow was directed up into the ice, providing accommodation space for sediment transport and then deposition; silt and clay was removed as flow waned. This process must have had enough

energy to transport the observed boulders and be rapid enough to stop sorting or stratification during deposition.

5.1.2. Glacial History

The regional glacial history was determined through 1:125 000 surficial geology mapping and ice flow indicator measurements of the Winter Lake, Lac de Gras and Aylmer Lake map areas (Dredge et al., 1994; Dredge et al., 1995; Kerr et al., 1996; Ward et al., 1997). The local glacial history matches the glacial history of the wider region. Ice flow indicators measured during this project record the earlier ice flow directions encountered in the Lac de Gras and Aylmer Lake areas, which had not previously been observed in the Winter Lake map area.

The distribution and genesis of sediments observed are a function of the glacial history of the area. During the Late Wisconsinan glaciation, till formed and was deposited at the base of the LIS as blankets and veneers. The dominant ice-flow direction to the northwest is indicated by streamlined bedforms such as crag-and-tails and striations. During deglaciation, glaciofluvial and glaciolacustrine sediments were deposited by meltwater. Meltwater was focused in corridors, eroding till and depositing eskers, hummocks, and veneers of sand and gravel. These corridors are indicated on the map by sublinear assemblages of glaciofluvial deposits, scoured bedrock and discontinuous till deposits that have been modified by meltwater.

The large-scale mapping provides a higher resolution for the distribution of sediments and landforms found in meltwater corridors, allowing for refinement of the depositional history of these features. Given the observed geomorphic relationships, meltwater corridor features represent the combined result of episodic meltwater events occurring in a time-transgressive manner as the glacier retreated. First meltwater eroded previously emplaced sediments and bedrock, then deposited glaciofluvial hummocks, and finally deposited eskers and glaciofluvial sands and gravels.

Glaciolacustrine sediments were deposited in transient glacial lakes that formed in depressions in front of the retreating ice as represented by shorelines and rare deposits of silt and clay. Holocene deposits are dominantly organics that form in poorly drained areas and rare alluvial deposits in small creeks. Permafrost is ubiquitous and has modified

all existing surficial materials to various degrees, as evidenced by the pervasive frost boiling of till and ice-wedge polygons in sandy deposits.

The study of surficial geology and glacial history of the Beauparlant Lake area was required to delineate subglacial meltwater corridors, sediments reworked by meltwater processes and all other sediments in the area. This step was necessary so that the effects of deglacial meltwater processes on KIMs samples could be effectively evaluated. The applications of surficial geology mapping and glacial history reconstruction can be applied to property scale surficial mineral exploration. This glacial history aids in our understanding of transport history of the sediments in the area and ice-flow histories can be used to aid in the interpretations of surficial exploration datasets. The recognition of areas modified by meltwater can aid in planning of sediment sampling programs and the interpretation of anomalies found in these sediments.

5.1.3. Sedimentology of Glacial Deposits

Grain size and pebble lithology analyses were completed on 46 sediment samples collected from three sampling areas. Sampling areas are focused across subglacial meltwater corridor margins. Samples include unmodified till and sediments collected within subglacial meltwater corridors. Meltwater corridor samples include a range of sediments: reworked till, glaciofluvial sand and gravel and glaciofluvial hummock sediments. Given the focus on glaciofluvial hummocks, samples collected from hummock landforms have been categorized together. Before this study, it was thought that there was a difference in grain size distribution between glaciofluvial hummocks and till, however a focused study on the grain size of glaciofluvial hummocks had not been completed.

The results of this study confirm that there is a significant difference in the grain size distributions in till and glaciofluvial hummocks. Till samples have more silt and clay than glaciofluvial hummocks and other sediments in subglacial meltwater corridors. This reflects the difference in depositional processes between till and glaciofluvial hummocks. This result supports the hypothesis that glaciofluvial hummock sediments have been modified by meltwater and provides a potential explanation for the higher KIM contents observed in subglacial meltwater corridor sediments.

Differences in the grain size distributions of subglacial meltwater corridor sediments and till should be considered during drift prospecting programs. A meltwater corridor sample containing less silt and clay than a till sample could have increased concentrations of indicator minerals as the relative percentage of sand size-fractions containing indicator minerals will be higher in the meltwater modified sample. Therefore, the KIM results from samples collected from within subglacial meltwater corridors should not be compared to those in till samples.

5.1.4. Kimberlite Indicator Mineral Counts

It was hypothesized that deglacial meltwater processes responsible for the change in grain size distribution between till and glaciofluvial hummocks may affect KIM concentrations. Pyrope is the most abundant KIM recovered during this study. The abundance of pyrope coupled with well-defined diamond fertility chemical constraints make it the most useful KIM for analysis.

There is a difference in pyrope concentrations amongst till and meltwater corridor sediments. Sediments within the subglacial meltwater corridors, have higher average contents of pyrope grains than till samples. This means the delineation of subglacial meltwater corridors is imperative when analyzing KIM datasets. The difference in pyrope counts is likely attributed to meltwater processes that remove silt and clay leading to a relative increase in sand size-fractions picked for KIMs.

Subglacial meltwater corridor sediments should be avoided as a sampling medium as they can be mistaken for till and have a different transport history. If samples must be collected from within subglacial meltwater corridors because of location and scale of sampling grid, the results must not be compared to till samples directly; differences in transport and depositional histories will result in concentration of KIMs in the corridor sediments. Instead, the sample transport history should be interpreted in a similar way to esker sediments, with an understanding that they are a second derivative of bedrock and have a more complex transport history. To use these sediments as a vector towards mineralization you first must trace the anomaly up flow along the meltwater corridor before conducting further till-based exploration closer to the source.

5.1.5. Mineral Chemistry and Matrix Geochemistry

KIM chemistry and matrix geochemistry datasets were compared between till and meltwater corridor sediments to establish trends that may suggest differences in depositional history and thus provenance. Matrix geochemistry is consistent between till and subglacial meltwater corridor sediments. The chemistry of pyrope grains is consistent for till and sediments within the meltwater corridors, except for samples collected from Transect 3. These general trends suggest that meltwater corridor sediments are derived from till with the same mineral chemistry and geochemistry as adjacent unmodified till. This could mean that meltwater corridor sediments are sourced from relatively nearby till and have a relatively short transport distance.

The chemistry of pyrope grains reveals that 10% of pyropes are harzburgitic in composition falling within the G10 field of Cr_2O_3 and CaO compositions. Of the G10 pyropes, eight of them fall above the graphite-diamond constraint meaning that these pyropes have a high potential to be associated with diamond bearing kimberlites. Most G10 pyropes were recovered from Transect 1 and the surrounding area. The relatively high concentration of G10 pyropes from this area, especially given that many were recovered from unmodified till is worth future investigation. The higher G10 pyrope contents in till samples collected from Transect 1 suggest these samples are more likely related to diamond bearing kimberlites and targeted sampling in this area may reveal kimberlite dispersal trains in till.

Of the 53 visually identified Cr-diopside grains, mineral chemistry analysis revealed that 9 of them had been misidentified. Mineral chemistry analysis show that these misidentified grains were all epidote group mineral grains. This suggests that the epidote group of minerals can be mistaken for Cr-diopside grains during visual indicator mineral picking. Therefore, mineral chemistry analysis of Cr-diopside grains is crucial to confirm mineralogy. Mineral chemistry analysis can also aid in the determination of mineral source which can improve the delineation of dispersal patterns and provide more accurate exploration targets.

5.2. Future Work

5.2.1. Repeatability

This is one of the first academic studies to assess the effects of deglacial meltwater on KIM concentrations in subglacial meltwater corridor affected sediments. The results of this study show promising correlations between KIM counts and material type as it relates to sedimentology and deglacial meltwater processes. These results have important implications for diamond exploration. This was a relatively small study with three short transects composed of 20 samples or less that are within 10 km of each other. The study area is small enough that it cannot account for regional differences in subglacial meltwater corridor characteristics. Therefore, the replication of this study in other parts of the diamond prospective SGP are needed to increase the confidence in the observed correlations.

The repeatability of this study would be best assessed in an area with a known kimberlite source and associated dispersal train in subglacial till that is crosscut by a subglacial meltwater corridor. This would assure high KIM counts in both unmodified subglacial till and subglacial meltwater corridor sediments and allow for direct comparison between material groups.

5.2.2. Transport History and Material Source

During this project, a new question arose: what is the transport history of subglacial meltwater corridor sediments, and more specifically where is the source of glaciofluvial hummock sediment? Understanding the transport histories of subglacial meltwater corridor sediments is important if we are to effectively interpret exploration datasets from these sediments. Beyond applications in mineral exploration, an understanding of transport history of subglacial meltwater corridor sediments would allow for further interpretation of the genesis of these features and the landforms that we find within them.

A longitudinal study of clast lithology and angularity along a subglacial meltwater corridor that crosscuts chemically and mineralogically distinct bedrock units would be very useful in developing a range of transport distances experienced by the materials found in subglacial meltwater corridors.

5.2.3. Sediment Reworking by Meltwater

This thesis focused on sediment reworking associated with erosional deglacial meltwater processes responsible for the formation of subglacial meltwater corridors. However, sediment reworking caused by short-lived glacial lakes are likely to have influences on material sedimentology and potentially KIM concentrations. A similar study to this one that focuses on identifying areas affected by short-lived glacial lakes and a comparison of the sedimentology, KIM concentrations and geochemistry of these sediments with unmodified till would be useful in furthering our understanding of the effects of sediment reworking by deglacial meltwater processes.

5.2.4. Glaciofluvial Hummock Genesis

Determining the genesis of glaciofluvial hummocks was not the main focus of this project; however, using the distribution, morphology, field observations and sedimentological data of glaciofluvial hummocks, an interpretation of their genesis was proposed. More focused and detailed study of glaciofluvial hummocks is required to better constrain our understanding of how they form. Some ideas for useful field studies would be test-pitting glaciofluvial hummocks with an excavator to create exposures so that in-situ sedimentology could be observed. Ground penetrating radar or seismic studies could also be used to determine the stratigraphy of hummocks.

References

Aylsworth, J.M., and Shilts, W.W., 1989. Bedforms of the Keewatin Ice Sheet, Canada: Sedimentary Geology, 62: 407–428.

Box, J. E., and Ski, K., 2007. Remote sounding of Greenland supraglacial melt lakes: implications for subglacial hydraulics: Journal of Glaciology, v. 53, no. 181: 257-265.

Campbell, J., McMartin, I., and Dredge, L., 2013. Morphology, architecture and associated landform-sediment assemblages of meltwater corridors north of Wager Bay, Nunavut. CANQUA-CGRC Biennial Meeting: Edmonton.

Cameron, E.M., Hamilton, S.M., Leybourne, M.I., Hall, G.E.M., and McClenaghan, M.B. 2004. Finding deeply buried deposits using geochemistry. Geochemistry: Exploration, Environment, Analysis, 4: 7–32. Geological Society of London.

Chu, V., 2014. Greenland ice sheet hydrology: A review: Progress in Physical Geography, v. 38, no. 1: 19-54.

Cookenboo, H.O., and Grütter, H.S. 2010. Mantle-derived indicator mineral compositions as applied to diamond exploration. Geochemistry: Exploration, Environment, Analysis, 10: 81–95.

Cowton, T., Nienow, P., Sole, A., Wadham, J., Lis, G., Bartholomew, I., Mair, D., and Chandler, D., 2013. Evolution of drainage system morphology at a land-terminating Greenlandic outlet glacier: Journal of Geophysical Research-Earth Surface, v. 118, no. 1: 29-41.

Crabtree, D.C. 2003. An overview of the Ontario Geological Survey's KIM data base: Interpretation of chromite and Cr-diopside data from regional surveys; *in* Thorleifson, H. and McClenaghan, M.B., (orgs.), Indicator Minerals in Mineral Exploration, Proceedings of a Short Course, March 8, Prospect. Develop. Assoc. Can: 35-43.

Cummings, D.I., Kjarsgaard, B.A., Russell, H.A.J., and Sharpe, D.R. 2011. Eskers as mineral exploration tools. Earth-Science Reviews, 109: 32–43.

Dahlgren, S., 2013. Subglacialy eroded meltwater hummocks: Master of Science thesis, University of Gothenburg, Gothenburg, Sweden, 49 pp.

Dalton, A.S., Margold, M., Stokes, C.R., Tarasov, L., Dyke, A.S., Adams, R.S., Allard, S., Arends, H.E., Atkinson, N., Attig, J.W., Barnett, P.J., Barnett, R.L., Batterson, M., Bernatchez, P., Borns, H.W., Breckenridge, A., Briner, J.P., Brouard, E., Campbell, J.E., Carlson, A.E., Clague, J.J., Curry, B.B., Daigneault, R.-A., Dubé-Loubert, H., Easterbrook, D.J., Franzi, D.A., Friedrich, H.G., Funder, S., Gauthier, M.S., Gowan, A.S., Harris, K.L., Hétu, B., Hooyer, T.S., Jennings, C.E., Johnson, M.D., Kehew, A.E., Kelley, S.E., Kerr, D., King, E.L., Kjeldsen, K.K., Knaeble, A.R., Lajeunesse, P., Lakeman, T.R., Lamothe, M., Larson, P., Lavoie, M., Loope, H.M., Lowell, T.V., Lusardi, B.A., Manz, L., McMartin, I., Nixon, F.C., Occhietti, S., Parkhill, M.A., Piper, D.J.W., Pronk, A.G., Richard, P.J.H., Ridge, J.C., Ross, M., Roy, M., Seaman, A., Shaw, J., Stea, R.R., Teller, J.T., Thompson, W.B., Thorleifson, L.H., Utting, D.J., Veillette, J.J., Ward, B.C., Weddle, T.K., and Wright, H.E. 2020. An updated radiocarbon-based ice margin chronology for the last deglaciation of the North American Ice Sheet Complex. Quaternary Science Reviews, 234: 106-223.

Deblonde, C.,Cocking, R.B, Kerr, D.E., Campbell, J, Eagles, S., Everett, D. Huntley, D., Inglis, E., Parent, M.,,Plouffe, A., Robertson, L. Smith, I.R.., and Weatherston, A., 2018. Surficial Data Model: the science language of the integrated Geological Survey of Canada data model for surficial geology maps. Geological Survey of Canada, Open File 8236.

Dredge, L.A., Nixon, F., and Richardson, R., 1985. Surficial Geology, Northwestern Manitoba: Geological Survey of Canada, "A" Series Map 1608A, 1:500 000.

Dredge, L.A., Ward, B.C., and Kerr, D.E., 1994. Glacial geology and implications for drift prospecting in the Lac de Gras, Winter Lake, and Aylmer Lake map areas, central Slave Province, Northwest Territories; - in Current Research 1994-C; Geological Survey of Canada: 33-38.

Dredge, L. A., Ward, B. C., and Kerr, D. E., 1995. Surficial geology, Aylmer Lake, District of Mackenzie, Northwest Territories, Map 1867A: Geological Survey of Canada, 1:125 000.

Dreimanis, A., 1989. Tills, their genetic terminology and classification. In: Goldthwait, R.P., Matsch, C.L. (Eds.), Genetic Classification of Glacigenic Deposits. Balkema, Rotterdam:17–84.

Dyke, A. S., 2004. An outline of North American deglaciation with emphasis on central and northern Canada: *in* Quaternary glaciations: Extent and chronology, *eds.* Ehlers, J., Gibbard, P.L., v. 2: 373-424.

Dyke, A. S and Prest, V.K., 1987: Paleogeography of northern North America, 18 000 – 5 000 years ago; Geological Survey of Canada, Map 1703A, scale 1; 12 500 000.

Fipke, C. E., Dummet, H. T., Moore, R. O., Carlson, J. A., Ashley, R. M., Gurney, J. J. & Kirkley, M. B. 1995. History of the discovery of diamondiferous kimberlites in the Northwest Territories, Canada. In: Extended Abstracts Volume, Sixth International Kimberlite Conference, Novosibirsk, Siberia: 158–160.

Fipke, C.E., Gurney, J.J., Moore, R.O., and Nassichuk, W.W. 1989: The development of advanced technology to distinguish between diamondiferous and barren diatremes; Geological Survey of Canada, Open File 2124: 1175pp.

Grütter, H.S., Gurney, J.J., Menzies, A.H., and Winter, F. 2004. An updated classification scheme for mantle-derived garnet, for use by diamond explorers. Lithos, 77: 841–85.

Grütter, H.S., Sweeney, R.J., 2000. Tests and constraints on single-grain Cr-pyrope barometer models: some initial results. Ext.Abstr. GAC/MAC Annual Joint Meeting, Calgary.

Gurney, J. J. 1984. A correlation between garnets and diamonds. In: Glover, J. E. & Harris, P. G. (eds) Kimberlite Occurrence and Origins: A basis for Conceptual Models in Exploration. University of Western Australia, Perth, 8: 376–383.

Haiblen, A. M., 2016. Glacial History and Landform Genesis in the Lac de Gras Area, Northwest Territories: Master of Science thesis, Simon Fraser University, Burnaby, Canada, 152pp.

Haiblen, A.M., Ward, B.C., Normandeau, P.X., Elliott, B., and Pierce, K.L., 2018. Detailed field and LiDAR based surficial geology and geomorphology in the Lac de Gras area, Northwest Territories (parts of NTS 76C and 76D); Northwest Territories Geological Survey, NWT Open Report 2017-016, 28 pages, 2 maps at 1:20 000 scale.

Hrabi, R.B and Grant J.W., 1999. Geology, Winter Lake Supracrustal Belt, Northwest Territorries; Geological Survey of Canada, Open File 3676, scale 1:50 000.

Henderson, P.J., 2000. Drift composition and surficial geology, MacQuoid Lake area (NTS 55 M/7 and 55 M/10), Kivalliq region, Nunavut: a guide to drift prospecting. Geological Survey of Canada, Open File 3944. 44 pp.

Kerr, D., Knight, R., Sharpe, D., and Cummings, D., 2014a. Reconnaissance surficial geology, Lynx Lake, Northwest Territories, NTS 75-J: Geological Survey of Canada, 1:125 000.

Kerr, D. K., RD, Sharpe, D., and Cummings, D., 2014b. Surficial geology, Walmsley Lake, Northwest Territories, NTS 75-N, Canadian Geoscience Map-140: Geological Survey of Canada, 1:125 000.

Kerr, D. E., Ward, B. C., and Dredge, L. A., 1996. Surficial Geology, Winter Lake, District of Mackenzie, Northwest Territories, "A" Series Map 1871A: Geological Survey of Canada, 1:125 000.

Knight, J., 2018. An interpretation of the deglaciation history of the southern Slave Province using 1:50 000 surficial geology maps; Northwest Territories Geological Survey, NWT Open Report 2017-018, 70 pp.

Layton-Matthews, D., Hamilton, C., and McClengahan, M.B., 2014. Mineral chemistry: modern techniques and applications to exploration, In: Application of Indicator Mineral Methods to Mineral Exploration, (eds) M.B. McClenaghan, A. Plouffe, and D. Layton-Matthews; Geological Survey of Canada, Open File 7553.

Levson, V.M., 2001. Regional till geochemical surveys in the Canadian Cordillera: sample media, methods and anomaly evaluation. In: McClenaghan, M.B. Bobrowsky, P.T., Hall, G.E.M. & Cook, S.J. (eds) 2001. Drift Exploration in Glaciated Terrain. Special Publication, 185. Geological Society, London:45-68.

Malvern Instruments, 2007. Mastersizer 2000 User Manual: Worcestershire, United Kingdom: Malvern Instruments, 95 pp.

McClenaghan, M.B. 2005. Indicator mineral methods in mineral exploration. Geochemistry: Exploration, Environment, Analysis, 5: 233–245.

McClenaghan, M.B. and Kjarsgaard, B.A. 2001. Indicator mineral and geochemical methods for diamond exploration in glaciated terrain in Canada. In: McClenaghan, M.B. Bobrowsky, P.T., Hall, G.E.M. & Cook, S.J. (eds) 2001. Drift Exploration in Glaciated Terrain. Special Publication, 185. Geological Society, London: 83–123.

McClenaghan, M.B., Plouffe, A., McMartin, I., Campbell, J.E., Spirito, W.A., Paulen, R.C., Garrett, R.G., and Hall, G.E.M. 2013. Till sampling and geochemical analytical protocols used by the Geological Survey of Canada. Geochemistry: Exploration, Environment, Analysis, 13: 285–301.

McClenaghan, M.B., Spirito, W.A., Plouffe, A., McMartin, I., Campbell, J.E., Paulen, R.C., Garrett, R.G., Hall, G.E.M., Pelchat, P., and Gauthier, M.S., 2020. Geological Survey of Canada till-sampling and analytical protocols: from field to archive, 2020 update; Geological Survey of Canada, Open File 8591.

McClenaghan, M.B., Thorleifson, L.H., and DiLabio, R.N.W. 2000. Till geochemical and indicator mineral methods in mineral exploration. Ore Geology Reviews, 16: 145–166.

McClenaghan, M.B., Ward, B.C., Kjarsgaard, I.M., Kjarsgaard, B.A., Kerr, D.E., and Dredge, L.A. 2002. Indicator mineral and till geochemical dispersal patterns associated with the Ranch Lake kimberlite, Lac de Gras region, NWT, Canada. Geochemistry: Exploration, Environment, Analysis, 2: 299–319.

McMartin, I., Godbout, P.-M., Campbell, J. E., Tremblay, T., Behnia, P. 2020. A new map of glacigenic features and glacial land systems in central mainland Nunavut, Canada. Boreas, 50: 51–75.

Miller, J.K. 1984. Model for elastic indicator trains in till. In: Prospecting in Areas of Glaciated Terrain 1984. Institution of Mining and Metallurgy, London: 69-77.

Morris, T.F., Sage, R.P., Ayer, J.A., and Crabtree, D.C. 2002. A study of clinopyroxene composition: Implications for kimberlite exploration; Geochem. Explor. Analy., v2, no4: 321-331.

Ojala, A.E.K., Peterson, G., Mäkinen, J., Johnson, M.D., Kajuutti, K., Palmu, J-P., Ahokangas, E., Öhrling, C. 2019. Ice-sheet scale distribution and morphometry of triangular shaped hummocks (murtoos): a subglacial landform produced during rapid retreat of the Scandinavian Ice Sheet. Annals of Glaciology 60(80): 115–126.

Parent, M., Beaumier, M., Girard, R., Paradis, S.J., 2004. Diamond exploration in the Archean craton of northern Quebec: Kimberlite indicator minerals in eskers of the Saindon–Cambrien corridor. Géologie Québec MB 2004-02: 16 pp.

Peterson, G., Johnson, M.D., Dahlgren, S., Påsse, T., and Alexanderson, H. 2018. Genesis of hummocks found in tunnel valleys: an example from Hörda, southern Sweden. GFF, 140: 189–201.

Peterson, G., and Johnson, M.D. 2018. Hummock corridors in the south-central sector of the Fennoscandian ice sheet, morphometry and pattern. Earth Surface Processes and Landforms, 43: 919–929.

Porter, Claire; Morin, Paul; Howat, Ian; Noh, Myoung-Jon; Bates, Brian; Peterman, Kenneth; Keesey, Scott; Schlenk, Matthew; Gardiner, Judith; Tomko, Karen; Willis, Michael; Kelleher, Cole; Cloutier, Michael; Husby, Eric; Foga, Steven; Nakamura, Hitomi; Platson, Melisa; Wethington, Michael, Jr.; Williamson, Cathleen; Bauer, Gregory; Enos, Jeremy; Arnold, Galen; Kramer, William; Becker, Peter; Doshi, Abhijit; D'Souza, Cristelle; Cummens, Pat; Laurier, Fabien; Bojesen, Mikkel, 2018. "ArcticDEM", Harvard Dataverse, V1.

Quirt, D.H. 2004. Cr-diopside (clinopyroxene) as a kimberlite indicator mineral for diamond exploration in glaciated terrains; *in* Summary of Investigations 2004, Volume 2, Saskatchewan Geological Survey, Sask. Industry Resources, Misc. Rep. 2004-4.2, CD-ROM, Paper A-10: 14p.

Rampton, V. N., 2000. Large-scale effects of subglacial meltwater flow in the southern Slave Province, Northwest Territories, Canada: Canadian Journal of Earth Sciences, 37: 81-93.

Rampton, V. N., and Sharpe, D. R., 2014. Detailed surficial mapping in selected areas of the southern Slave Province, Northwest Territories: Geological Survey of Canada, Open File 7562, 31 pp.

Sacco, D.A., McKillop, R .M., Ward, B.C., and Ellis, S. 2018. Surficial Geology and Till Sampling Suitability for NTS Map Sheets 075M09, parts of 075N05/06/11/12, and parts of 076D05/06/07/10/11/12, Slave Geological Province, Northwest Territories. Northwest Territories Geological Survey, NWT Open Report 2018-015, Scale 1:50 000.

Siegert, M.J., 2000. Antarctic subglacial lakes: Earth-Science Reviews, 50: 29-50.

Smith, B. E., Gourmelen, N., Huth, A., and Joughin, I. 2017. Connected subglacial lake drainage beneath Thwaites Glacier, West Antarctica, The Cryosphere, 11: 451–467.

Sparks, R.S.J., Baker, L., Brown, R.J., Field, M., Schumacher, J., Stripp, G., and Walters, A. 2006. Dynamical constraints on kimberlite volcanism. Journal of Volcanology and Geothermal Research, 155: 18–48.

Spirito, W.A., McClenaghan, M.B., Plouffe, A., 2011. Till sampling and analytical protocols for GEM projects: from field to archive; Geological Survey of Canada, Open File 6850: 84 p.

Stevens, L. A., Behn, M. D., McGuire, J. J., Das, S. B., Joughin, I., Herring, T., Shean, D. E., and King, M. A., 2015. Greenland supraglacial lake drainages triggered by hydrologically induced basal slip: Nature, v. 522, no. 7554: 73-76.

St Onge, D., 1984. Surficial deposits of the Redrock Lake area, District of Mackenzie: Current Research, Part A; Geological Survey of Canada, Paper no. 84-1A: 271-276.

St Onge, D., and Kerr, D., 2014. Reconnaissance surficial geology, Joe Lake, Nunavut, NTS 66-J, south half: Geological Survey of Canada, 1:125 000.

Thompson, P.H. and Kerswill, J.A., 1994. Preliminary geology of the Winter Lake – Lac de Gras area, District of Mackenzie, Northwest Territories; Geological Survey of Canada, Open File 2740 (revised), scale 1:250 000 with marginal notes.

Tremblay, T., Ryan, J.J., James, D.T., Kjarsgaard, I.M., 2009. Kimberlite indicator mineral survey and ice flow studies in Boothia mainland (NTS 57A, 57B, 57C, and 57D), Kitikmeot region, Nunavut. Geological Survey of Canada, Open File 6040. 27 pp.

Utting, D. J., Ward, B. C., and Little, E. C., 2009. Genesis of hummocks in glaciofluvial corridors near the Keewatin Ice Divide, Canada. Boreas, 38: 471-481.

Ward, B. C., Dredge, L. A., and Kerr, D. E., 1997, Surficial geology, Lac de Gras, District of Mackenzies, Northwest Territories (NTS 76-D): Geological Survey of Canada, 1:125 000.

Wentworth, C.K. 1922. A Scale of Grade and Class Terms for Clastic Sediments. Journal of Geology, 30: 377–392.

Wingham, D., Siegert, M., Shepherd, A., Muir, A. 2006. Rapid discharge connects Antarctic subglacial lakes. Nature, 440: 1033–1036.

Appendix A.

Surficial Geology North of Beauparlant Lake, Northwest Territories, part of NTS 86A09

Description:

This pdf file contains the 1: 15 000 map with full legend and marginal notes. This map is intended for publication as an NTGS open file.

File name:

Surficial_Geology_Beauparlant_Lake.pdf

Appendix B. Field Notes

Supplementary Data File

Description:

This appendix includes scanned copies of the notes taken during the field work portion of this thesis and a table of the sample names, coordinates, and material types. This appendix includes two files: a pdf of the field notes and an excel spreadsheet of the sample IDs and locations.

File names:

Field_Notes.pdf

Sample_Locations.xlsx

Appendix C. Grain size Data

Supplementary Data File

Description:

Results of grain size analysis, including masses of each grain size-fraction and cumulative and differential percentages of each grain size-fraction for each sample.

File name:

Grain size_Analysis_Appendix_C.xlsx

Appendix D. Clast Lithology

Supplementary Data File

Description:

Results of clast lithology analysis including lithology counts, angularity, and shape values for each sample.

File name:

Clast_Analysis_Appendix_D.xlsx

Appendix E. KIM Counts

Supplementary Data File

Description:

The results of visual identification of KIM grains for each sample, completed by Overburden Drilling Management. The mass of the <2.0 mm size-fraction is included as well as normalized KIM counts. KIM counts are normalized to 10 kg of <2.0 mm size-fraction.

File name:

KIM_Counts_Appendix_E.xlsx

Appendix F. Electron Microprobe Data

Supplementary Data File

Description:

Results of Electron Microprobe analysis, containing the weight percent oxide of all analytes for each point analysis. Mineral grain IDs correspond with associated sample numbers. There are two files in this appendix. One is the Garnet mineral chemistry results, the other is the Clinopyroxene mineral chemistry results.

File name:

Garnet_Chemistry.xlsx

Clinopyroxene_Chemistry.xlsx

Appendix G. Matrix Geochemistry

Supplementary Data File

Description:

Results of geochemical analysis of the matrix of each sample, completed by ALS global. Each analyte column includes the ALS package code completed, the method of digestion and the unit of the results.

File name:

ALS_Matrix_GeoChem_Appendix_G.xlsx